Copyright Warning & Restrictions

The copyright law of the United States (Title 17, United States Code) governs the making of photocopies or other reproductions of copyrighted material.

Under certain conditions specified in the law, libraries and archives are authorized to furnish a photocopy or other reproduction. One of these specified conditions is that the photocopy or reproduction is not to be "used for any purpose other than private study, scholarship, or research." If a, user makes a request for, or later uses, a photocopy or reproduction for purposes in excess of "fair use" that user may be liable for copyright infringement,

This institution reserves the right to refuse to accept a copying order if, in its judgment, fulfillment of the order would involve violation of copyright law.

Please Note: The author retains the copyright while the New Jersey Institute of Technology reserves the right to distribute this thesis or dissertation

Printing note: If you do not wish to print this page, then select "Pages from: first page # to: last page #" on the print dialog screen

ABSTRACT

PROCESSING OF CDS/CDTE SOLAR CELL AND THE GROWTH MODEL OF CDTE THIN FILM

by
Guogen Liu

Cadmium telluride is the only thin film photovoltaic (PV) technology to surpass crystalline silicon PV in the cost. The most common CdTe solar cells consist of a simple p-n heterojunction structure containing a p-doped CdTe layer and n-doped cadmium sulfide (CdS) layer, which acts as a window layer. Cadmium Sulfide (CdS) thin films are often deposited on glass substrates coated with TCO layers by the close-spaced sublimation (CSS) or sputter techniques in industrial because of in-line production integration. It is seldom reported that CdS is deposited by the chemical bath deposition (CBD) batch process. The bottleneck of CBD for commercial application is its low production rate and waste water treatment. This dissertation reports how to produce different thickness large area (100cm2) CdS thin film by CBD. The influence of the solution temperature and concentration on the thickness of CdS is investigated. This dissertation also reports a growth model for CdTe deposition including diffusion limited and sublimation limited. The model was consistent with experimental observations and showed very good agreement over a range of operating conditions.

PROCESSING OF CDS/CDTE SOLAR CELL AND THE GROWTH MODEL OF CDTE THIN FILM

By
Guogen Liu

A Dissertation
Submitted to the Faculty of
New Jersey Institute of Technology
in Partial Fulfillment of the Requirements for the Degree of
Doctor of Philosophy in Chemical Engineering

Otto H. York Department of
Chemical, Biological and Pharmaceutical Engineering

August 2016

.

APPROVAL PAGE

PROCESSING OF CDS/CDTE SOLAR CELL AND THE GROWTH MODEL OF CDTE THIN FILM

Guogen Liu

Dr. Ken K. Chin, Dissertation Advisor Professor of Physics, Director of CNBM Photovoltaic Material Research Center, NJIT	Date
Dr. Laurent.Simon, Dissertation Advisor Associate Professor of Otto H. York Department of Chemical, Biological and Pharmaceutical Engineering	Date
Dr. Alan E. Delahoy, Committee Member Research Professor of Physics, NJIT	Date
Dr. Reginald P Tomkins, Committee Member Professor of Otto H. York Department of Chemical, Biological and Pharmaceutical Engineering	Date
Dr. Xiaoyang Xu, Committee Member Assistant Professor of Otto H. York Department of Chemical, Biological and Pharmaceutical Engineering	Date
Dr. George E. Georgiou, Committee Member University Lecturer of Physics, NJIT	Date

BIOGRAPHICAL SKETCH

Author: Guogen Liu

Degree: Doctor of Philosophy

Date: August 2016

Undergraduate and Graduate Education:

- Doctor of Philosophy in Otto H. York Department of Chemical, Biological and Pharmaceutical Engineering,
  New Jersey Institute of Technology, Newark, NJ, 2016

- Master of Chemical Engineering,
  Beijing University of Chemical Engineering, Beijing, P. R. China, 2007

- Bachelor of Chemical Engineering,
  Nanchang University, Jiangxi, P. R. China, 2004

Major: Chemical Engineering

Presentations and Publications:

Guogen Liu, Zimeng Chen, George E. Georgiou, Ken K. Chin, "The Growth Model of CdTe Thin Film by Close Spaced Sublimation," at 42th IEEE Photovoltaic Conference, (June 2015).

Zimeng Cheng, Alan E. Delahoy, **Guogen Liu**, Shou Peng, Congxiao Wang, Jingong Pan, Xin Cao and Ken K. Chin, "Modelling of The Nonstoichiometric Composition Shift In Physical Vapor Deposition of CdTe Thin Films Based on Experimental Results," EUPVSEC, (2015).

Guogen Liu, Zimeng Chen, Ken K. Chin, Robert B. Barat, George E. Georgiou, Alan E. Delahoy, "CdS Thin Film Grown by Aerosol-Assisted Deposition Method," at 38th IEEE Photovoltaic Conference, (June 2012).

Guogen Liu, Zimeng Chen, Ken K. Chin, Robert B. Barat, Alan E. Delahoy, George E. Georgiou, "Preparation and characterization of high efficiency CdS/CdTe solar cell, " at VIII th Annual Graduate Student Research Day, NJIT, Newark, NJ, (Nov 2012).

Poonam Kharangarh, Durgamadhab Misra, George E. Georgiou, Alan E. Delahoy, Zimeng Cheng, **Guogen Liu**, Halina Opyrchall, Timothy Gessert and Ken K. Chin, "Investigation of Defects in n+CdS/p-CdTe Solar Cells," Proc. of 38th PVSC, Austin, TX USA , p. 1286, Jun 2012.

Guogen Liu, Zimeng Chen, Ken K. Chin, Robert B. Barat, George E. Georgiou, "Large Area CdS Thin Film Grown By Chemical Bath Deposition," In proceedings of 37th IEEE Photovoltaic Conference, June 2011.

Guogen Liu, Zimeng Chen, Ken K. Chin, Robert B. Barat, George E. Georgiou, "Preparation and characterization of CdS/CdTe solar cell," at VIth Annual Graduate Student Research Day, NJIT, Newark, NJ, Nov 2010.

To my family: Fuliang Liu, Aimei Xu, Qiaozhen Liu

ACKNOWLEDGMENT

I would like to express my deep gratitude and sincere appreciation to my advisors, Prof. Ken K. Chin and Prof. Laurent Simon, for their constant support and guidance throughout this work. Their valued advice, encouragement, and constructive criticism have been a great source of inspiration in the fulfillment of this thesis. I would also like to express my gratitude and thanks to all my committee members Dr. Reginald P. Tomkins, Dr. George E. Georgiou, Dr. Alan E. Delahoy and Dr. Xiaoyang Xu for their interest, useful suggestions, and support in this study.

The valuable discussions and constructive suggestions from Tim Gessert and Jim Sites are greatly acknowledged. Many thanks to Chemical Engineering and CNBM for their funding support.

Finally, I would also like to thank all my colleagues for their help and support in my work.

TABLE OF CONTENTS

TABLE OF CONTENTS
(Continued)

Chapter **Page**

TABLE OF CONTENTS
(Continued)

Chapter **Page**

LIST OF TABLES

Table **Page**

LIST OF FIGURES

LIST OF FIGURES
(Continued)

Figure **Page**

LIST OF FIGURES
(Continued)

Figure **Page**

LIST OF FIGURES
(Continued)

Figure **Page**

LIST OF FIGURES
(Continued)

Figure **Page**

LIST OF ABBREVIATIONS

AM1.5	Standard solar spectrum
CdTe	Cadmium Telluride
CdS	Cadmium Sulfide
TCO	Transparent Conducting Oxide
CBD	Chemical Bath Deposition
CSS	Closed Spaced Sublimation
PV	Photovoltaic
CSP	Solar Concentrated Power
DC	Direct Current
AC	Alternating Current
CSS	Closed Spaced Sublimation
PV	Photovoltaic
CSP	Solar Concentrated Power
DC	Direct Current
AC	Alternating Current
CIGS	Copper Indium Gallium Selenide
CIS	Copper Indium Selenide
CdCl2	Cadmium Chloride
A-Si	Amorphous Silicon
NREL	National Renewable Energy Lab
FTO	Fluorine-Doped Tin Oxide

ITO	Indium Tin Oxide
PVD	Physical Vapor Deposition
CVD	Chemical Vapor Deposition
AAD	Aerosol-Assisted Deposition

CHAPTER 1

INTRODUCTION

1.1 Why Renewable Energy?

Energy is the capacity of a physical system to perform work. It is available in several forms such as thermal, light, electrical, chemical and mechanical energy (Table 1.1). Energy can be classified by different ways (Gurmit Singh, 2013). We can also classified by kinetic energy and potential energy. Kinetic energy results from matter moving or in use. It is defined as the work needed to accelerate a body of a given mass from rest to its stated velocity; Potential energy is due to the position, structure of matter or composition. It is the energy associated with forces of attraction and repulsion between objects. Any object that is lifted from its resting position has stored energy because it has a potential to do work when released.

Table 1.1 Energy Form

Form of Energy	Example
Thermal(heat) Energy	Flame
Electrical Energy	Electrical light
Light	Sun
Chemical Energy	Coal, Oil, Natural gas
Mechanical Energy(Motion)	Car, Aircraft

Source: (Gurmit Singh, 2013)

The resource of energy includes fossil fuel and renewable energy.

1.1.1 Fossil Fuels

Fossil fuels are referred to nonrenewable energy sources because they cannot be restored. They include natural gas, petroleum (oil), and coal.

Natural Gas

Natural gas is primarily methane and is piped into homes and office buildings for heating, cooking, washing and drying. It is the raw material for producing other chemicals and is the cleanest fossil fuel. Natural gas is found in deep underground natural rock formations.

Petroleum or Oil

Petroleum is a flammable liquid consisting of a complex mixture of hydrocarbons and other liquid organic compounds that are found beneath the earth's surface. It is the black and thick liquid. To make it useful, it is refined. Refining produces the gasoline portion which is used for transportation. Products from the remaining portions include synthetic rubber, detergents, fertilizers, textiles, paints, and pharmaceuticals.

Coal

Coal is a combustible black rock usually occurring in coal beds. Coal is the largest source of energy and the most abundant fossil fuel. It is not a widely used energy source due to the cost of mining. It also causes pollution. There are two ways to mine coal: underground mining and strip mining.

Fossil fuels are derivatives of plant and animal fossils that are million years old. Fossil fuels are the major energy sources but lead to disastrous effects such as air

pollution. Burning of fossil fuels releases nitrogen dioxide, sulfur dioxide, carbon dioxide, nitrogen monoxide, carbon monoxide etc., which affect human health. They are non-renewable sources of energy. Their source is limited and they are depleting at a faster rate.

There are many disadvantages of fossil fuel (Rinkesh, 2013):

1. Environmental Hazards

Pollution is a serious disadvantage of fossil fuels. They give out carbon dioxide, a greenhouse gas which is the main aspect of global warming. The temperature rise in earth has resulted in melting of polar ice caps, flooding of low-lying areas, rising in sea levels. Fossil fuels also give out sulfur dioxide gas which is the factor for acid rain. Acid rain leads to destruction of monuments consisted of brickwork or marbles.

2. Human Health Getting Affected

Fossil fuels cause the worn-out of the ozone layer. Ozone holes let the harmful UV rays enter the earth surface and may cause diseases like cancer.

3. Non-Renewable

Fossil fuels will deplete some day. Since they are non-renewable, it is likely that fuels expenses will increase greatly in the near future. It would take millions of years to replace coal, and oil.

1.1.2 Renewable Energy (Chris Woodford, 2015)

Renewable energy comes from resources which are naturally replenished on a human time scale. It includes solar, wind power, hydroelectric, ocean tides, geothermal, biomass and nuclear fission.

Solar

Solar energy is the radiant light and heat from the sun. It includes solar heating, solar photovoltaics, solar thermal electricity, solar architecture and artificial photosynthesis. The sun is the supplier of energy which runs the water cycle. The uneven heating of the earth produces wind energy. Solar energy can serve to cook food, heat water and generate electricity. It is still the cleanest energy source.

Wind power

The wind comes from the movement of the atmosphere driven by differences in temperature. Wind energy can be used to pump water or generate electricity. Areas where winds are stronger and more constant are preferred locations for wind farms.

Hydroelectric

Hydroelectricity is the electricity generated by hydropower. It is the most widely used form of renewable energy. The water collected behind dams provides a source of energy for the production of electricity. The enormous power of falling water turns the giant turbines which drive the generators and produce electricity.

Ocean Tides

Ocean Tides are the rise and fall of sea levels caused by the combined effects of the gravitational forces of the Moon and the Sun and the rotation of the Earth. Ocean tides are very powerful forces.

Geothermal

Geothermal energy is thermal energy generated and stored in the Earth. The geothermal energy of the Earth's crust originates from the original formation of the planet (20%) and from the radioactive decay of minerals (80%).

Biomass

Biomass is biological material from living organisms. As a renewable energy source, biomass can either be used directly or indirectly. Biomass can be transformed into energy in three ways: thermal conversion, chemical conversion and biochemical conversion.

There are many advantages of renewable energy (Mariska de Wild-Scholten, et al. 2009)

1. Environmental Benefits

Renewable energy technologies are clean sources of energy that have much lower environmental impact than conventional energy technologies.

2. Energy for our children

Renewable energy will not run out, unlike coal, oil and gas which are finite and will someday be depleted.

3. Reduces Transmission Losses and Infrastructure Costs

Distributed renewable energy production means putting modest-sized generators closer to load. This means less electricity lost in transmission and less stress on the electricity grid, especially reducing demand for new, long-distance high-voltage transmission lines that cost approximately $3 million per mile.

4. Increases Economic Development

Smaller-scale, distributed renewable energy projects are more likely to tap into local talent for financing, construction, maintenance and retain more of the project's cash flow in the local economy. Renewable electricity (Figure 1.1) comprised an estimated 22.8%

of global electricity in 2014. While renewable capacity continues to rise at a rapid rate from year to year.

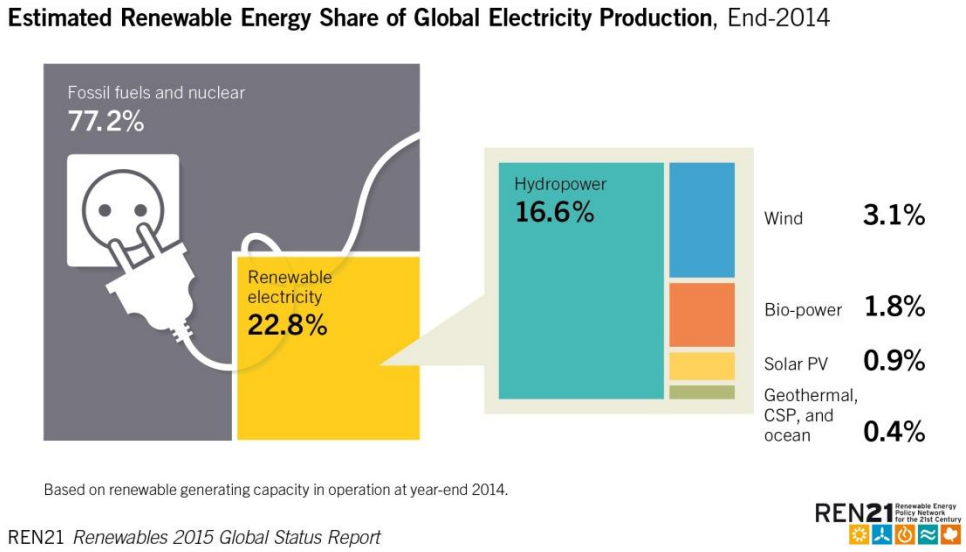

Figure 1.1 Renewable energy share of global electricity production in 2014.
Source: (José González, 2015)

1.2 Why Solar Energy and Solar Cell?

Solar energy is the energy from the sun, which provides consistent and steady source of solar power throughout the year. As our natural resources decline in the future, it is important to move towards renewable sources. The sun is the most plentiful energy source for the earth. All wind, fossil fuel, hydro and biomass energy comes from sunlight. Solar energy falls on the surface of the earth at a rate of 120 petawatts which is the most plentiful renewable resource. As showed in Figure 1.2, there is more than enough solar irradiation available to satisfy the world's energy demands. On average, each square meter is exposed to generate 1,700kwh of energy every year. The yearly energy of solar irradiance on Earth is much higher than fossil fuel resources as shown in Figure 1.2.

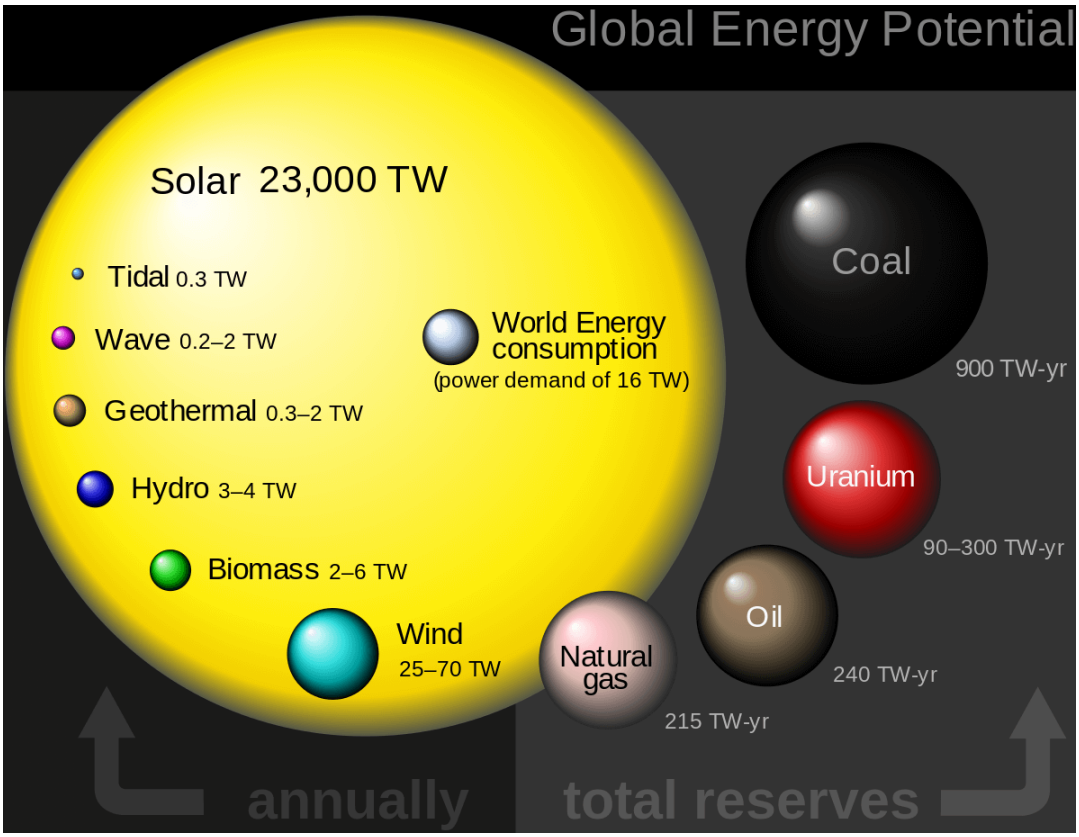

Figure 1.2 World's energy consumption vs. annual solar energy potential.

Source: http://learn.revolvesolar.com/the-sun-to-rule-them-all-solar-energys-potential

Solar radiation is the largest energy flow entering the terrestrial ecosystem. There is about 23,000TW that hits the surface of the earth, which is more than 1,000 times of the current global consumption (Figure 1.2). Solar energy is one of the best renewable energy sources with least negative impacts on the environment. The temperature difference between the sun and the earth is the driving force of solar energy. The sun emits electromagnetic radiation with spectral distribution determined by the temperature. Figure 1.3 shows the spectral irradiance at different positions in the atmosphere.

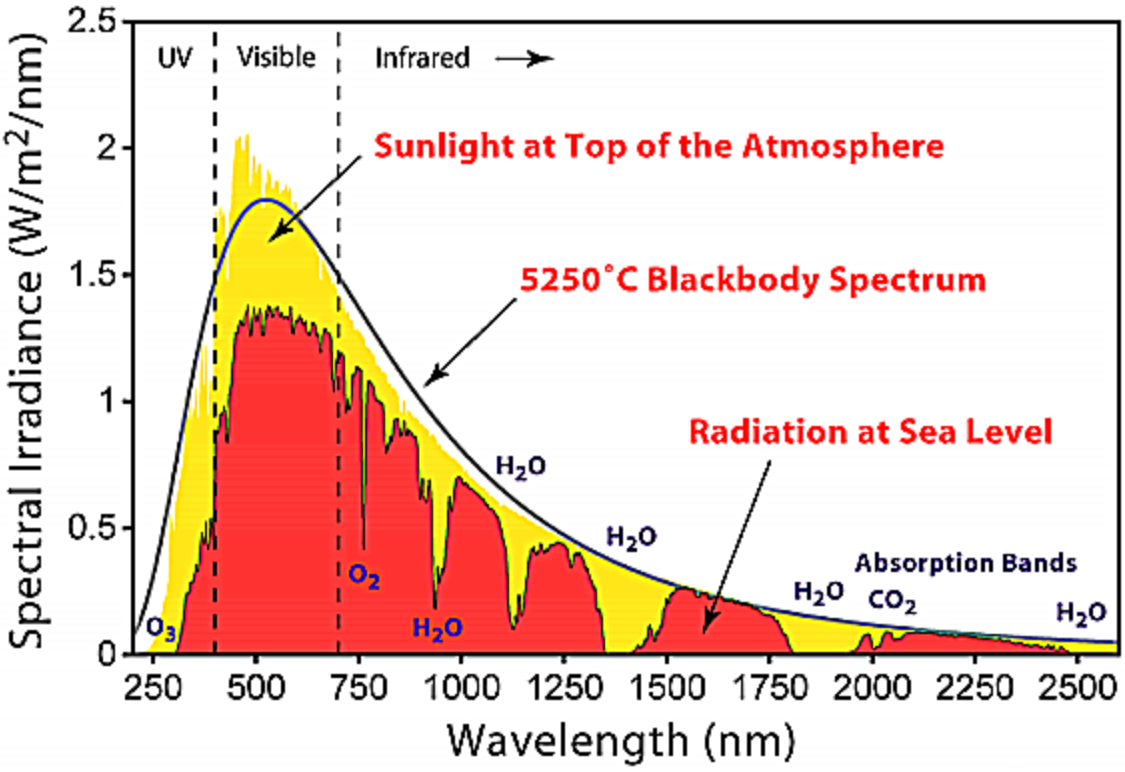

Figure 1.3 Spectral irradiance of the solar spectrum.

Source: (Solar irradiance, 2015)

Solar energy can be used by small-scale photovoltaic (PV) cells. The PV systems feed into electricity grids. The costs of solar energy technologies have dropped substantially over the last 30 years because of the fast development of solar energy technology. The solar energy technologies can be divided into passive and active. Passive solar energy technology merely collects the energy without converting into other forms. Active solar energy technology converts it for other applications and can be broadly classified into two groups: (I) solar thermal and (II) photovoltaic (PV). Solar thermal technology (Figure 1.4**)** uses solar heat to produce hot water for showers etc.

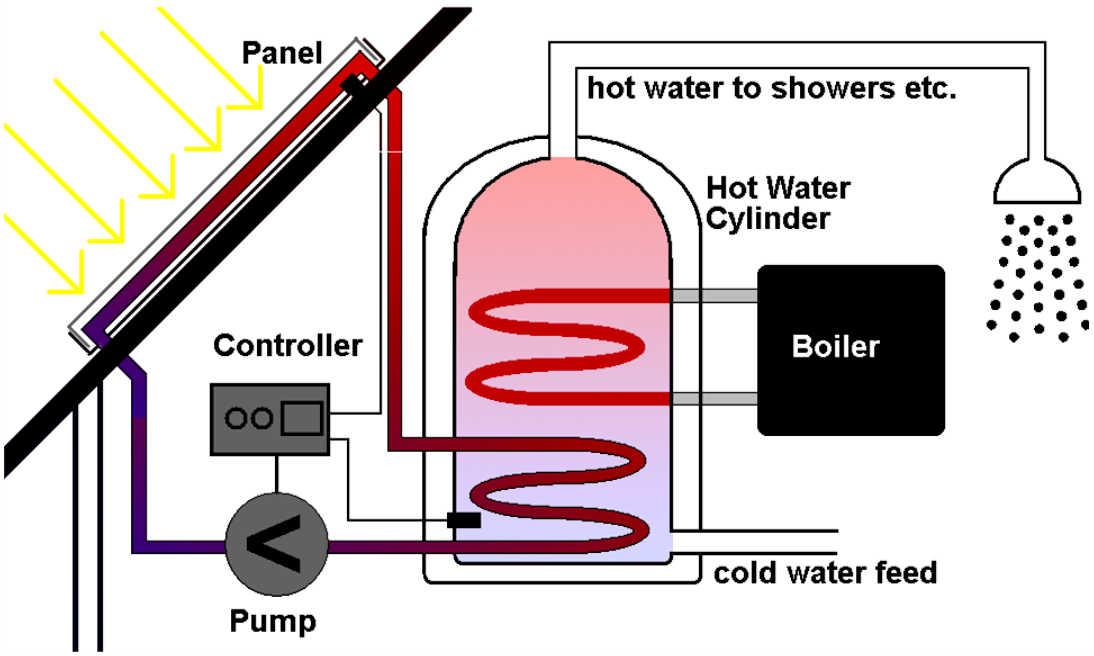

Figure 1.4 Solar thermal energy diagram solar water heating system.

Source: http://info.cat.org.uk/questions/solar-water-heating/how-does-solar-water-heating-work

The PV technology (Figure 1.5) converts light into electrical energy. Solar energy comes to earth in the form of photons which are collected by solar photovoltaic (PV) panels. The photons excite the potential energy in the solar panel and electricity in the form of DC current and voltage is generated. DC power is like the energy stored in batteries. The power from the solar array (DC current) goes to an electrical component called Inverter which converts it to AC (Alternating Current). The power is then sent to your electrical circuit breaker box which is attached to the grid.

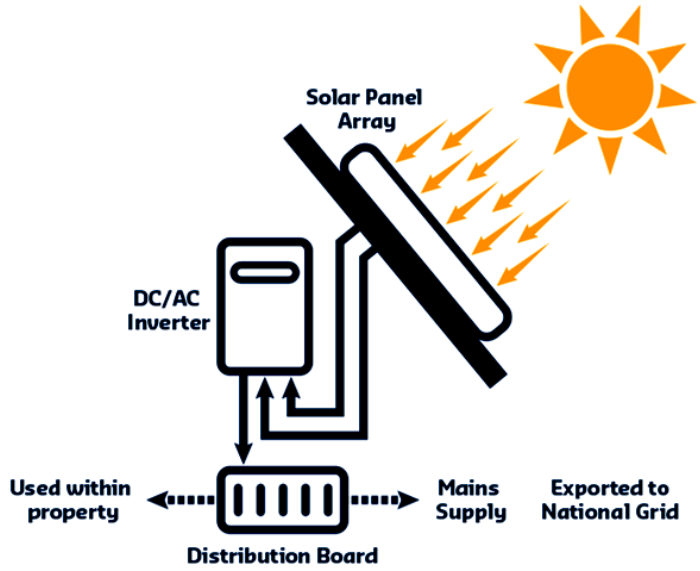

Figure 1.5 PV working system.

Source: http://www.aessolar.co.uk/

There are two types of PV technology (Figure 1.6) available in the market: (a) crystalline silicon-based PV cells and (b) thin film technologies. It is made out of a range of different semi-conductor materials, including amorphous silicon, cadmium-telluride (CdTe) and copper indium gallium selenide (CIGS).

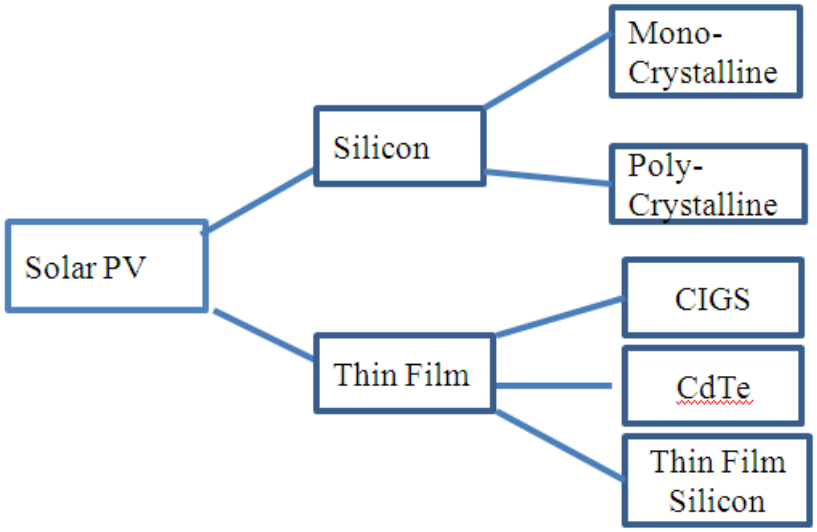

Figure 1.6 Solar cell classification.

Crystalline silicon (c-Si) is produced by refining sand to a higher purity of 5N (99.999%). Silicon is grown from a small seed crystal which is slowly pulled out of a poly-silicon melt into a cylindrical shaped ingot. The ingot is cut into wafers using a diamond saw. Solar cells made of c-Si are made from wafers between 160 to 240 micrometers thick.

Thin-film technologies reduce the amount of active material in a cell. Most sandwich active material between two panes of glass. Since silicon solar panels only use one pane of glass, thin film panels are approximately twice as heavy as crystalline silicon panels. Cadmium telluride (CdTe) is one of the most promising thin film materials. Its record efficiency was boosted to more than 20% by First Solar. Amorphous silicon (a-Si) is a non-crystalline and the most well-developed thin-film technology. a-Si is attractive as a solar cell material because it's an abundant, non-toxic material. It requires a low processing temperature and enables a scalable production upon a flexible, low-cost substrate with little silicon material required. CIGS cell uses an absorber made of copper, indium, gallium, selenide (CIGS). It is one of three mainstream thin-film technologies, the other two being cadmium telluride and amorphous silicon.

The global solar PV market increase every year. More than 139 GW was installed in 2013 (Figure 1.7).

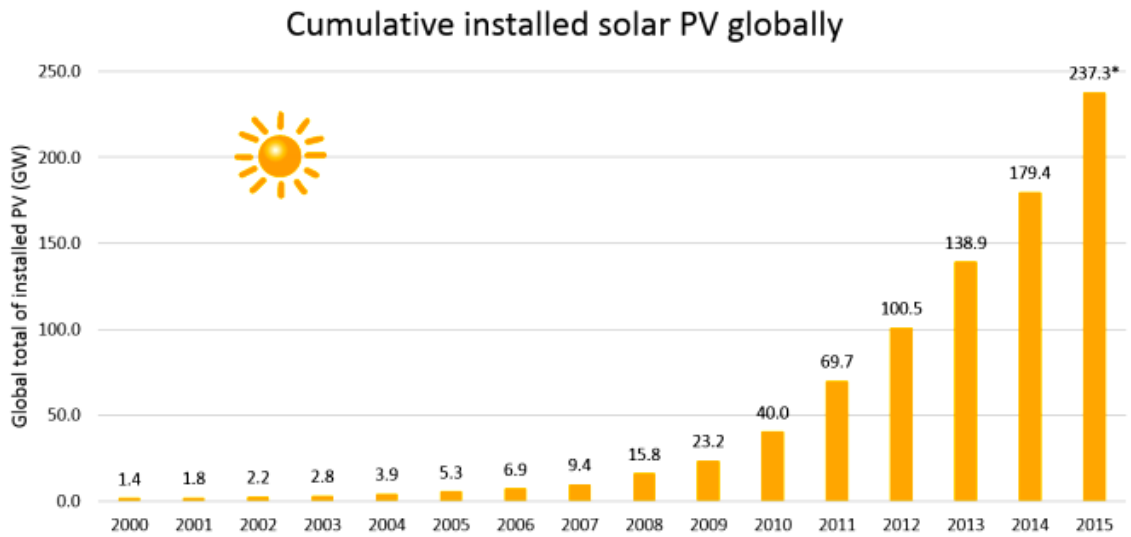

Figure 1.7 Solar PV total global capacity(2000–2015).

Source: https://charlieonenergy.wordpress.com/2015/12/07/solar-and-moores-law/

There are five criteria for evaluating the value of energy source:

1. Availability - Is the energy source available and for how long? Fifteen years is considered to be near, fifteen to fifty years is intermediate, and over fifty years is considered to be long.
2. Energy Yield - How much of other energy is needed to produce the energy? Rider University uses a net energy ratio, "Energy produced divided by energy expended during production." The higher the ratio, the better the energy.
3. Cost - How much does the energy cost to develop and manufacture? If it needed high-technology to produce nuclear energy, it may be a detriment to its use.
4. Environment - How does the energy affect the environment? Does the extracting, transporting and using the source outweigh the effects on the environment?

5. Renewable – Does the energy source come from a renewable energy? Is it sustainable? Rider University experts say: "Why develop it if you're just going to run out of it?"

The Advantages of Solar Energy:

1. Raw materials are renewable and unlimited.

The amount of available solar energy is roughly 1,000 times that currently required by humans. Sunlight is everywhere and the resource is inexhaustible.

2. Solar power is low-emission

A solar power system produces no pollution at all. Solar panels are very clean, although they impose environmental costs through manufacture and construction. These environmental tolls are negligible compared with the damage inflicted by conventional energy sources. Solar energy is an excellent alternative for fossil fuels like coal and petroleum.

3. Solar power is suitable for remote areas

Solar power can generate electricity no matter how remote the area. Even in areas that are inaccessible to power cables, solar power can produce electricity. Solar energy can drastically improve quality of life for millions of people who live in the dark.

4. Solar panels produce no noise

The generation of electricity through solar power produces no noise. Wind turbines create some noisy.

5. Solar power is economical

Solar panels and installation involve high initial expenses, but this cost is soon offset by savings on energy bills. Eventually they produce a profit on their use. Payback times may be as short as five years.

In summary, solar energy offers advantages to conventional fossil fuels and other renewable energy systems. Solar energy is obviously environmentally advantageous compare to any other energy source. It does not deplete natural resources, does not cause CO_2 or other gaseous emission into air or generates liquid or solid waste products.

1.3 Why CdTe Thin Film Solar Cell?

Cadmium telluride (CdTe) is a photovoltaic (PV) technology based on the use of a thin film of CdTe to absorb and convert sunlight into electricity. CdTe is the second most utilized solar cell material in the world. It is the first and only thin film photovoltaic technology to surpass crystalline silicon PV in cheapness. It is one of the most competitive photovoltaic devices as far as cost and efficiency are concerned. It has a large optical absorption coefficient. Only a small amount of CdTe (2-8 microns thick) is needed for the absorber layer (100 times thinner than typical crystalline-Si solar cells). Moreover, the band gap of CdTe matches the solar spectrum quite well. It is quite close to the band gap which produces the highest theoretical conversion efficiency.

CdTe is an excellent semiconductor and absorbs a very wide range of the solar spectrum. It performs better under hot conditions due to a high temperature coefficient, is well suited to high-volume manufacturing. This combination of factors gives CdTe PV a unique combination of economic and environmental benefits over other PV technologies.

CdTe is a very stable crystalline compound. CdTe solar cells can be fabricated with a variety of deposition techniques, such as close-spaced sublimation, vapor-transport deposition, physical-vapor deposition, sputter deposition, electro-deposition, metal-organic chemical-vapor deposition, spray deposition, and screen-print deposition. Among those technologies, Close spaced sublimation (CSS) has attractive features for high-rate deposition of CdS/CdTe thin film solar modules. Besides, the new efficiency record 21.5% is also produce by FSLR.

CdTe panels have several advantages over traditional silicon technology. These include:

1. Ease of manufacturing

The necessary electric field stems from properties of cadmium sulfide and cadmium telluride. It is simpler compared to the multi-step process of joining two different types of doped silicon in a silicon solar panel. First Solar is the biggest thin film solar cell company and produces CdTe solar cell (Figure 1.8) by the VTD. It is very simple and high efficient.

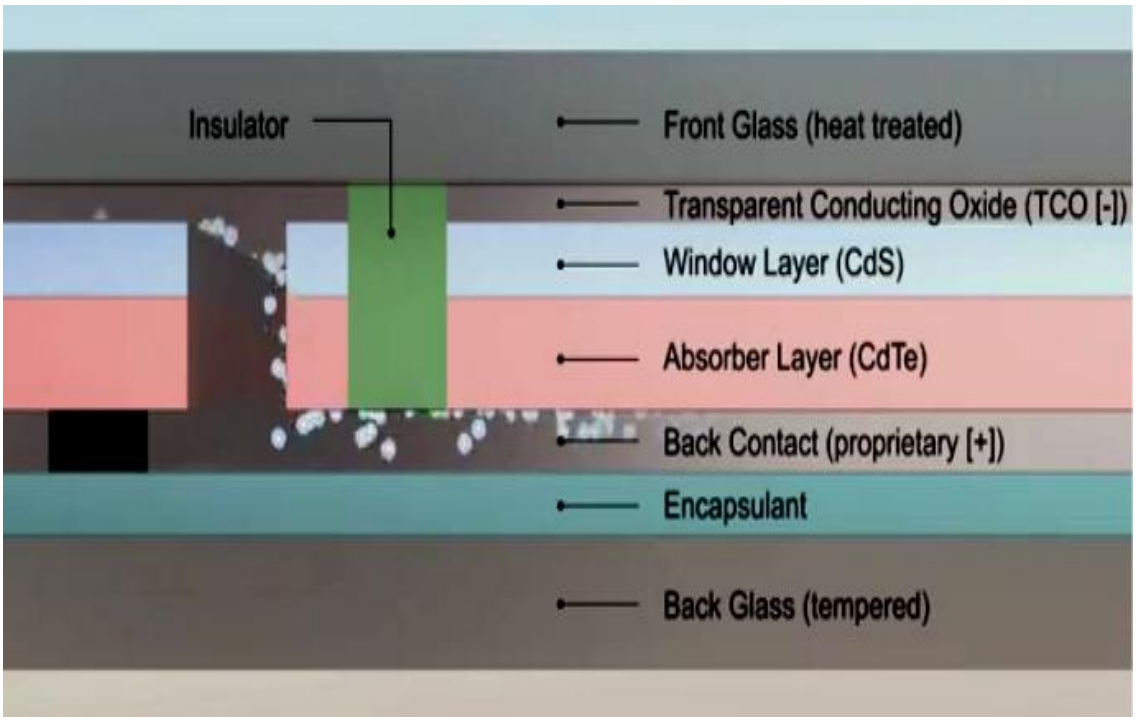

Figure 1.8 First Solar CdTe structure.

Source: http://www.firstsolar.com/

2. Good match with sunlight

Cadmium telluride absorbs sunlight at close to the ideal wavelength, capturing energy at shorter wavelengths than silicon panels. CdTe PV modules are reportedly at the higher end of the reliability spectrum.

3. Cadmium is abundant

Cadmium is abundant, produced as a by-product of other important industrial metals such as zinc. Besides, the price is much cheaper than the silicon prices.

4. The efficiency of CdTe increase fast

The new record of lab efficiency increase to 22.1% by First Solar and the panel efficiency reach 18.2% by First Solar. Both the solar cell and solar panel efficiency increase about 3%

within 2 years. The efficiency increase of CdTe efficiency in recent years is “unrivaled” in the solar PV industry.

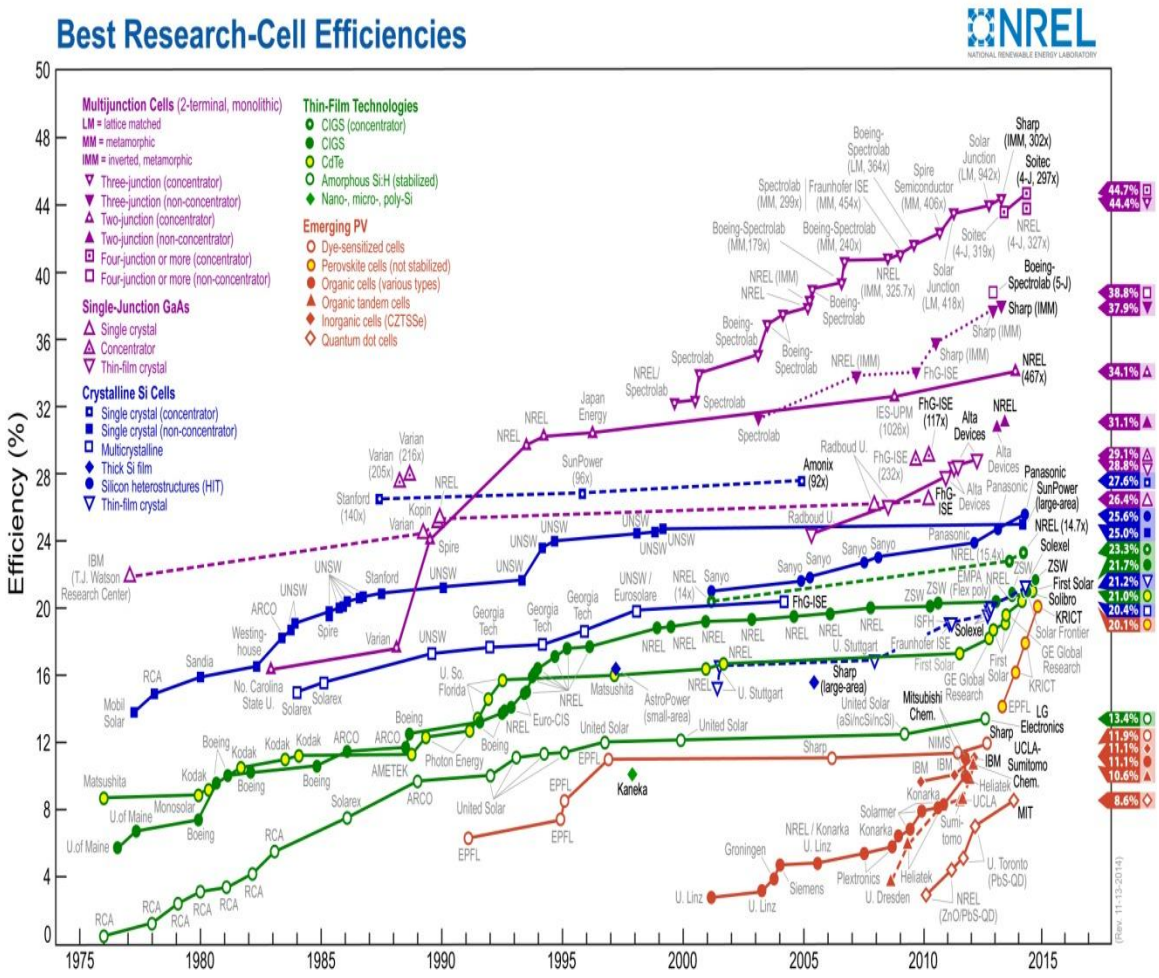

Figure 1.9 Best research-cell efficiencies.

Source: http://energyinformative.org/nrel-efficiency-record-two-junction-solar-cell

Figure 1.9 shows steady efficiency growth over the years for all the different solar cell technologies. The module efficiency numbers are lower than the efficiency in the lab, but those lab-modules might be achieved in the near future. From Figure 1.9, we can find the efficiency increase great in past 10 years, especially for the thin film solar cell efficiency.

Table 1.2 I–V Parameters for Record Cells

Year	Team	Efficiency	Voc	Jsc	FF
1993	USF	15.8%	843	25.1	74.5%
1997	Matsushlta	16.0%	840	26,1	73.1%
2001	NREL	16.4%	848	25.9	74.5%
2001	NREL	16.4%	845	26.1	75.5%
2011	FSLR	17.3%	845	27.0	75.8%
2012	GE	18.3%	857	27.0	79.0%
2012	FSLR	18.7%	852	28.6	76.7%
2013	FSLR	19.0%	872	28.0	78.0%
2016	FSLR	22.1%	925	30	80%

Table 1.2 indicates the fast development of CdTe in the past 20 years. Optical losses have been minimized to a great degree. An overlay of the quantum efficiency (QE) curves of the 16.7%, 17.3%, 18.3%, 18.7% is shown in Figure 1.10. CdS window layer loss has been nearly eliminated leading to relatively square QEs. First Solar has been able to demonstrate a significant improvement in Voc to 903 mV. The newly identified boundaries to be discovered for CdTe cell efficiency should be a Voc of 925 mV, Jsc of 30 mA/cm^2, and an FF near 80%, which equate to a cell efficiency of 22.1%.

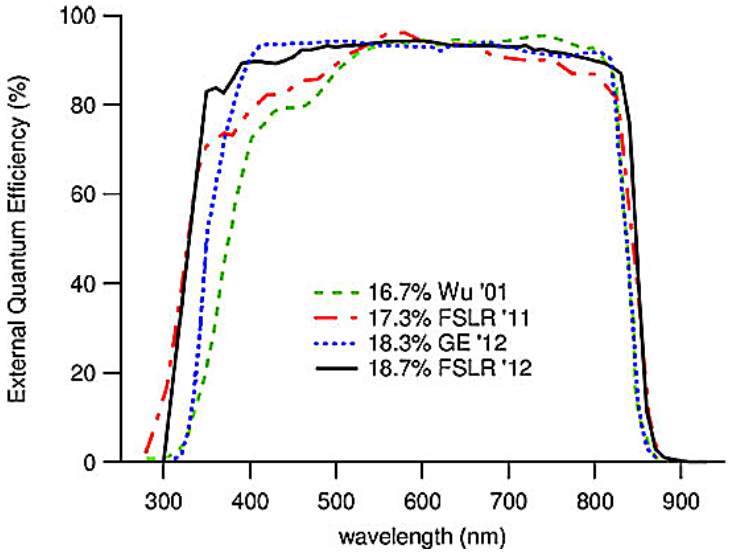

Figure 1.10 Quantum efficiency (QE) curves of the last four cell records.

Source: http://www.firstsolar.com/

First Solar's certified record cell characteristics and the module designs described in Figure 1.11. It shows the results given the assumptions of the module design characteristics as described above.

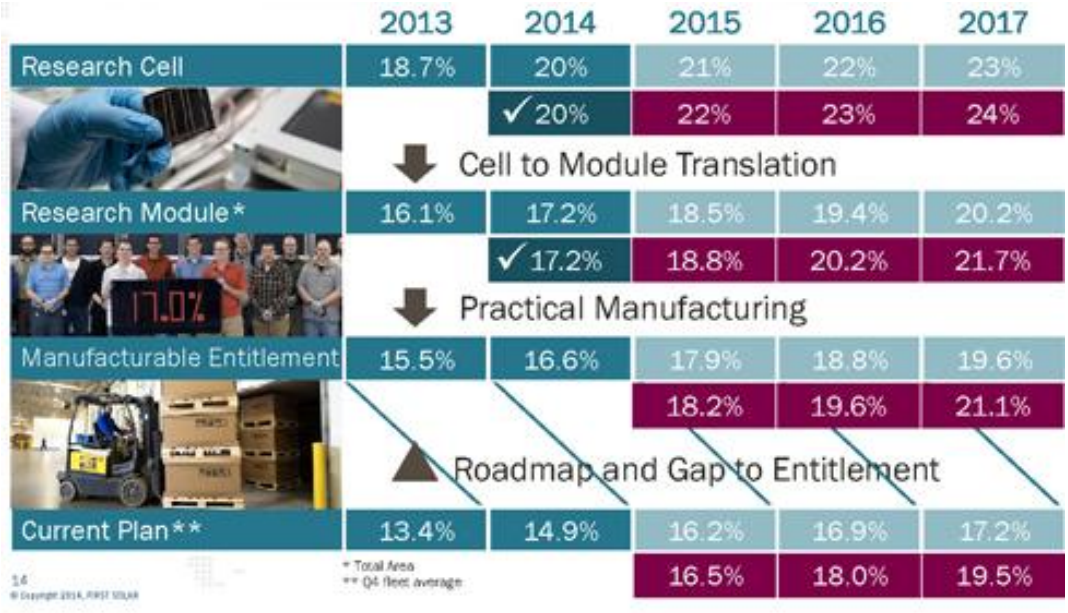

Figure 1.11 First Solar CdTe solar cell efficiency roadmap.

Source: http://www.firstsolar.com/

5. Significantly higher temperature resistance

In addition to the highest theoretical efficiency and lowest inherent manufacturing costs, CdTe thin film module technology has a significant performance advantage compared to conventional crystalline silicon solar modules (Figure 1.12).

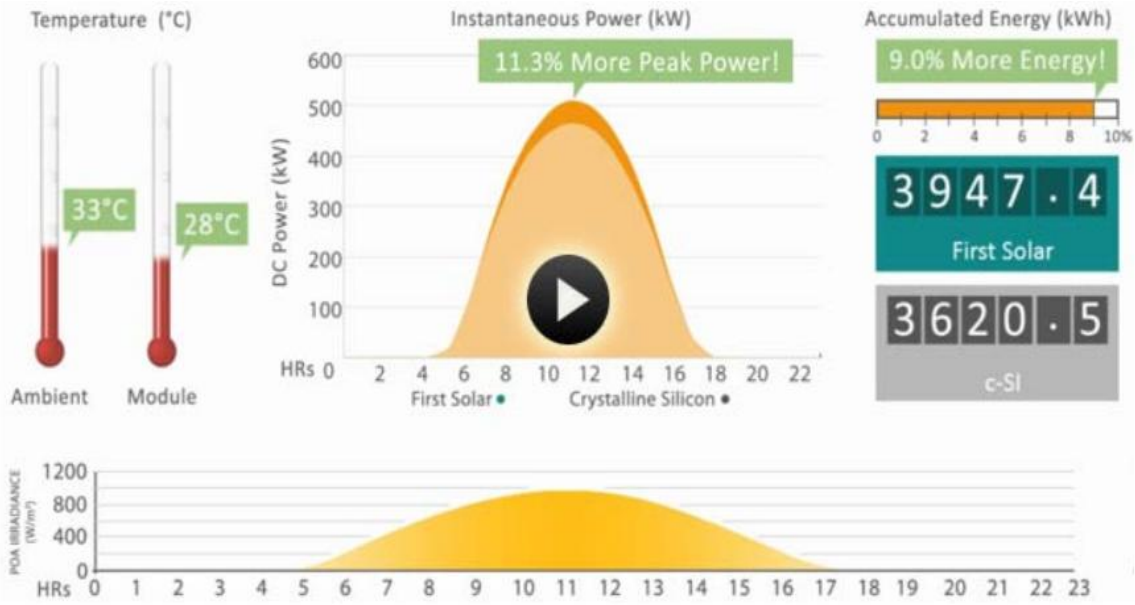

Figure 1.12 Performance comparison between CdTe and crystalline silicon.

Source: http://www.firstsolar.com/en/Technologies-and-Capabilities/PV-Modules/First-Solar-Series-3-Black-Module/CdTe-Technology.aspx

Based on actual data, the First Solar system produced 11.3% more peak power and 9% more energy (kWh) than the crystalline silicon system. CdTe thin-film solar panels lose less efficiency in high temperatures and make them more competitive in hot climates like deserts.

6. Fastest energy payback and carbon reductions

CdTe thin film module technology produces the smallest carbon dioxide in all PV technology (Figure 1.13). CdTe thin film module technology also has the fastest energy payback time in the industry (less than 1 year).

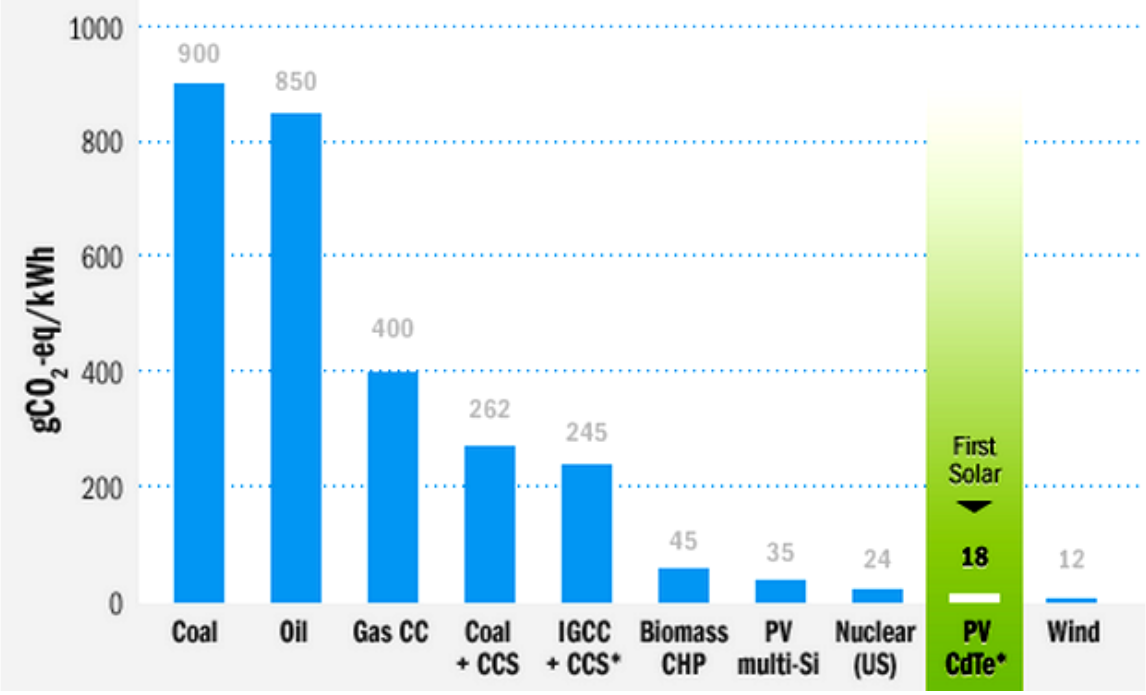

Figure 1.13 CO2 emissions comparison for different energy.

Source: http://www.firstsolar.com

1.4 Structure of CdS/CdTe Solar Cell

The CdS/CdTe solar cell is composed of four main layers (Figure 1.14) that are:

1. Transparent Conducting Oxide (TCO) as a front contact;

2. CdS film as window layer;

3. CdTe film which is the absorber layer;

4. The back contact on top of CdTe.

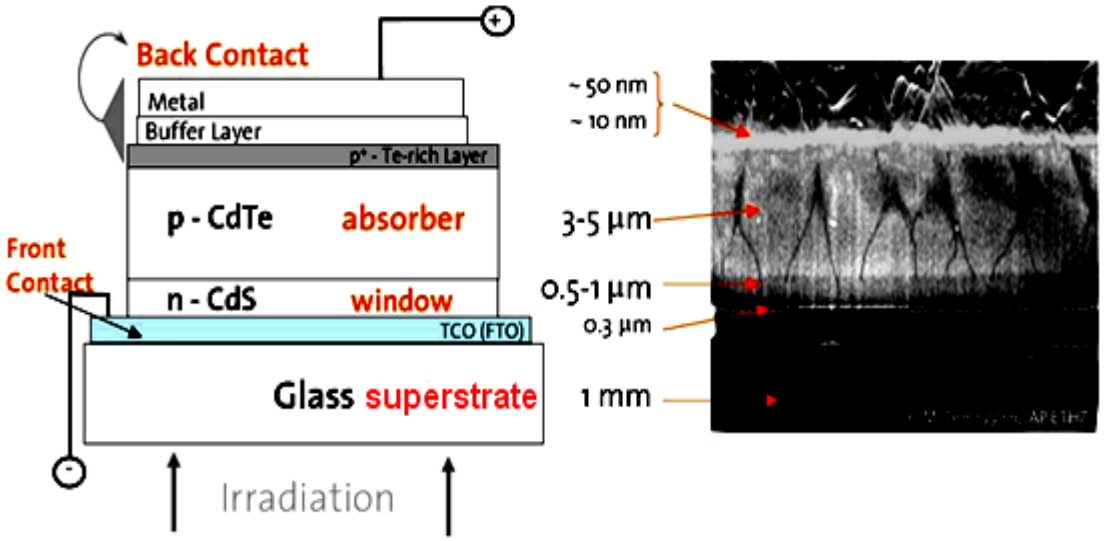

Figure 1.14 Structure of CdS/CdTe solar cell.

Source: (Lukas Kranz, et al., 2013)

The functions of the different layers are as follows:

Transparent Conducting Oxide (TCO) Coated Glass: TCOs are thin films of metal oxides that exhibit both optical transparency and electrical conductivity. It is on top of the glass. The solar cell is deposited on a 2-4 mm substrate of ordinary window glass, because it is transparent, strong and cheap. It protects the active layers from the environment and provides the device's mechanical strength. Some glass may have an anti-reflective coating to enhance its optical properties. The TCO is between the glass and the CdS layer for CdS/CdTe solar cell. The major TCOs include tin oxide (SnO_2), indium oxide (In_2O_3), indium tin oxide (ITO), and zinc oxide (ZnO) (Table 1.3). ITO has been the dominant TCO, but the price of indium metal has varied over the range of $100-1000/kg in the last 15 years. ITO is widely used because of its electrical conductivity, optical transparency and the ease to be deposited as a thin film.

Table 1.3 Common TCO Materials

Main Component	Dopant
Tin Oxide (SnO_2)	Fluorine (F)
	Antimony (Sb)
Indium Oxide (In_2O_3)	Tin (Sn)
	Zinc (Zn)
Zinc Oxide (ZnO)	Aluminum (Al)
	Boron (B)
	Gallium (Ga)

Source: https://www.materialsnet.com.tw/eng/TCO.html

Table 1.4 shows the record of high carrier mobility of certain TCOs.

Table 1.4 Record High Carrier Mobility of Certain TCOs

TCO	Abbreviation	μ ($cm^2/V\,s$)	ρ ($10^{-4}\,\Omega\,cm$)
ZnO:Al	AZO	47.6	0.85
ZnO:Ga	GZO	30.9	0.81
ZnO:Al		44.2	3.8
ZnO:Al		49.5	2.9
ZnO:Al		52	7.1
ZnO:Al			2.0
ZnO		120	4.6
In_2O_3:Ti	ITiO	105	1.9
In_2O_3:Ti		159	0.9
In_2O_3:Mo	IMO	130	1.7
In_2O_3:Mo		70.2	1.6
In_2O_3:Sn	ITO	103	0.44
In_2O_3:Sn		42	0.77
In_2O_3: H	IO:H	140	2.9
SnO_2:F	FTO	70	7.0
TiO_2:Nb	TNO	22	2.4
Cd_2SnO_4	CTO	68	
a-Zn_2SnO_4	ZTO	32	57

Source: (Alan E. Delahoy, et al., 2011)

In those TCO materials, Indium tin oxide is usually acts as the front contact to the device. However, due to the high temperature at which CdTe is deposited and/or treated in presence of Cl, some In can diffuse from the ITO into the subsequent deposited layers. In order to avoid the In diffusion, a buffer layer such as SnO_2 or ZnO is interposed between ITO and CdS. A buffer layer thickness of 100-200nm can be sufficient to hinder the In-diffusion. The buffer layer is also call as HRT (High Resistive Transparent). The HRT materials were summarized in Table 1.5.

Table 1.5 Influence of HRT to the Efficiency of Solar Cell

TCO	Buffer (nm/type)	d_f (CdS) (nm)	V_{oc} (mV)	J_{sc} (mA/cm^2)	FF (%)	Eff (%)
ITO	None	0	440	25.0	47	5.0
ITO	None	50	590	23.9	47	6.6
ITO	None	110	790	20.3	70	11.3
ITO	$20In_2O_3$	30	652	23.9	52	8.1
ITO	$50In_2O_3$	<20	754	26.2	60	11.9
ITO	$50In_2O_3$	100	790	21.8	70	12.0
ITO	$50Ga_2O_3$	40	760	24.0	62	11.4
SnO_2	None	0	440	18.0	46	3.5
SnO_2	None	90	753	22.8	63	10.8
SnO_2	$50SnO_2$	<20	790	26.0	68	13.8
ITO	None	$30Cd_{0.95}Zn_{0.05}S$	750	23.2	62	10.8

Source: (Brahim Dahmani, et al.,2003)

The High Resistive Transparent (HRT) layers (Table 1.5) in CdTe solar cells include SnO_2, Al_2O_3, $ZnSnO_4$ et al. It improves the efficiency of CdTe solar cell.

Cadmium Sulphide (CdS) Window Layer: The polycrystalline CdS layer is n-type doped and provides one half of the p-n junction. Being a wide band gap material (Eg ~ 2.4 eV at 300K), it is transparent down to wavelengths of around 515 nm. Below that

wavelength, some of the light will still pass through to the CdTe, due the thinness of the CdS layer (~ 100 nm).

When the CdS film thickness has been reduced, the absorption loss also reduces, which improves mainly Jsc and η. Figure 1.15 shows the effects of CdS layer reduction on the cell of Jsc, Voc, FF and η. Figure 1.15 shows that Jsc improved greatly with reduced CdS layer but Voc was not affected and FF was affected a little bit. To get higher efficiency CdTe solar cells, it is better to keep the CdS thickness to about 50-80nm.

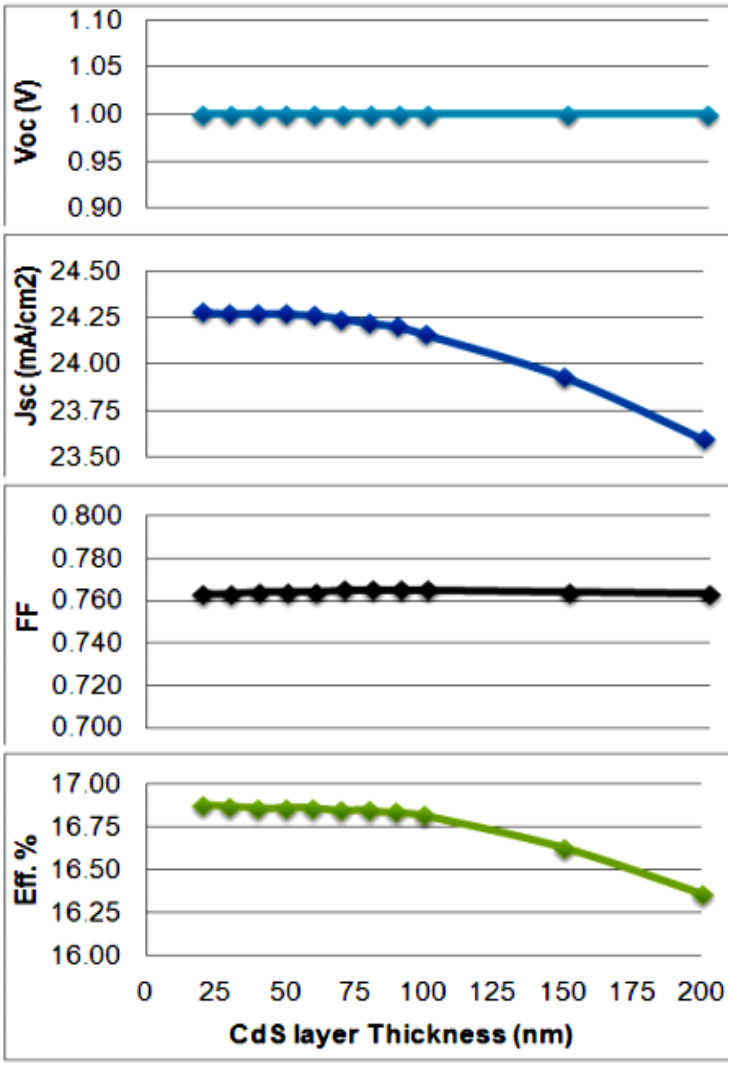

Figure 1.15 Effect of CdS film thickness on cell output parameters.

Source: (M. A. Matin, et al., 2009)

Cadmium Telluride Absorber Layer: The CdTe layer is p-type doped. Its energy gap (1.50-1.52 eV) is ideally suited to the solar spectrum. It acts as an efficient absorber and is used as the p side of the junction. The thickness of this layer is in the range of 1 - 6 μm. It is clear from the Figure 1.16 that all the solar cell output parameters are almost constant above the CdTe thickness of 2 μm.

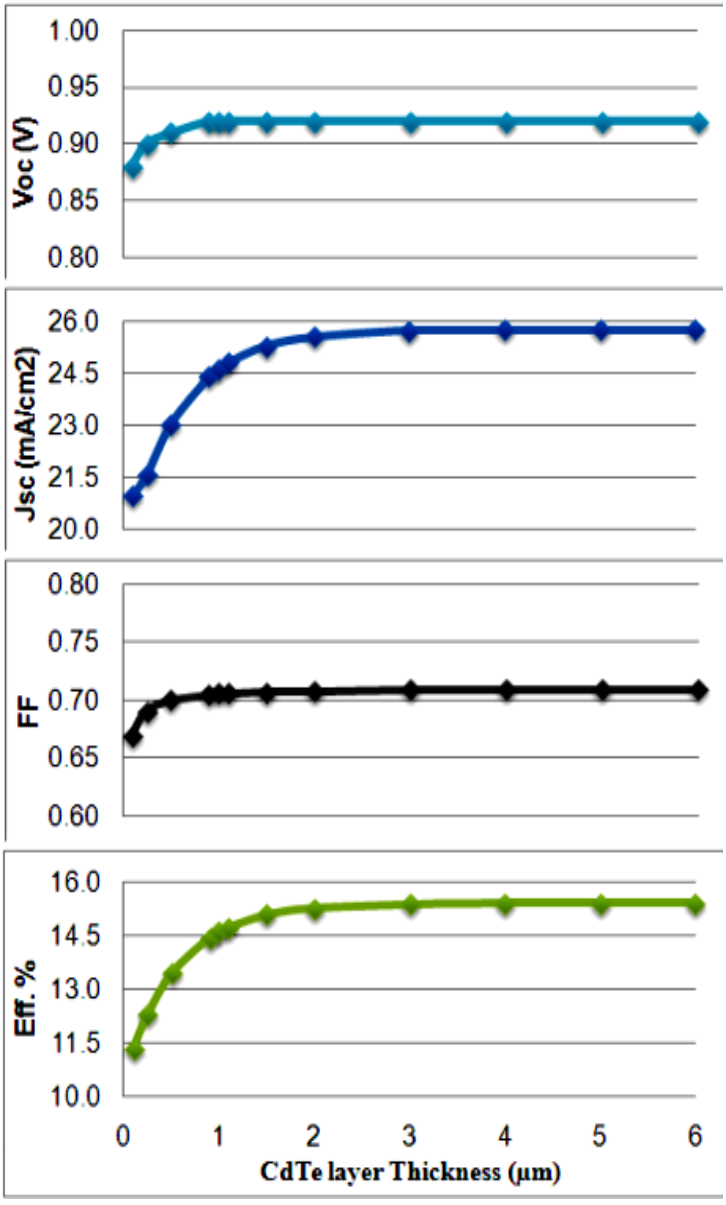

Figure 1.16 Effect of CdTe film thicknesses on cell parameters.

Source: (M. A. MATIN, et al., 2009)

Back Contact: The 'back contact' on the CdTe is very important because it influences the efficiency and long-term stability of solar cells. The development of an efficient and long-term stable electrical contact on p-type CdTe is very difficult because of both the high electron affinity and energy band-gap of CdTe. Gold was used in the research lab due to its high conductivity. Industrially, contacts are a closely guarded secret. Most labs and probably as many industries use copper telluride compositions as the back surface of the CdTe.

1.5 Pilot Line for CdTe Modules

1.5.1 CNBM CTF Solar

CTF was founded by the founding fathers Dr. Dieter Bonnet. He created the world's first functioning cadmium telluride (CdTe) solar cell in 1969. In the 1990s, Bonnet and his co-founders Dr. Michael Harr and Karl-Heinz Fischer pioneered the commercial production of CdTe modules (Figure 1.17) by constructing the first factory in Germany. Later on, the know-how and the experience in designing and implementing of solar factories were transferred to CTF Solar Gmbh.

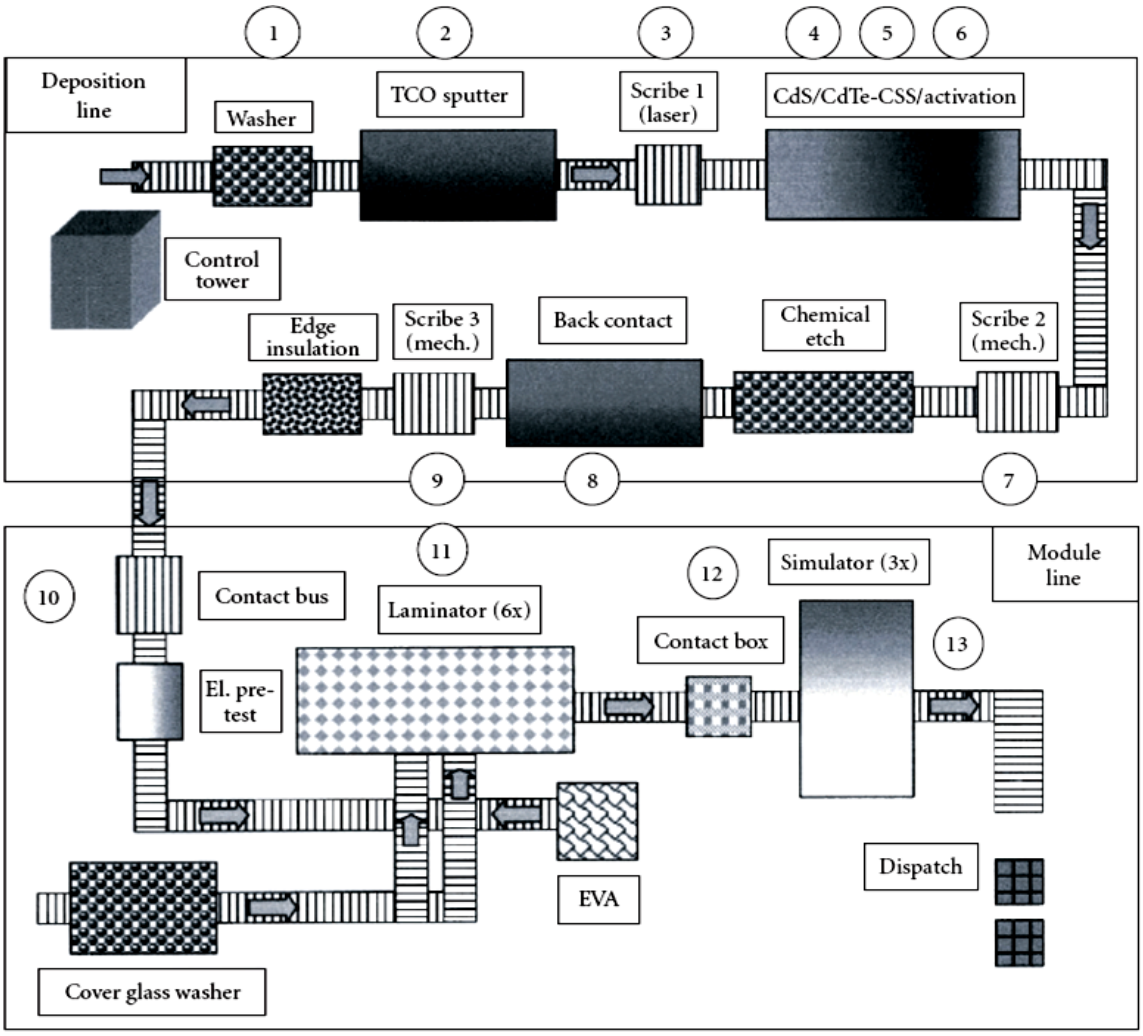

Figure 1.17 Schematic of CTF production line for CdTe solar modules.

Source: (Michael Powalla et al. 2007)

In 2008, the company was acquired by Roth & Rau Group with the purpose to develop and sell turnkey production lines for the production of CdTe solar modules. In February 2011, Roth & Rau has sold its Roth & Rau CTF Solar GmbH (CTF) subsidiary off to CTIEC (China Triumph International Engineering Corporation), a company of the Beijing-based CNBM Group (China National Building Materials).

Table 1.6 shows the each step for the production of CdTe solar modules. Figure 1.17 illustrates a module processing line like the one used for CdTe module production. The numbers relate to Table 1.6 which describes the processing steps for CdTe modules.

Table 1.6 Processing Steps for the Production of CdTe Thin-Film Solar Modules

Step no.	CdTe
1	Cleaning of glass superstrate
2	Deposition of front contact (SnO_2, etc.)
3	Scribing of front contact
4	Deposition of n-CdS film
5	Deposition of p-CdTe film
6	"Activation"
7	Scribing of semiconductor film
8	Deposition of back contact
9	Scribing of back contact
10	Attachment of contact-bus structure
11	Lamination with back glass plate
12	Contact box attachment
13	Measurement, classification

Source: http://www.ctf-solar.com/

1.5.2 Abound Solar

In 1980, Abound Solar's founders began do research in CdTe thin-film deposition. In 1991, W.S. Sampath, a professor at Colorado State University, patented a process for low-cost metal deposition within a vacuum. By 1998, the team had developed a pilot production process featuring an inline, single-vacuum semiconductor deposition tool. By

2004, the founding team had scaled up the technology glass panels of 16 by 16 inches in size. In 2006, AVA Solar, Inc (Abound's former name) was formed with private funding from local angel investors to commercialize the technology. In 2010, Abound received a $400 million loan from the U.S. government. In 2012, Abound Solar announced it suspended operations and file for bankruptcy.

Abound Solar produced CdTe thin-film solar modules by CSS developed at Colorado State University.

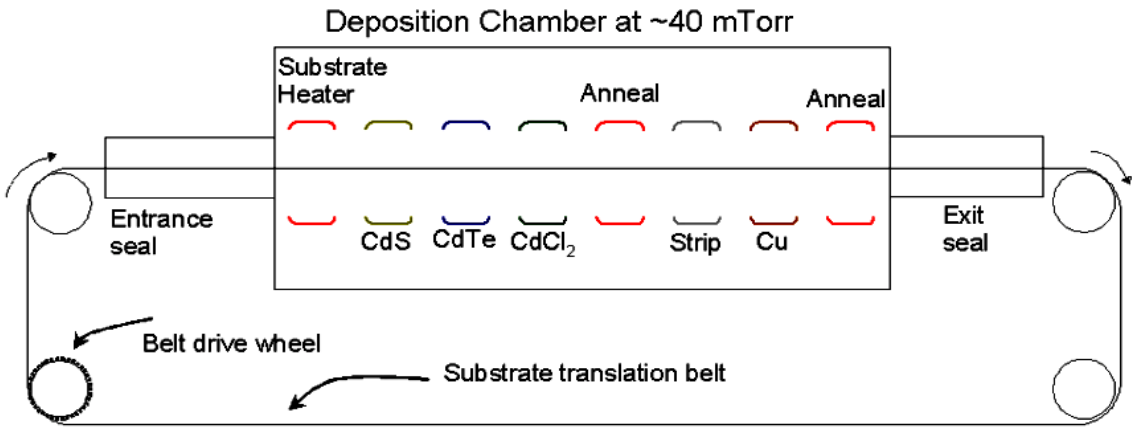

Figure 1.18 Schematic of Abound production line for CdTe solar modules.

Source: https://en.wikipedia.org/wiki/Abound_Solar

Figure 1.18 is the production line of Abound. The substrates are loaded onto a continuous belt. Within the chamber, a different processing station waits the substrate at each of the standing positions. The first station is a substrate heater, which brings the glass to 600 ◦C in two minutes. CdS and CdTe depositions occur at the next two stations, followed by a $CdCl_2$ deposition and then anneal. A Cu-containing compound is then evaporated onto the film stack and annealed for two minutes at 200 ◦C. After that, a

graphite layer (~2 μm) is spray-deposited onto the film-stack, followed by an electrodag contact layer (~100 μm), which contains Ni as the electrode metal.

1.5.3 PrimeStar Solar

PrimeStar Solar was founded in 2006. The goal is to make large scale, clean, renewable, cost competitive CdTe solar panel which are much cheaper than conventional crystalline silicon PV. PrimeStar Solar has an experienced and competitive team in thin film PV and deposition equipment. Its products are used in solar PV power plant, rooftop and ground mounted applications and designed to enable economically competitive large scale solar PV power plants.

In 2008, PrimeStar Solar, Inc. operates as a subsidiary of GE Energy Management and was acquired by GE Energy in 2011. In August 2013, GE announced an IP sharing and commercial partnership with First Solar. At the same time, GE announced the end of its CdTe solar manufacturing operations.

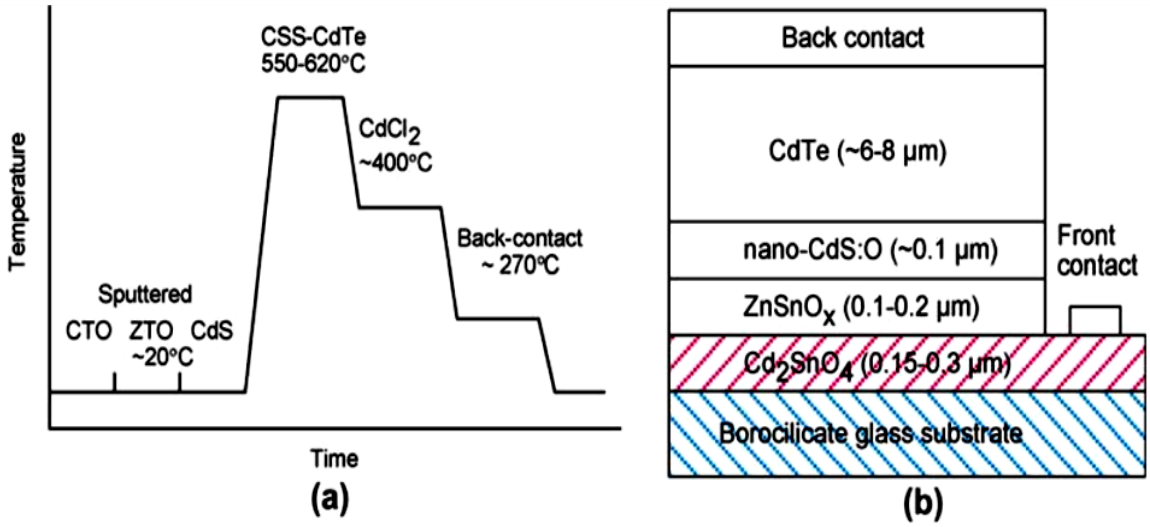

Figure 1.19 (a)Schematic of PrimeStar production line for CdTe solar modules.
(b) A borosilicate glass/CTO/ZTO/nano-CdS:O/CdTe device structure.

Source: https://en.wikipedia.org/wiki/PrimeStar

GE's PrimeStar CdTe technology use CSS process (Figure 1.19) while First Solar use vapor transport deposition (VTD). Using this deposition technology, GE had achieved a CdTe cell efficiency record of 19.6% in 2013. In February of 2014, First Solar hit a world record CdTe cell efficiency record of 20.4%, as verified by NREL. This beat the GE record and was a big improvement on its previous record of 18.3% over 12 months earlier.

The drawback of CSS is that it required the high quality and expensive glass to deposit. After the Abound bankrupt, Prime Star learned from First Solar and improved their manufacture process to Figure 1.20.

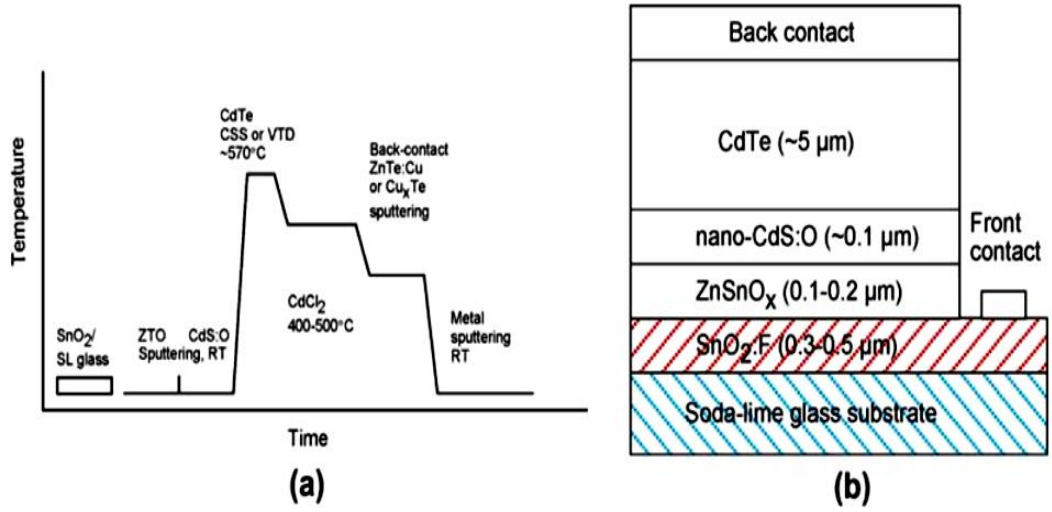

Figure 1.20 (a) Improved schematic of PrimeStar novel manufacturing process.
(b) A soda-lime glass/SnO2/ZTO/nano-CdS:O/CdTe device structure.

Source: http://www.primestaraviation.com/

1.5.4 First Solar

First Solar, Inc. is the number one thin film company. Their CdTe solar panels is the most competitive in the market.

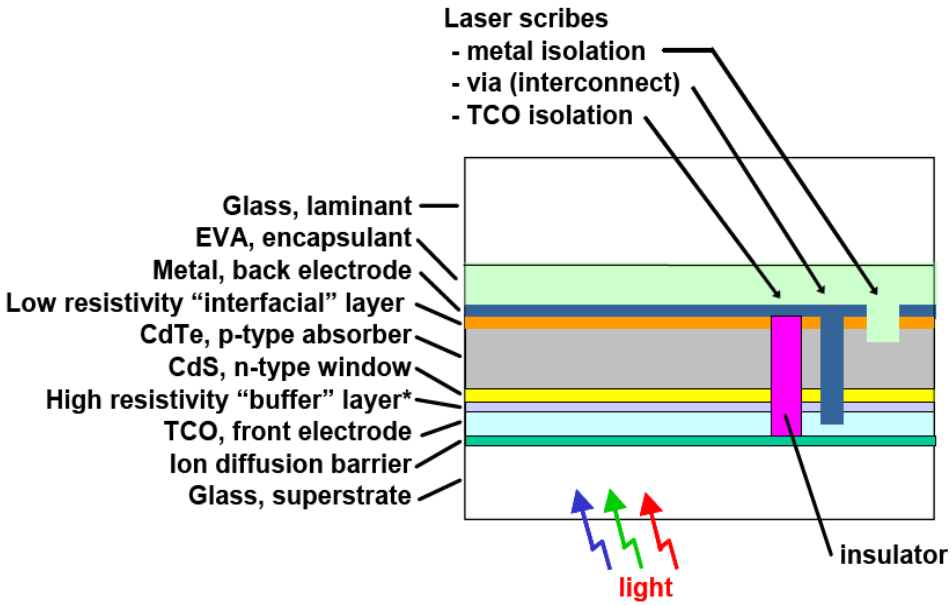

Figure 1.21 Structure of First Solar CdTe panels.

Source: http://photovoltaicell.com/n-type-photovoltaic-cell/

In 2009, First Solar became the first solar panel manufacturing company to lower its manufacturing cost to $1 per watt and produced CdTe panels (Firgure 1.21) with an efficiency of about 14 percent at a reported cost of 59 cents per watt in 2013.

First Solar manufactures CdTe PV modules and created a world record-breaking cell with 22.1% efficiency in the laboratory in February 2016 and a world record-breaking PV module with 18.2% efficiency in Sep. 2015. Figure 1.22 shows the each step for First Solar CdTe solar panel production.

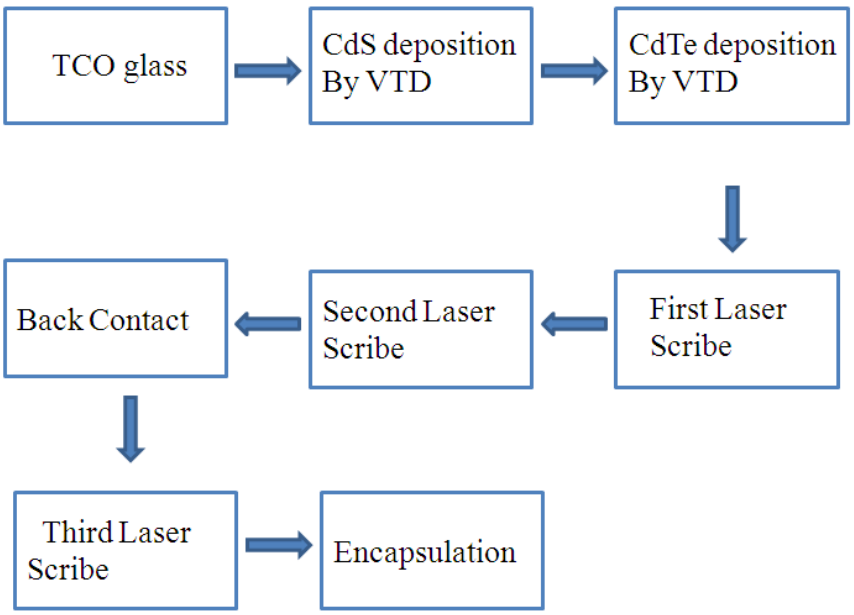

Figure 1.22 CdTe solar cell process by First Solar.

First Solar uses vapor transport deposition (VTD) to deposite CdS and CdTe layers in TCO glass. It applies a proprietary back contact and cell series interconnect to the device structure. VTD (Figure 1.23) has the attractive feature of decoupling the source and substrate environments. The manufacturability of this process has been demonstrated by First Solar using moving substrates with high throughput.

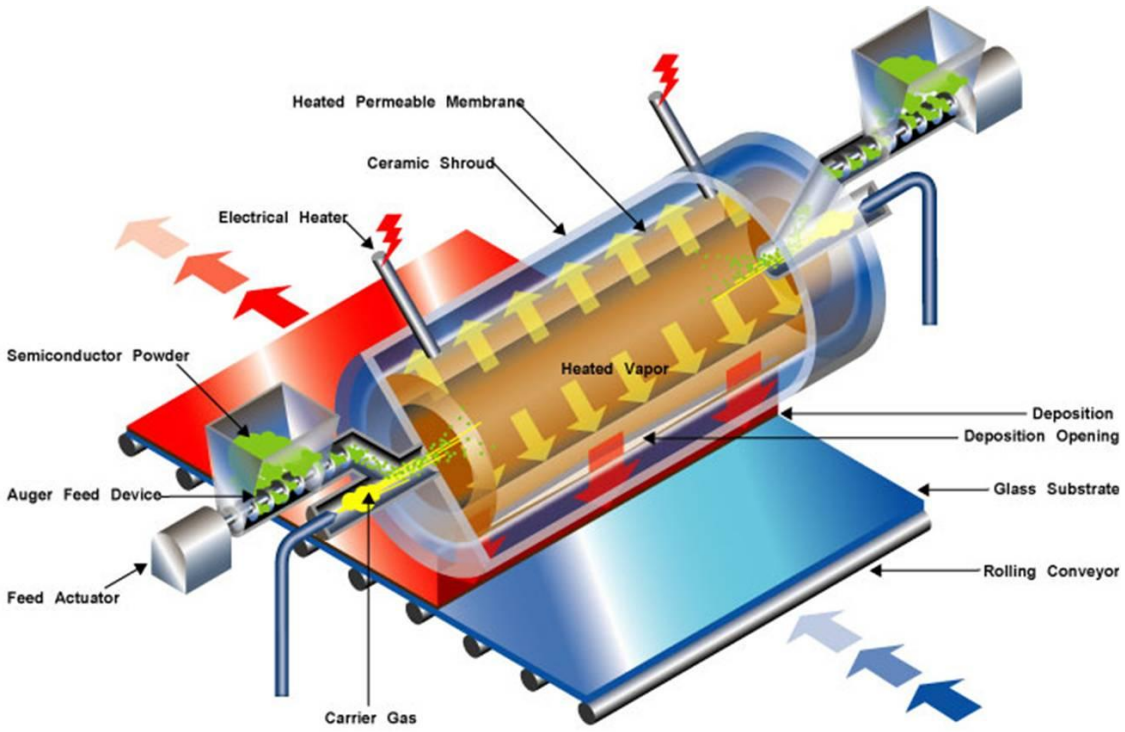

Figure 1.23 VTD structure of First Solar.

Source: http://www.firstsolar.com

CHAPTER 2

DEPOSITION OF HIGH EFFICIENT CDTE SOLAR CELL

2.1 Introduction

CdTe solar cells are one of the most promising candidates for photovoltaic energy conversion because of the great potential of low cost, high efficiency, reliable and stable thin film solar cell fabrication. First, the cell is produced from polycrystalline materials and glass, which are potentially much cheaper than other counter parts. Second, the polycrystalline layers of a CdTe solar cell can be deposited using a variety of different low cost techniques. Third, CdTe has a high absorption coefficient. And finally, CdTe has a direct optical band-gap of 1.50-1.52 eV which is very close to the optimum band-gap for solar cells. It is the only thin film technology with lower costs than conventional solar cells made of crystalline silicon.

CdTe PV is a solution to key ecological issues including climate change, energy security, and water scarcity because CdTe PV has the smallest carbon footprint, lowest water use and shortest energy payback time of all solar technologies. CdTe's short energy payback time is less than a year. It enables for faster carbon reductions without short-term energy deficits. With about 5 percent of worldwide PV production, CdTe technology accounted for more than half of the thin film market in 2013. A prominent manufacturer of CdTe thin film technology is the company First Solar, based in Tempe, Arizona.

In this chapter, we introduce each step of CdTe deposition process and our experiment to get 13.7% solar cell and the methods to improve the efficiency.

2.2 Preparation of CdS/CdTe Solar Cell

The CdTe/CdS thin film solar cell is the most suitable to be fabricated thin films. The processes are quite simple and fast. There are five main steps to deposit the CdS/CdTe solar cell (Figure 2.1): 1, TCO deposition; 2, CdS deposition; 3, CdTe deposition; 4, $CdCl_2$ treatment; 5, back contact. For each step, they are many different methods to prepare it. We will briefly introduce the advantage of each method.

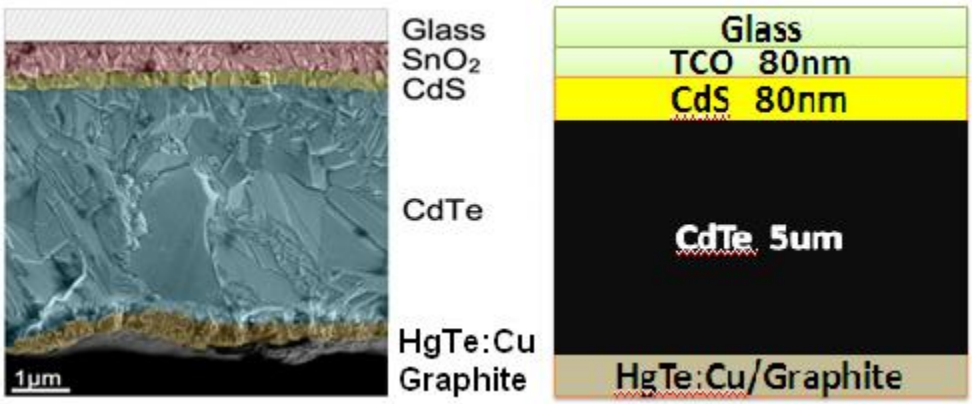

Figure 2.1 CdS/CdTe solar cell device structure.

2.2.1 Transparent Conducting Oxides (TCO) Deposition

The common TCO materials are fluorine-doped tin oxide (FTO) and indium tin oxide (ITO), which can be prepared by various techniques such as physical vapor deposition (PVD), chemical vapor deposition (CVD), direct current (DC), RF magnetron sputtering, electron beam evaporation, spray pyrolysis, and the sol-gel method. Among these, the RF magnetron sputtering method is the most compatible with the circuit processing, which can continuously produce high-quality films at a lower processing temperature. In our experiment, we brought the TCO Corning glass. The substrate is first cleaned by

sonication in a 1% solution of Liquinox soap in hot deionized (DI) water, followed by five rinses/sonication in DI water (two of which are in hot DI water).

2.2.2 CdS Deposition

Cadmium sulfide (CdS), due to its wide band gap (2.42 eV), photoconductivity, and high electron affinity, is known to be an excellent hetero junction partner for p-type cadmium telluride (CdTe). In the past few decades, several techniques such as thermal evaporation, radio frequency sputtering, physical vapor deposition, pulsed laser evaporation, molecular beam epitaxy, electro deposition, spray pyrolysis, metal organic chemical vapor deposition, successive ionic layer adsorption reaction, screen printing, close spaced vapor transport, and chemical bath deposition (CBD) have been used in the deposition of CdS thin films. Although other techniques have been used in the deposition of CdS, chemical bath deposition is known to enhance the performance of cadmium sulfide window used in solar cell applications. Besides, CBD has the advantages of being a simple, low temperature, and inexpensive large-area deposition technique.

CdS by Chemical Bath Deposition (CBD)

Deposition of CdS using CBD is based on the slow release of Cd^{2+} ions and S^{2-} ions in an aqueous alkaline bath and the subsequent condensation of these ions on substrates suitably mounted in the bath. The slow release of Cd^{2+} ions is achieved by adding a complexing agent (ligand) to the Cd salt to form some cadmium complex species which, upon dissociation, results in the release of small concentrations of Cd^{2+} ions. The S^{2-} ions are supplied by the decomposition of thiourea or sodium thiosulfate.

We cut glass to 4*6 inch. The glass is cleaned by sonication in a 1% solution of Liquinox soap in hot DI water. Then we scrub the glass and wash with acetone and methanol and rinse five times with de-ionized water. Then the substrates were dried in N_2. The cleaned substrates were placed, four at a time, in the beaker with 1200ml DI water as shown in Figure 2.2 and 2.3.

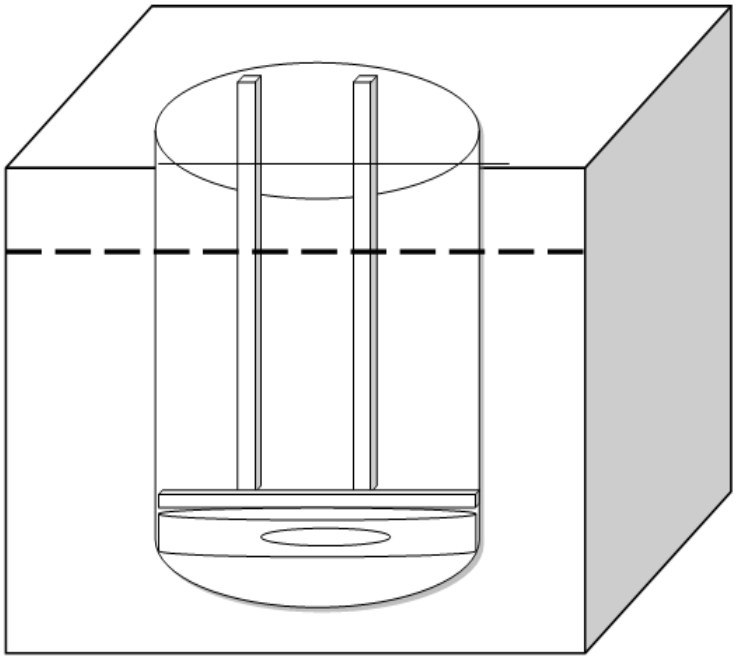

Figure 2.2 Schematic diagram of the CBD.

Then we put 5.3 ml 0.1 M Cadmium chloride ($CdCl_2$), 9.2 ml 1M Ammonium acetate (NH_4AC) and 15 ml 15M Ammonia (NH_4OH) into the beaker. After the temperature reaches 88℃, the thiourea is added by a titrator in four aliquots of 2 ml, 10 min apart. The total deposition time, after the first addition of thiourea, is 38 min. The substrates are then removed from the bath, placed in warm DI water, and given three sonications (about 2 min each) to remove loosely adhere CdS particulates. The films are then blown dry with N_2 and stored in Fluoroware containers.

Figure 2.3 Chemical bath deposition (CBD) setup.

The deposited CdS film (Figure 2.4) is about 83nm this as measured by a Dektak profiler. The CdS films are very uniform, with less than 5% deviation from center to the edge.

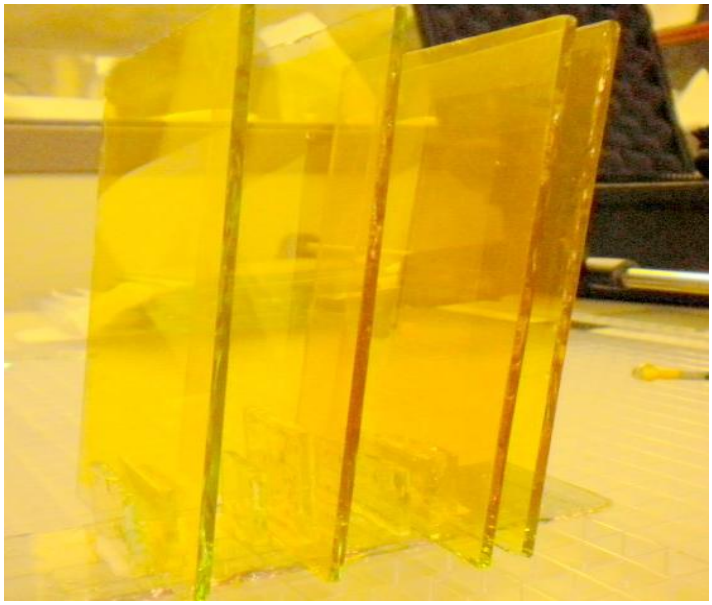

Figure 2.4 CdS this film.

CdS by Aerosol-Assisted Deposition (AAD)

CBD for industrialization is low efficiency and produce great waste water. There is a new method to produce CdS deposition by aerosol-assisted deposition method (AAD) The new method increase the production rate and greatly decrease waste water.

We cut glass to 4*6 inch. The glass is cleaned by sonication in a 1% solution of Liquinox soap in hot DI water. Then we scrub the glass and wash with acetone and methanol and rinse five times with de-ionized water. Then the substrates were dried in N_2. The cleaned substrates were placed on the heater as shown in Figure 2.5

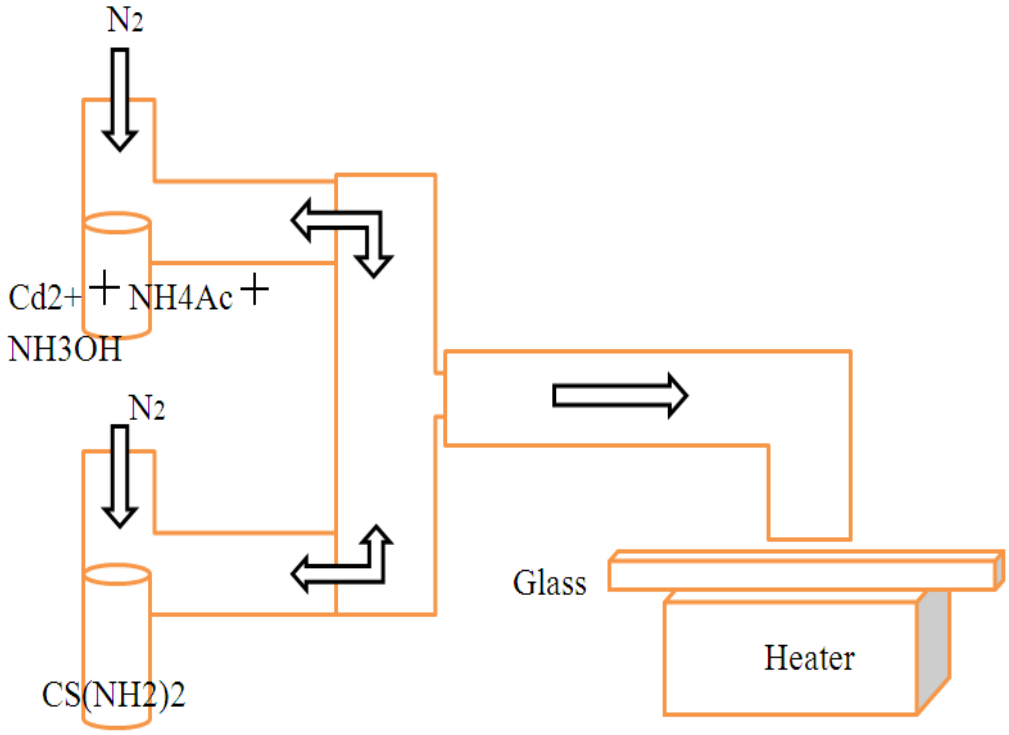

Figure 2.5 Schematic diagram of the AAD.

Then we put 5.3 ml 0.1 M Cadmium chloride ($CdCl_2$), 9.2 ml 1M Ammonium acetate (NH_4AC) and 15 ml 15M Ammonia (NH_4OH) into one beaker and put the

thiourea into the other beaker (Figure 2.6). Then we use the N_2 gas to carry them to the glass. The Total deposition is about 30 minutes and we get very thin film CdS.

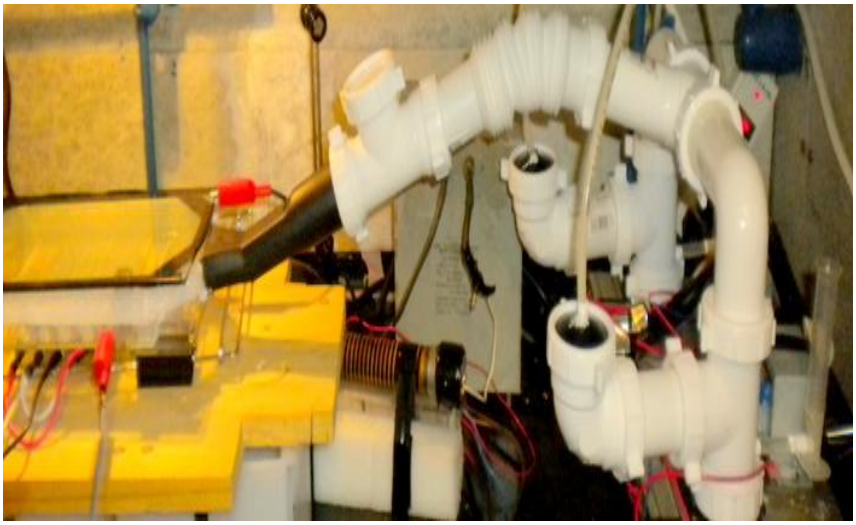

Figure 2.6 Aerosol-Assisted Deposition setup.

The mechanism of AAD of CdS deposition is shown in Figure 2.7. The Cd^{2+} ions combine with NH3 and form $Cd(NH_3)_4^{2+}$ which adsorb on the glass and gain energy to become active $Cd(NH_3)_4^{2+}$. $CS(NH_2)_2$ from another beaker was also absorb on the glass and gain energy to become active $CS(NH_2)_2$. Both active $Cd(NH_3)_4^{2+}$ and active $CS(NH_2)_2$ move around the glass and react to become CdS. CdS will stick on the glass and become very stable.

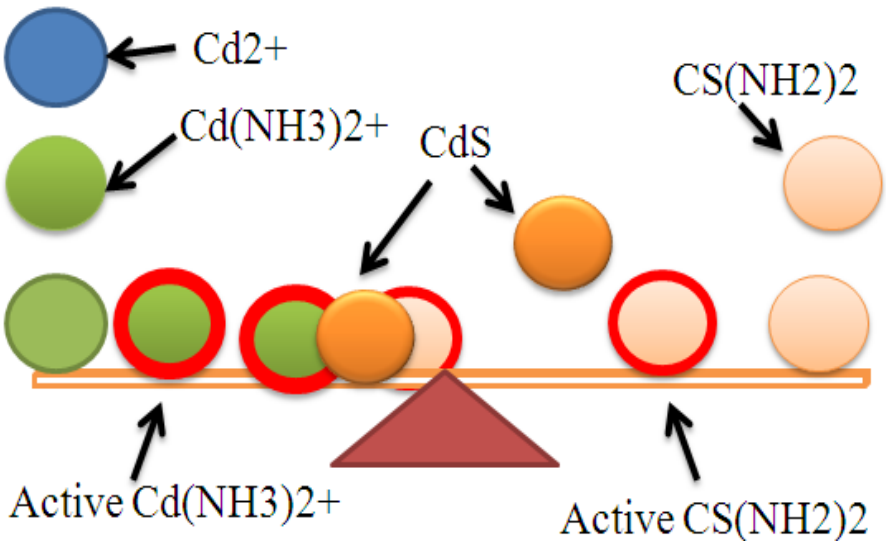

Figure 2.7 Mechanism of AAD.

2.2.3 CdTe Deposition

The CdTe film is deposited by a process such as close spaced sublimation, screen printing, spraying, electrodeposition, atomic layer epitaxy, physical vapor deposition, sputtering, chemical vapor deposition, molecular beam epitaxy, or laser ablation. Among those methods, the most popular one are closed space sublimation (CSS) and vapour transport deposition (VTD). For different methods, the substrate temperatures are also different, from 80 to about 630 ℃ depending on the deposition process. The thickness of CdTe films are also from 2 to 10 μm. In Figure 2.8, we introduce the difference between the two methods. It has widely been employed to deposit CdTe thin films for solar cells: 1, Closed Space Sublimation; 2, Vapour Transport Deposition. In our experiment, we use the CSS to deposit the CdTe.

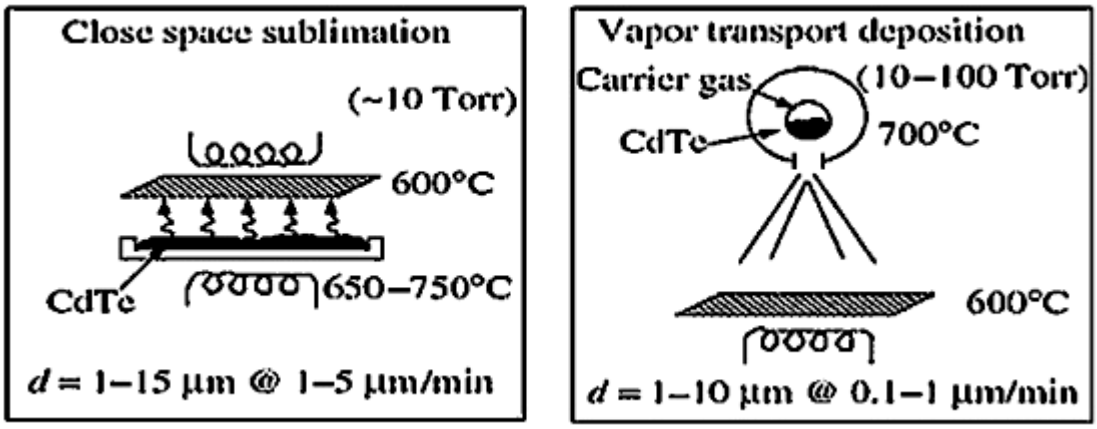

Figure 2.8 CSS and VTD system.

Source: (RC Powell, et al., 1998)

CSS of CdTe is based on the principle of reversible dissociation of CdTe at high temperatures. The elemental gases diffuse to the substrate, which is in close proximity to the source plate. The gases recombine on the substrate, which is kept at a temperature lower than the source. The CdTe source material is supported in a holder having the same area as the substrate; the source holder and substrate cover serve as suceptors for radiative heating and conduct heat to the CdTe source and the substrate (Figure 2.9).

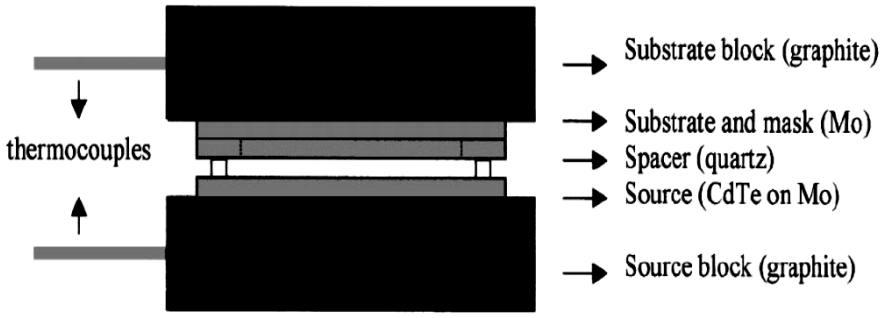

Figure 2.9 CSS deposition system.

Source: (Wagner Anacleto Pinheiro, et al., 2006)

The reactor consists of a source (CdS or CdTe) and a substrate. The source is in underside and the substrate is above. They are held by two graphite susceptors which set

one thermocouple to monitor the temperature of the source and the substrate. The aim of the CSS technique is to provide a temperature difference between the source and the substrate which enables diffusion controlled transport mechanism. An insulating spacer allows thermal isolation of the source from the substrate, so that a temperature differential can be sustained throughout the duration of the deposition. In the spacer, the ambient gas is input. It contains a nonreactive gas, such as N_2, Ar, or He. O_2 is also input with the inert gas, because a small amount of O_2 appears to be crucial for obtaining good film density and solar cell junction quality. When the deposition temperature is above 550 ℃, it exhibits nearly random orientation and normal grain size distribution. The CSS process yields the highest small-area cell performance of any process.

In our experiment, we deposit the CdTe in our CdS thin film by CBD. The CdS layer is removed from the back of the substrate by wiping with a swab dipped in concentrated HCl. The substrate is then rinsed in DI water, dipped in a dilute HCl in DI water solution (1:40 HCl : DI H_2O) for 5s, rinsed again, and dried with N_2 . The substrate is then loaded in the deposition chamber as shown in (Figure 2.10). The first stage of the deposition phase is hydrogen anneal. Annealing the substrate at 400 ℃ for 15 min in 30 torr H_2 is reported to reduce oxygen-related defects in the CdS thin film.

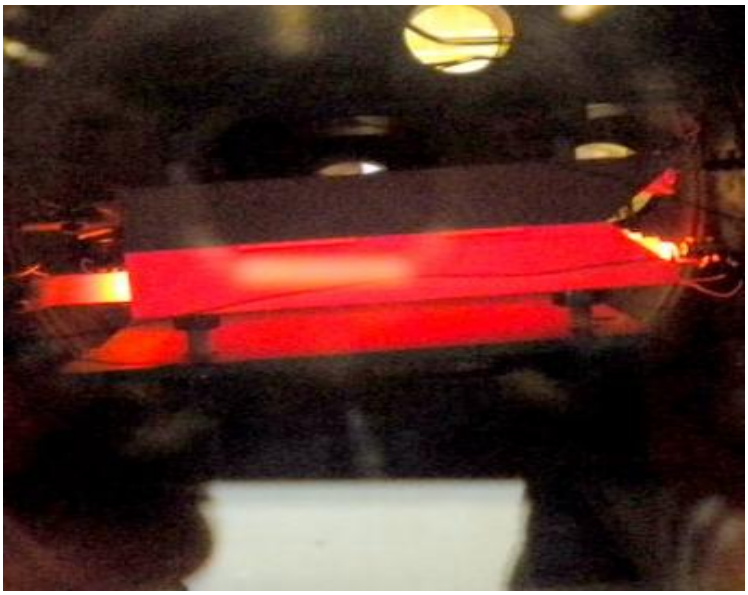

Figure 2.10 CSS deposition.

After cooling to 200℃, the CdTe deposition sequence is initiated. The chamber is pumped down to a background pressure of approximately 0.02 torr, and then He and O_2 are introduced. CSS of CdTe is based on the principle of reversible dissociation of CdTe at high temperatures. The gases recombine on the substrate, which is kept at a temperature lower than the source. Deposition process parameters include a 2 mm separation between the source and substrate, an oxygen partial pressure of 0.9 torr, and a helium partial pressure of 14.1 torr. The source and substrate are ramped together to 500℃, then the source temperature is ramped to 550℃. The substrate and source are then kept at 500℃ and 575℃, respectively, for 2 min. For these conditions, the resultant CdTe thickness is about 5-8um (Figure 2.11).

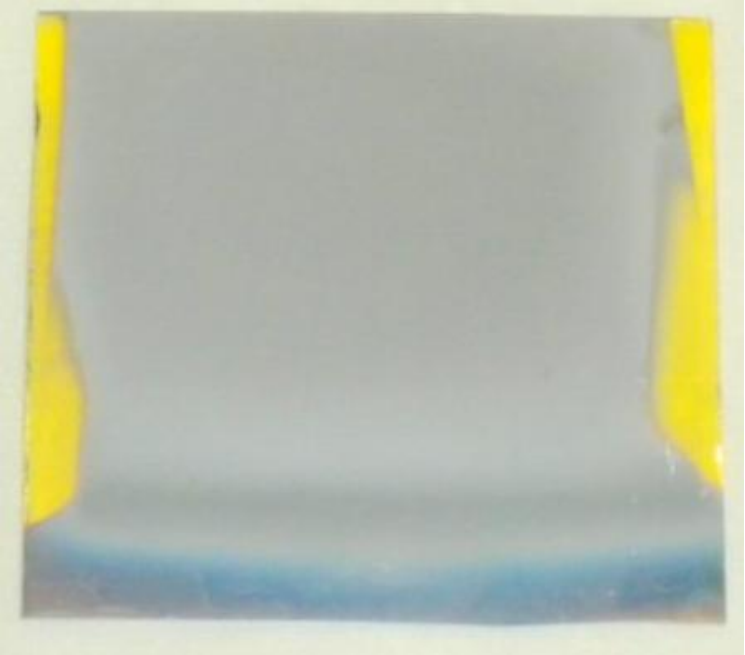

Figure 2.11 CdTe thin film by CSS.

The CdTe layer is very compact without pin-holes and voids. It is also very uniform and the grain size is about 3 um (Figure 2.12).

Figure 2.12 Microscope picture of CdTe.

Figure 2.13 shows the XRD patterns of the CdS and CdTe layers. As-deposited CdS films typically exhibit a strong cubic (111) orientation that has been reported to lie at an angle of 26.5 °(International Centre for Diffraction Data (ICDD) No. 75 – 1546, 80-0019 and 89-0440). As-deposited CdTe films also typically exhibit a strong cubic (111) orientation that has been reported to lie at an angle of 23.757 °(ICDD No. 15 – 0770).

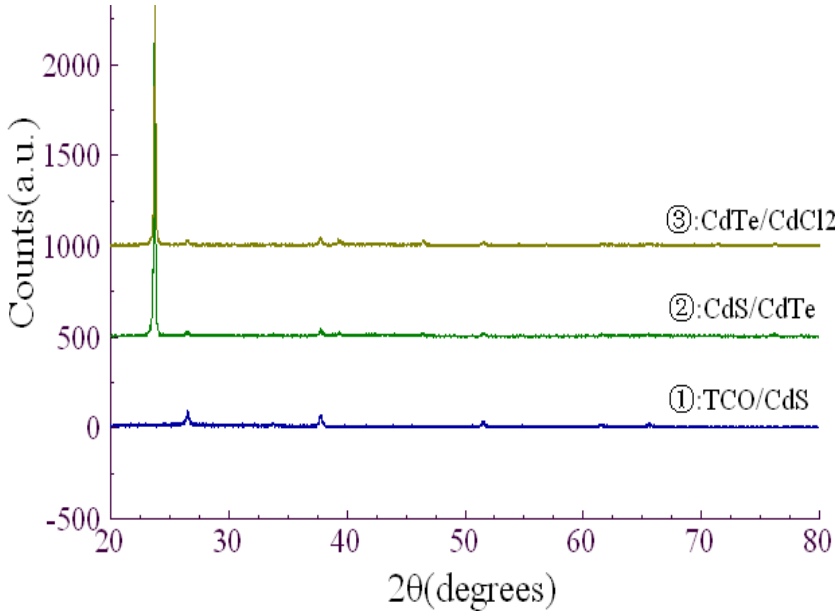

Figure 2.13 XRD of CSS CdTe thin film.

The individual crystallite grain size is determined using Scherrer's relationX-ray diffraction pattern of CdTe solar cell.

$$Mean\ Grain\ Size = \frac{S\lambda}{\beta cos\theta}$$

where S is the Scherrer constant (0.9), λ is the wavelength of the incident radiation, β is the full width at half maximum intensity (FWHM) and θ is the Bragg angle that corresponds to the peak under consideration. The FWHM exceeds upper limit of assumption which corresponds to at least 100nm. The calculated lattice constant from

(111) peak using Bragg condition is 6.496Å (2θ=23.725˚) grown on CBD CdS before $CdCl_2$ treatment and 6.489 Å (2θ=23.750˚) after the treatment.

The average grain size for 111 peak is 15nm and 16nm. It should be noticed that since 111 plane is parallel to the glass substrate. The calculate grain size is in the direction perpendicular to the glass substrate.

2.2.4 $CdCl_2$ Treatment

In CdTe solar cell, "$CdCl_2$ treatment" is the key step for great improvement of the solar efficiency. The treatment consists two parts: growth or post-growth heat treatment of CdTe layers. Post-growth heat treatment is usually carried out at temperatures in the range 350–450 ℃ for 20-60 min. This treatment drastically enhances the solar cell efficiency. The $CdCl_2$ treatment is usually applied for thin film CdTe layers grown by any large area deposition method. The $CdCl_2$ treatment is to spread a saturated solution or methanol on CdTe surface, allow the solvent to evaporate and then heat-treat the structure at high temperatures up to 450 ℃ for a selected period of time in air atmosphere.

For our experiment, the pieces are soaked in a 75%-saturated $CdCl_2$ in methanol solution (the saturated solution is 7.5 g $CdCl_2$ in 500 ml MeOH). The substrates are soaked for 15 min on a hot plate in a covered petri dish near the boiling point. After that soak, the pieces are taken out of the solution and immediately blown off with N_2. The pieces are then placed on an aluminum plate in a tube furnace that is purged with He. The furnace is then set at 360 ℃ and left on for 40 min with a flow of 100-sccm He and 25-sccm O_2 . After cooling to a maximum of 50 ℃, the pieces are rinsed in DI water to

remove any excess $CdCl_2$ while $CdCl_2$ is not typically found on the surface of the CdTe after anneal.

There are many advantages of $CdCl_2$ treatment:

1. Recrystallisation and Grain Growth

Numerous reports (Dharmadasa, I.M., et al. 2002; Green, M.A., 2013) conclude that the XRD peaks observed show recrystallisation and grain growth after $CdCl_2$ treatment. Heat treatment alone, without $CdCl_2$, also shows this trend, but the presence of $CdCl_2$ enhances the recrystallisation. This observation is widely accepted for CdTe layers consisting of small grains before post-deposition heat treatment.

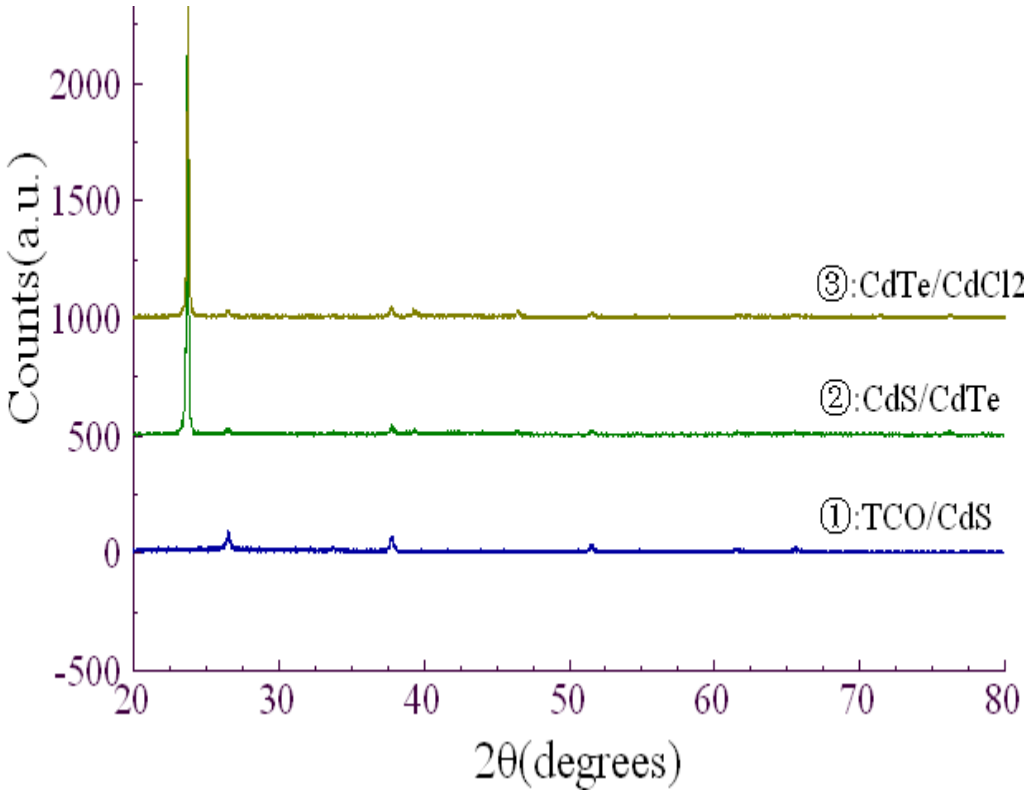

Figure 2.14 XRD of CSS CdTe thin film before and after the $CdCl_2$ treatment.

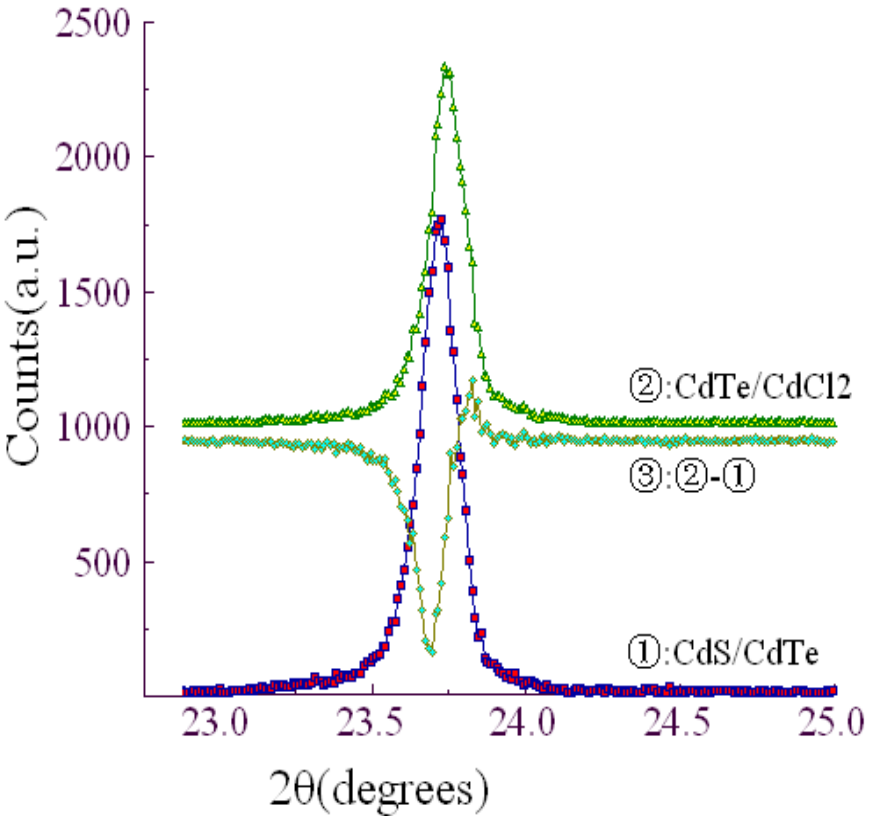

Figure 2.15 XRD of CSS CdTe thin film before and after the $CdCl_2$ treatment.

From Figures 2.14 and 2.15, we can find the grain size increase and the peak shift a little bit after the $CdCl_2$ treatment.

The increase of grain size was also proved by the optical microscope image of CdTe. It shows in Figures 2.16 and 2.17.

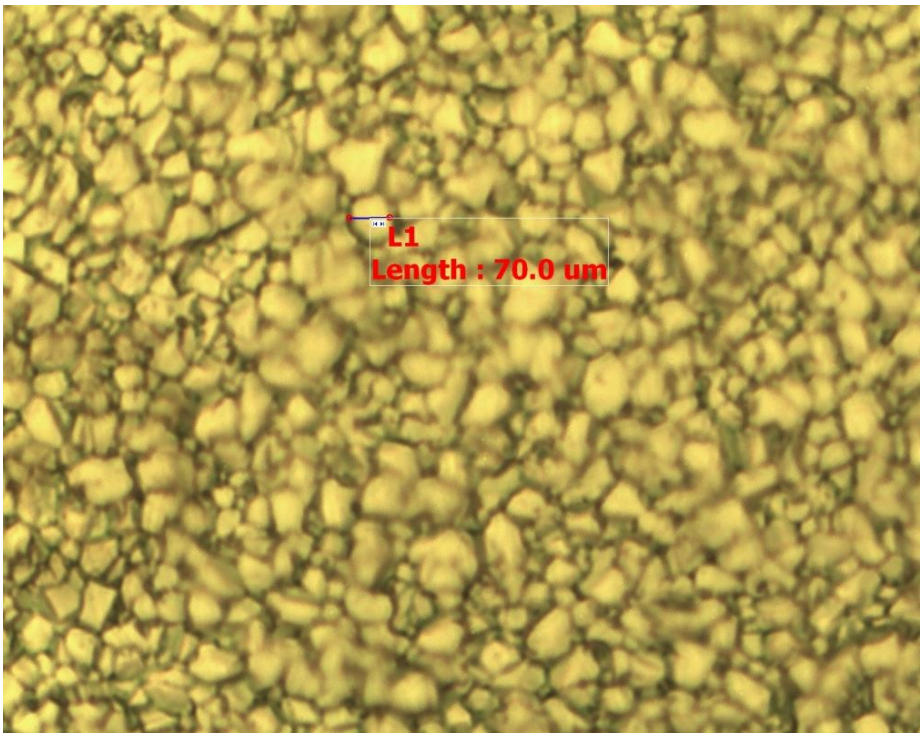

Figure 2.16 Optical CdTe before the $CdCl_2$ treatment.

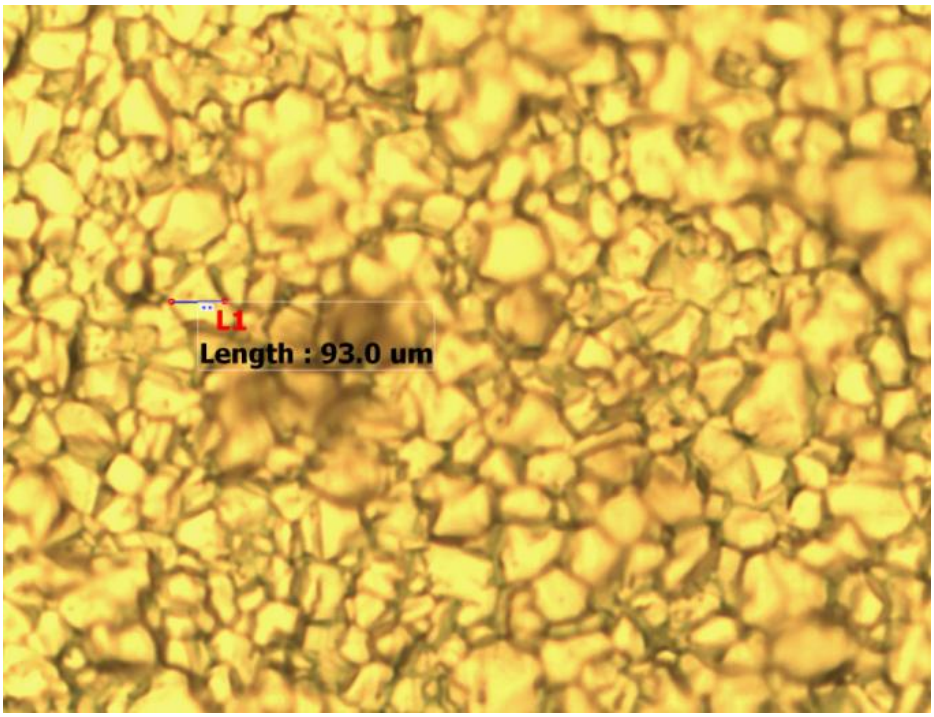

Figure 2.17 CdTe after the $CdCl_2$ treatment.

Figures 2.16 and 2.17 shows that the average grain size is 70um before the $CdCl_2$ treatment. After the $CdCl_2$ treatment, the average grain size increases to 93um.

2. Interactions at CdS/CdTe Interface

The $CdCl_2$ treatment enhances the diffusion of semiconductor (Figure 2.18). The $CdCl_2$ will diffusion to the CdS and CdTe interface and improve their interface and decrease the lattice mismatch (Figure 2.19). The production of a ternary compound (CdS_xTe_{1-x}) and creation of a graded band gap structure is benefit to device performance. Removal of lattice mismatch, stress, and surface states are the main advantages of this interface reaction that lead to the improvement of device performance.

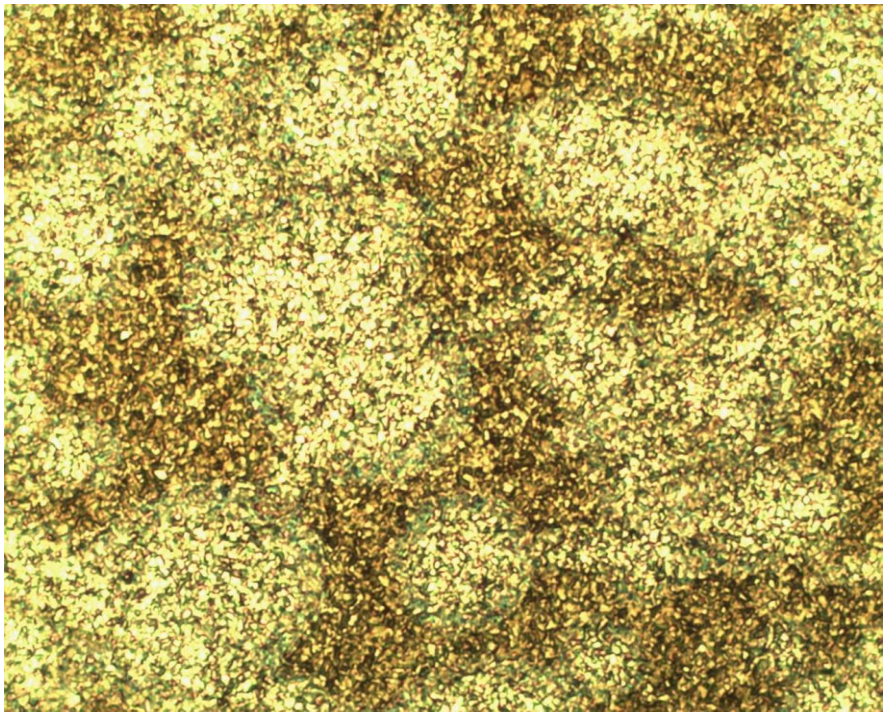

Figure 2.18 CdTe with the $CdCl_2$ treatment.

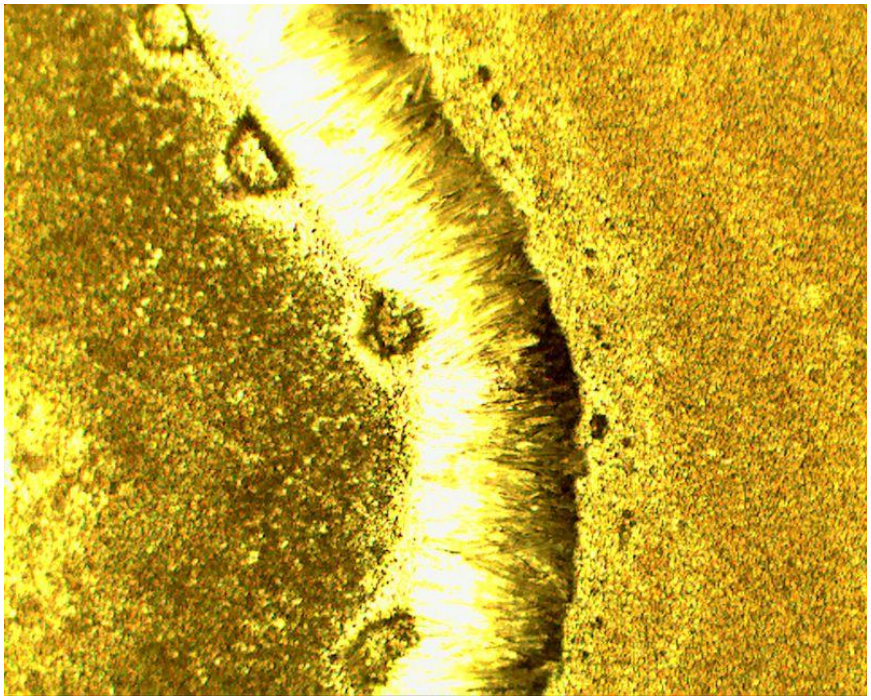

Figure 2.19 CdTe recrystallisation after the $CdCl_2$ treatment.

3. Increase in Surface Roughness

Results reported show that the surface roughness increases after $CdCl_2$ treatment. These observations agree well with recrystallisation and grain growth. In our experiment, the CdTe particles look very shining before $CdCl_2$ treatment (Figure 2.20). After the $CdCl_2$ treatment, the CdTe doesn't shining any more (Figure 2.21), which means that the $CdCl_2$ treatment increase the surface roughness of CdTe. It is also indicated by Cunningham that the CdTe (Cunningham, D. et al. 2002) surface become roughness after the $CdCl_2$ treatment. The surface roughness of thin films increases because of the columnar growth and re-crystallization. This surface roughness could create discontinuities in the back metal contact. This disadvantage can be removed by using thicker back electrical contacts in device fabrication.

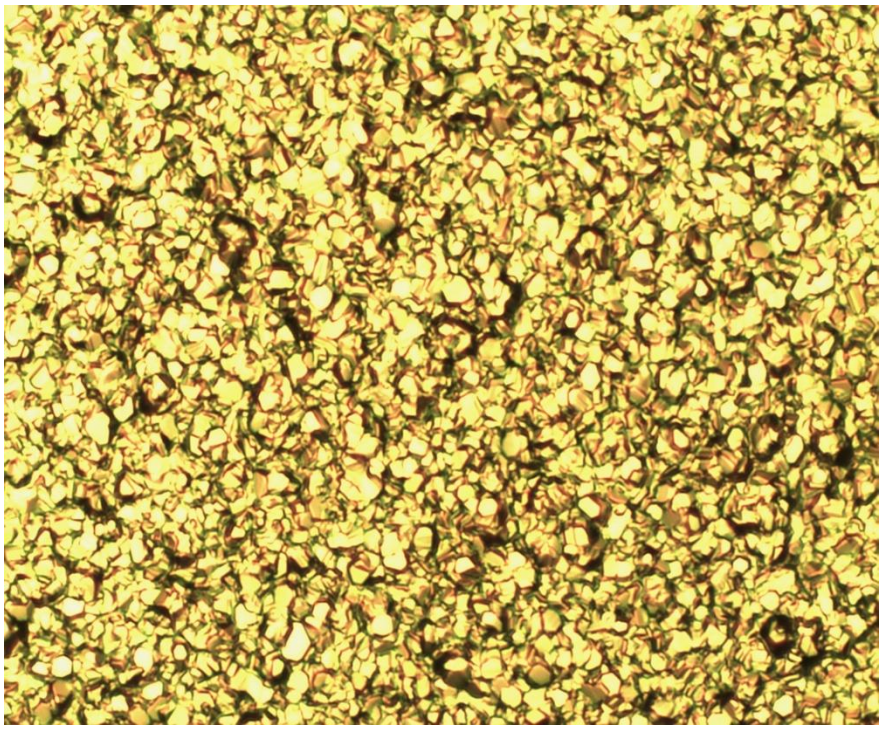

Figure 2.20 CdTe particles surface before the $CdCl_2$ treatment.

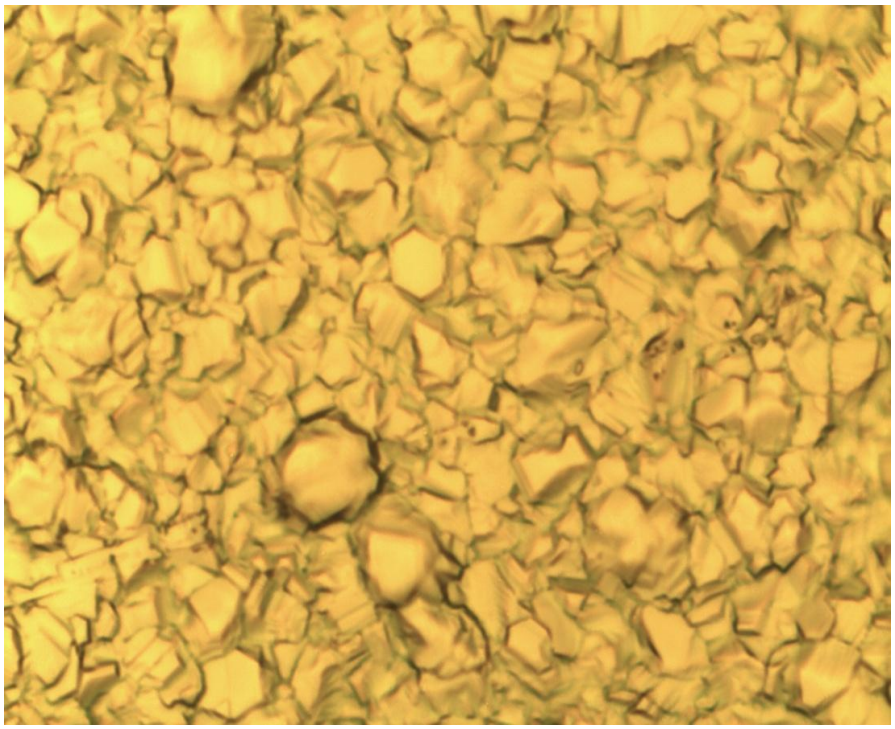

Figure 2.21 CdTe particle surface after the $CdCl_2$ treatment.

2.2.5 Back Contact

Among the II-VI compounds, CdTe is one of the most promising absorbers for use in inexpensive semiconductor solar cells. One of the major problems in CdTe solar cells is the poor contact stability. It is essential to develop a stable and low ohmic resistance electrical contact on CdTe for high efficiency and long term stability of CdTe/CdS solar cells. Since CdTe semiconductor has a high electron affinity, most metals form a non ohmic contact. The use of Cu at the back contact improves the contact to thin film CdTe solar cells, however the copper diffuses into the CdTe producing a heavily doped p- layer. It is generally unstable because Cu diffuses into the CdTe and the performance of the cell tends to degrade. The formation of an effective back contact depends on two key material properties: 1. The electron affinity of the material; 2. The doping level of the material.

There are several ways to make ohmic or pseudo-ohmic contacts to a CdTe.

The following are two of the most typical ways:

1. Use of a compound with a higher work function than p-CdTe.

2. Heavily doping the semiconductor adjacent to the contact to permit quantum mechanical tunneling through the surface barrier.

The first method involves a layer of semiconductor at the contact that will form a pseudo-ohmic contact to the metal. The second method is formed by doping the CdTe adjacent to the contact highly p-type to promote tunneling. It is important for Chemical etching of CdTe with Nitric-Phosphoric solution or Bromine-Methanol solution, which widens grain boundaries and leaves a metastable tellurium rich p+ CdTe surface which reduces the Schottky barrier.

In our experiment, the CdTe cells are then etched in 88:1:35 phosphoric acid: nitric-acid:DI-water (NP etch) to provide a clean, Te-rich surface (Figure 2.22). The samples are held in the etch 4 seconds past the point when the CdTe surface is completely covered with small bubbles (total etch time is about 35 s). The bubbles indicate that the initial oxide layer on the CdTe has been penetrated or it may be an indication of a transition to hydrophobic behavior after the Te layer is formed.

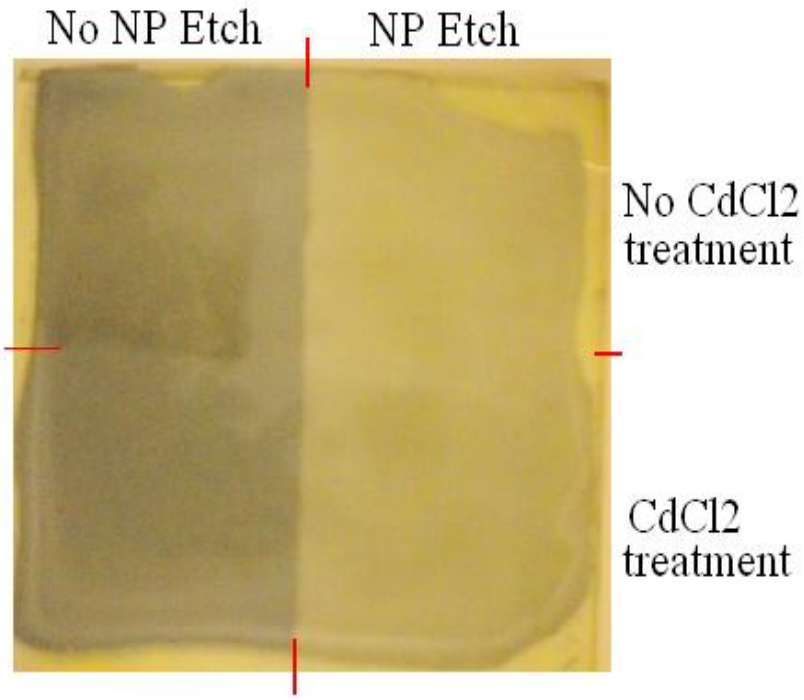

Figure 2.22 CdTe after NP etch.

Immediately on removal from the acid, the samples are rinsed with DI water. HgTe:Cu-doped graphite is then brushed on the cell as the back contact. The paste is made by stirring 4 g HgTe: Cu powder into 10 g graphite paste (Figure 2.23).

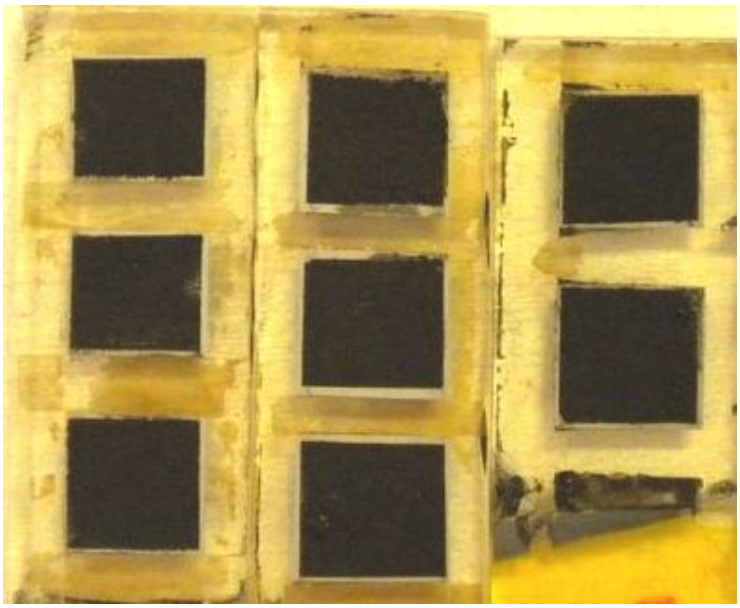

Figure 2.23 CdTe with graphite paste.

Next, the contact is annealed by placing the device in a tube furnace at 280 ℃ with a 100 sccm He flow for 30 min. A thin layer of silver paste is then applied to the back contact. The device is then placed in an oven at 100 ℃ for 1 h to cure the silver paste (Figure 2.24).

Figure 2.24 CdTe with silver paste.

2.3 CdTe Solar Cell Efficiency

In order to calculate the power conversion efficiency, it is necessary to locate maximum power and voltage and current. Solar cells are usually tested under standard testing conditions: air mass AM = 1.5, irradiance E= 1000W/m^2, temperature T = 25 ℃, and zero wind speed for no cooling effect. Adapting these values, the conversion efficiency can be calculated as

$$\eta(\%) = \frac{P_m}{P_{in}} * 100\% = \frac{V_{mp} I_{mp}}{EA} * 100\%$$

where P_{in} is the input power of incident light, and A is the area of the solar device(Figure 2.25).

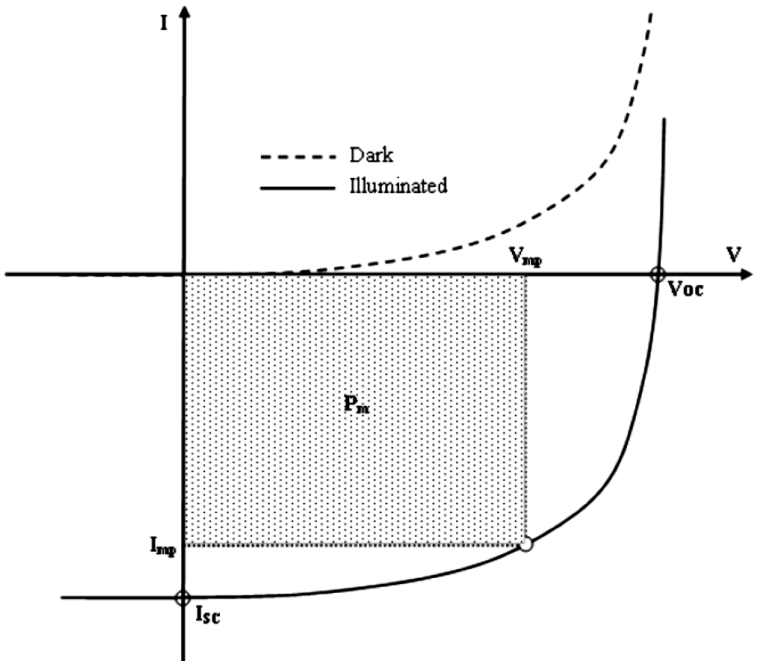

Figure 2.25 I-V characteristics of a solar cell.

Source: http://pvlab.epfl.ch/thin_film_on_glass

In order to maximize the output power it is desirable to increase both V_{oc} and I_{sc} while the shunt resistance should be as high as possible and the series resistance should

stay as low as possible. V_{oc} is limited by the bandgap energy of the absorbing material while I_{sc} depends on the absorption and charge transport properties. The shunt resistance describes the losses of the photo current due to defects introduced into the materials during the fabrication process. Figure 2.26 show the efficiency of our first CdTe solar cell. From the I-V curve, we can get the V_{oc} =0.5V, I_{sc} =20ma, FF= 38%, efficiency is only 3.9%.

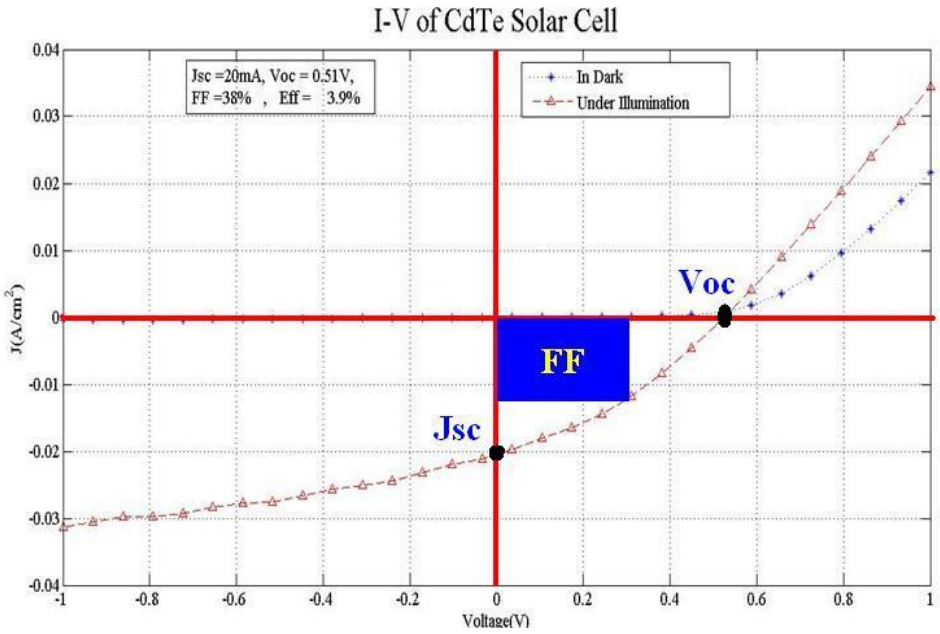

Figure 2.26 I-V characteristics of the first CdTe solar cell.

The series resistance in a solar cell has three causes: first, the movement of free carriers through the semiconductor; second the contact resistance between semiconductor and metal electrodes; and finally, resistance of the electrodes. The series resistance in a solar cell should be as low as possible in order to maximize power conversion efficiency. Another important parameter in the performance analysis of solar cells is fill factor (FF) which measures how close the real device is to the idealized model. An ideal device has

infinite shunt resistance and zero series resistance, giving an output voltage equal to V_{oc} and output current equal to I_{sc} , while having fill factor of 100%. Fill factor of a real device has a lower value and can be determined simply as a ratio of the area determined by V_{mp} and I_{mp} and the area defined by V_{oc} and I_{sc}

$$FF(\%) = \frac{V_{mp}I_{mp}}{V_{oc}I_{sc}} * 100\%$$

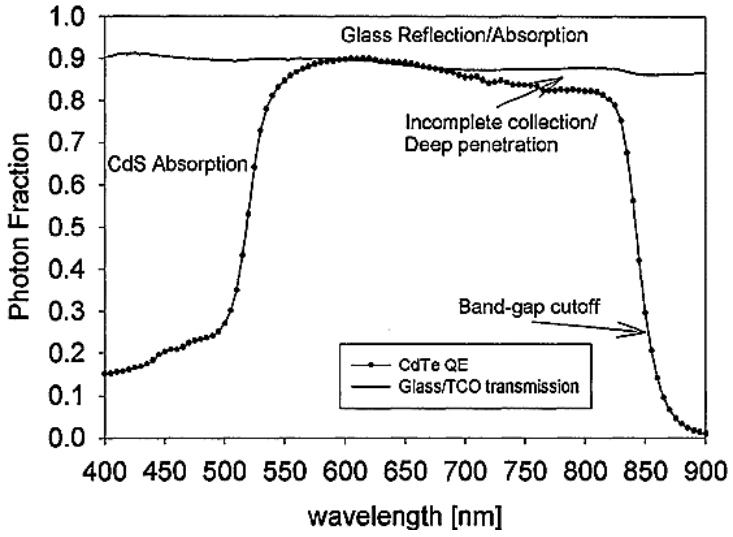

Figure 2.27 QE of CdTe solar cell.

Source: http://thegreenstalk.com/2010/08/

From Quantum Efficiency of CdTe solar cell (Figure 2.27), we can find that CdS absorption is the biggest loss for CdTe solar cell efficiency. To decrease the CdS absorption, we need to decrease the thickness of CdS and improve the quality of CdS. From Figure 2.28, we can see the quantum efficiency increase a lot by decrease the thickness of CdS.

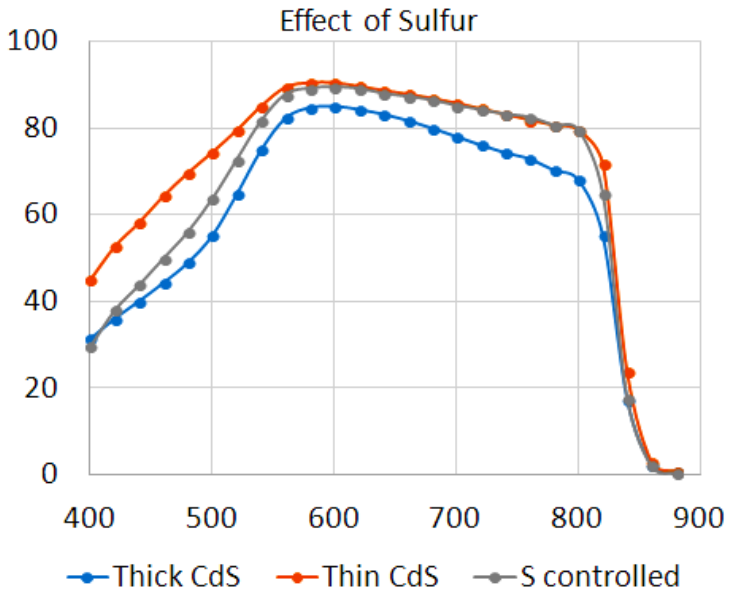

Figure 2.28 Effect of CdS thickness on QE.

Figure 2.29 are the latest CdTe solar cell efficiency device. The CdTe solar cell has increased the efficiency to 13.3%, Voc of 779 mV, Jsc of 23.8 mA/cm^2, and FF of 71.7%.

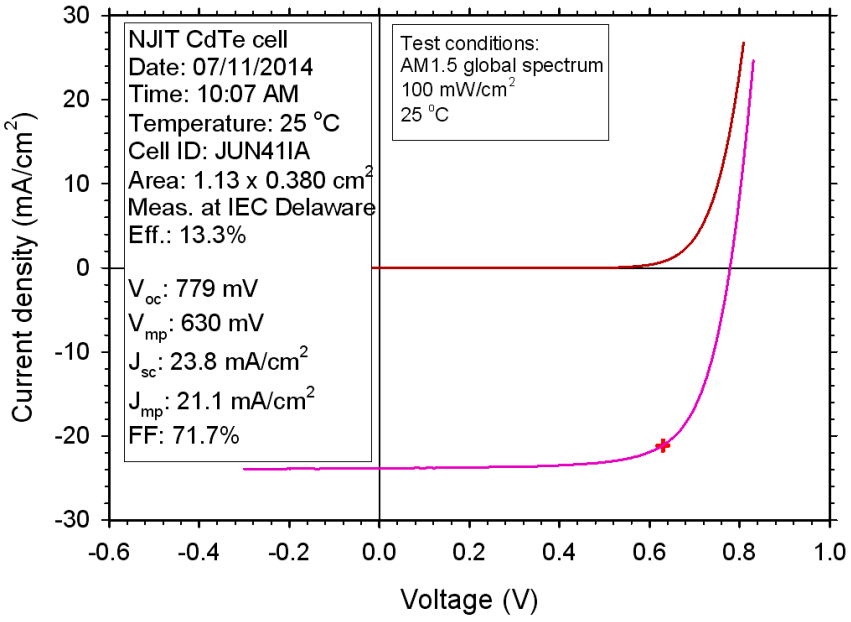

Figure 2.29 I-V characteristics of the latest CdTe solar cell.

Figure 2.30 is the QE of the latest CdTe with efficiency of 13.3%. From the QE picture, we can see the CdS absorption is the major impact for the CdTe efficiency. After the improvement of CdS, the efficiency increases greatly.

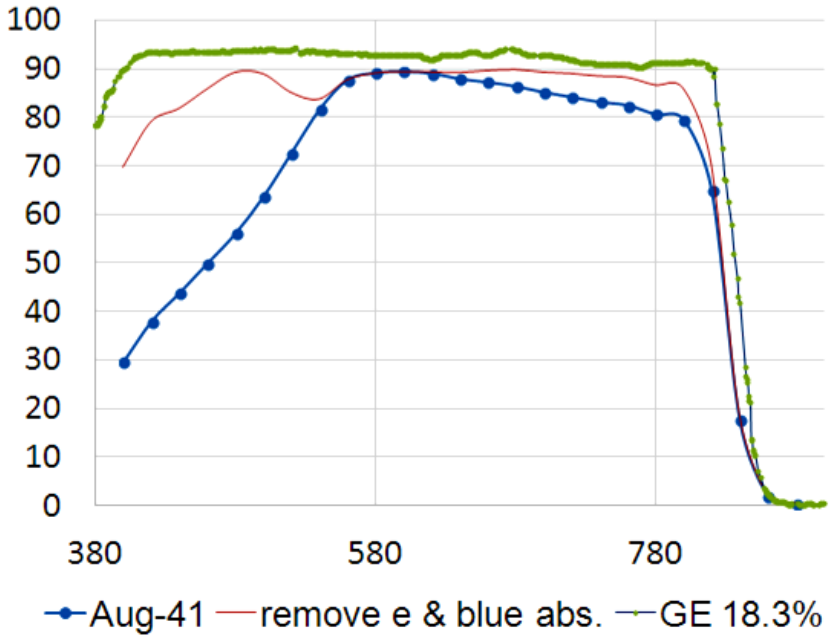

Figure 2.30 QE of NJIT CdTe solar cell.

CHAPTER 3

LARGE AREA CDS THIN FILM GROWN BY CHEMICAL BATH DEPOSITION

3.1 Introduction

Cadmium sulfide (CdS) is a semiconducting material used in a variety of applications. The wide band gap, low absorption loss, compact crystallographic cell structure and electronic affinity makes CdS is a promising opt-electronic device for making solar cells. CdS is an important wide band-gap semiconductor (Eg=2.42eV) used as window layer for cadmium telluride (CdTe) and copper Indium Gallium Selenide (CIGS) (Martinez M A, et al., 1999). It has also applications in various electro-optic and infrared devices (Kuhaimi S. A., 1998). The important thin film formation processes are based on liquid phase chemical techniques, gas phase chemical processes, glow discharge processes and evaporation methods. The methods employed for thin film deposition can be divided into two groups: physical or chemical (Figure 3.1).

In most heterojunction devices, high efficiency cells need high quality CdS window layer. Among these methods, CBD is a simple, convenient and cheap method to produce CdS thin films with high quality and low cost. The record efficiency for n-CdS/p-CdTe is obtained with CdS produced by CBD. The good quality of CdS by CBD may because of the good step coverage, low deposition temperature, chemical passivation and lacking of bombarding energetic species.

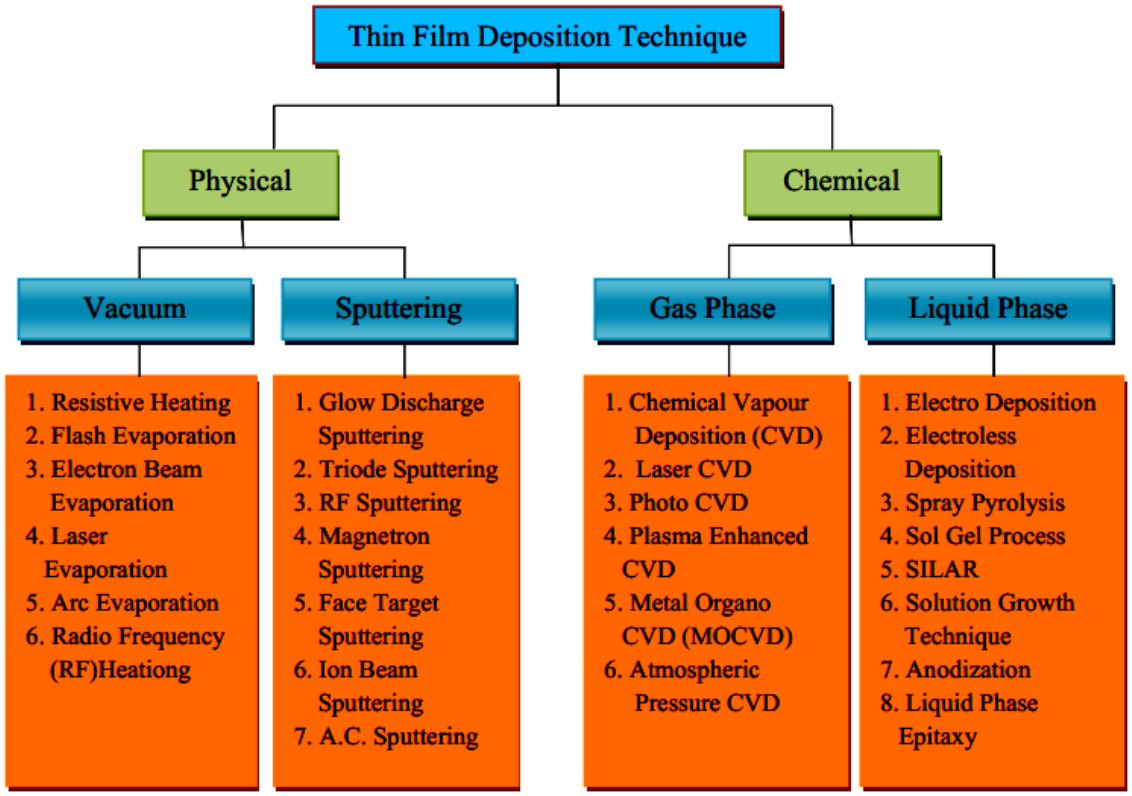

Figure 3.1 Classification of thin film deposition technique.

Source: (Santiago Arango, et al, 2012).

Over the years, different cadmium sources have been used in this process, such as cadmium sulfate, cadmium acetate, cadmium iodide/nitrate, and cadmium chloride. The effect of Cd source on the film properties has drawn attention for some time. The deposition process is based on the slow release of Cd^{2+} and S^{2-} ions. The amount of sulfide ions in the bath is controlled through setting up of appropriate chemical equilibrium. The anions and cations then react to form the compound. This technique is based on the controlled release of metal ion (M^{2+}) and sulphide (S^{2-}) in an aqueous bath. In this process, release of metal ion (M^{2+}) is controlled by using a suitable complexing

agent. The deposition begins with nucleation phase followed by growth phase (Figure 3.2).

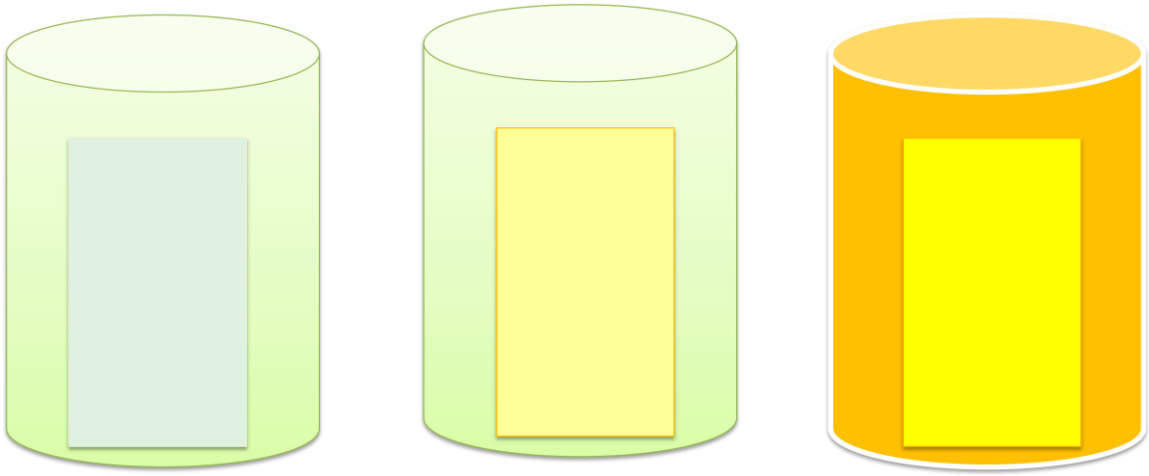

Figure 3.2 The sketch of process of forming CdS film.

Typical CBD processes for sulphides employ an alkaline medium containing the chalcogenide source, the metal ion and added base. A chelating agent is used to limit the hydrolysis of the metal ion. The technique under these conditions relies on the slow release of ions into an alkaline solution in which the free metal ion is buffered at a low concentration.

3.2 Preparation of CdS by CBD

We cut glass to 4*6 inch. The glass is cleaned by sonication in a 1% solution of Liquinox soap in hot DI water. Then we scrub the glass and wash with acetone and methanol and rinse five times with de-ionized water. Then the substrates were dried in N_2. The cleaned substrates were placed, four at a time, in the beaker with 1200ml DI water as shown in Figure 3.3.

Figure 3.3 Chemical bath deposition (CBD) setup.

Then we put 5.3 ml 0.1 M Cadmium chloride ($CdCl_2$), 9.2 ml 1M Ammonium acetate (NH_4AC) and 15 ml 15M Ammonia (NH_4OH) into the beaker. After the temperature reaches 88℃, the thiourea is added by a titrator in four aliquots of 2 ml, 10 min apart. The total deposition time, after the first addition of thiourea, is 38 min. The substrates are then removed from the bath. The substrates are then removed from the bath, placed in warm DI water, and given three sonications (about 2 min each) to remove loosely adhered CdS particulates. The films are then blown dry with N_2 and stored in Fluoroware containers.

The deposited CdS film is about 83nm this as measured by a Dektak profiler. The CdS films are very uniform, with less than 5% deviation from center to the edge.

1.3 Mechanism of CBD

The CBD of CdS deposition using CBD method can be proceeded by (i) heterogeneous mechanism (ion by ion) or (ii) homogenous mechanism (cluster by cluster).

For the homogenous mechanism, CdS grows colloidal particles in the bath solution which precipitate onto the substrate (Figure 3.4). The result is powdery and non-adherent films.

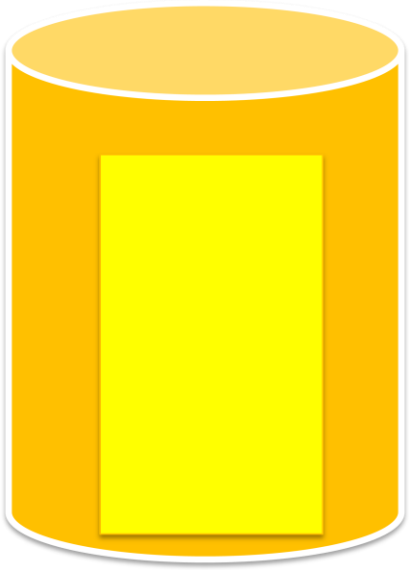

Figure 3.4 CdS deposited by homogenous mechanism.

The reactions for this mechanism and their equilibrium constants are as follows:

$$NH_3 + H_2O \rightleftharpoons NH_4^+ + OH^- \qquad K_1 = 1.8\times10^{-5}\ (300K) \qquad (3.3.1)$$

$$Cd^{2+} + 4NH_3 \rightleftharpoons Cd(NH_3)_4^{2+} \qquad K_2 = 1.88\times10^{14}\ (300K) \qquad (3.3.2)$$

$$Cd^{2+} + 2OH^- \rightleftharpoons Cd(OH)_2 \downarrow \qquad K_3 = 3.6\times10^{6}\ (300K) \qquad (3.3.3)$$

$$(NH_2)_2CS + 2OH^- \rightleftharpoons S^{2-} + 2H_2O + H_2CN_2 \qquad K_4 = 3.8\times10^{-3}\ (300K) \qquad (3.3.4)$$

$$S^{2-} + Cd^{2+} \rightleftharpoons CdS \downarrow \qquad K_5 = 7.1\times10^{28}\ (300K) \qquad (3.3.5)$$

For the heterogeneous mechanism, the reaction occurs on the substrate surface. CdS grows ion-by-ion on the substrate surface and is a well crystallized adherent film (Figure 3.5).

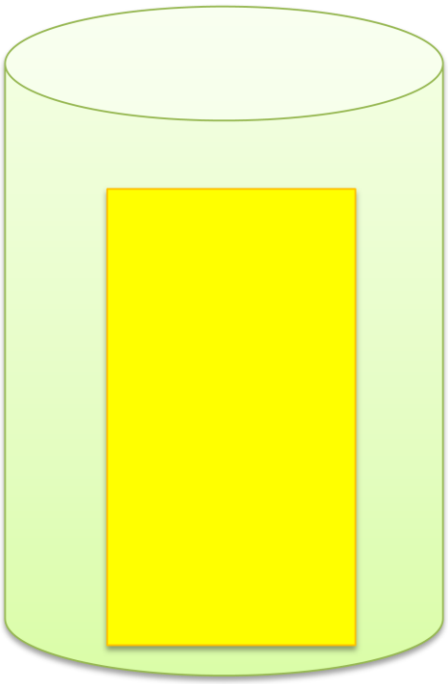

Figure 3.5 CdS growed by heterogeneous growth.

CdS deposition by the heterogeneous method has three growth regimes: an induction period with no growth, a linear growth period, and a colloidal growth period. The Cd^{2+} ions combine with NH_3 in the range of pH 10-11 and form $Cd(NH_3)_4^{2+}$ which adsorb on the glass. Then CdS will deposit on glass by reaction with the S^{2-} ions.

The desired heterogeneous reactions are:

Reversible absorption of cadmium hydroxide species

$$Cd(NH_3)_4^{2+} + 2OH^- + site \rightleftharpoons Cd(OH)_{2ads} + 4NH3\uparrow \quad (3.3.6)$$

Formation of surface complex with thiourea

$$Cd(OH)_{2ads} + S = C(NH2)2 \rightarrow [Cd(S = C(NH_2)_2)(OH_2)]_{ads} \quad (3.3.7)$$

Formation of CdS with site regeneration

$$[Cd(S = C(NH_2)_2)(OH_2)]_{ads} \rightarrow CdS \downarrow + CN_2H_2 + 2H_2O + site \quad (3.3.8)$$

Reaction (8) is the rate-limiting step in the heterogeneous mechanism.

3.4 Results and Discussion

3.4.1 The X-ray Diffraction (XRD) Measurement

Figure 3.6 shows the XRD pattern of film which reveals the formation of nano-crystalline CdS. The peaks at 2y positions of 27 ºand 52 ºcorresponds to the (111) and (311) planes of the cubic CdS phase, respectively. The XRD patterns obtained match with the JCPDS data. The widened peaks imply a small particle size of the product. According to Debye-Scherrer equation, the mean grain size is calculated to be approximately 4.3 nm.

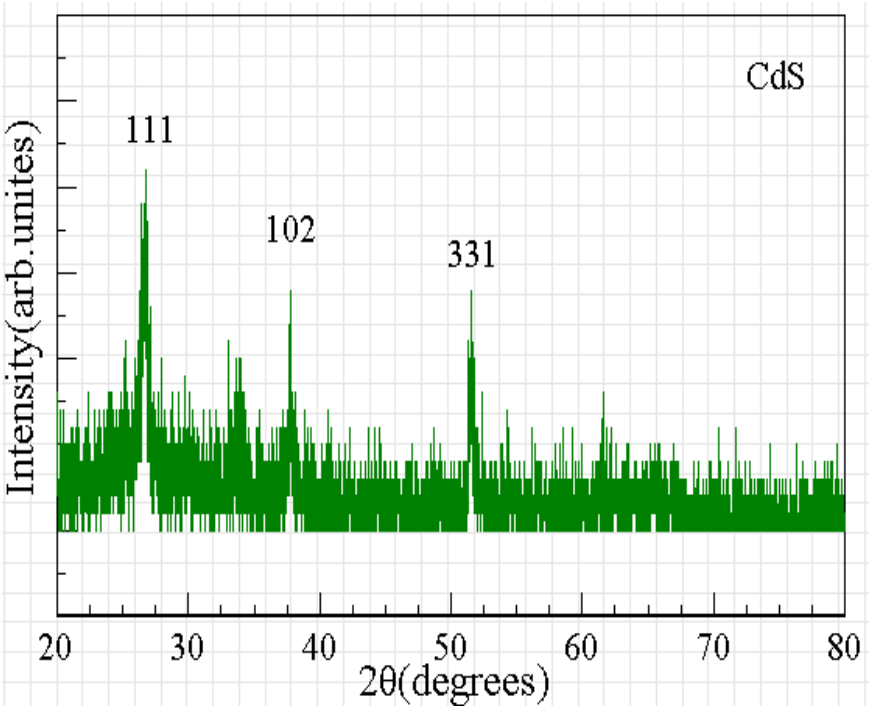

Figure 3.6 X-ray diffraction pattern of CdS.

3.4.2 Photoelectric Microscope Measurement

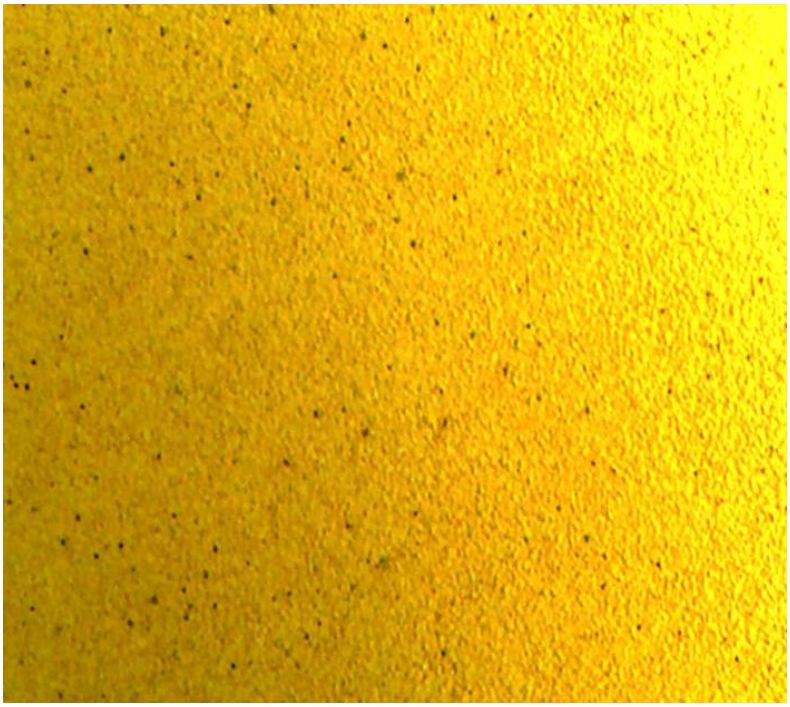

Figure 3.7 Photoelectric microscope of CdS.

Figure 3.7 shows the photoelectric microscope of CdS sample prepared by the CBD. From the picture, we can see the CdS is very compact and uniform. The results were confirmed by the test of Dektak profiler. It is around 80nm with less than 5% deviation.

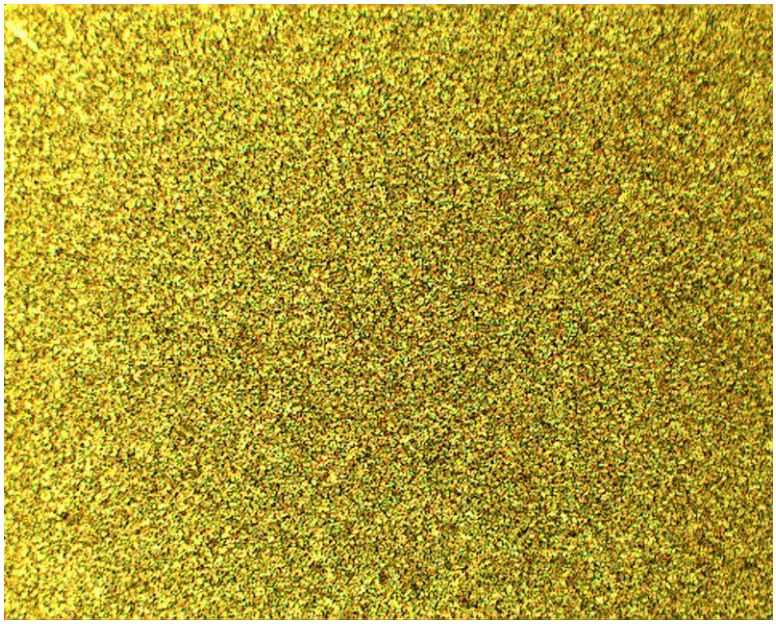

Figure 3.8 Photoelectric microscope of CdTe.

Figure 3.8 shows the photoelectric microscope of CdTe sample prepared by the CSS. From the picture, we can see the CdTe is very compact and uniform. It has good crystalline character and narrow size distribution.

3.4.3 J-V Curve for CdTe Solar Cell

It should be noted that this cell exhibits zero shunting in its dark J-V curve and a very flat illuminated J-V curve for V < 0.4 V indicating almost voltage-independent photocurrent collection. The Delaware-measured G values of 0.44 and 0.47 mS/cm^2 correspond to Rsc (=1/G) values of 2270 and 2130 Ω cm^2. We achieved conversion efficiency of 13.3%, with the parameters: Voc 779 mV, Jsc 23.8 mA/cm^2, FF 71.7% (Figure 3.9).

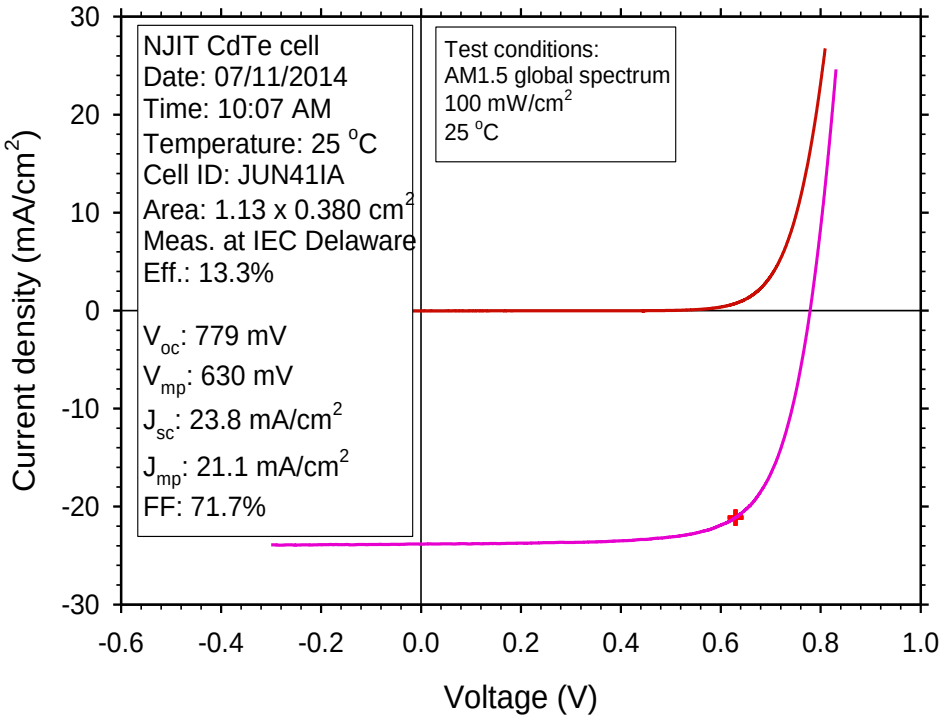

Figure 3.9 J-V curve for 13.3% NJIT CdTe cell.

3.4.4 Effect of Temperature on the Deposition Rate

With the increasing temperature, reaction (1) will shift to left and more NH_3 will be produced, which will promote the reaction (2). Then the concentration of $Cd(NH_3)_4^{2+}$ will increase and Cd^{2+} will decrease, which will promote the heterogeneous mechanism and impede the homogenous mechanism, because the increasing concentration of $Cd(NH_3)_4^{2+}$ will promote reaction (6) and the decreasing of Cd^{2+} will impede the reaction (3). The increase of temperature will also decrease the solubility of NH_3 in water and decrease the concentration of NH_3OH (see Figure 3.10).

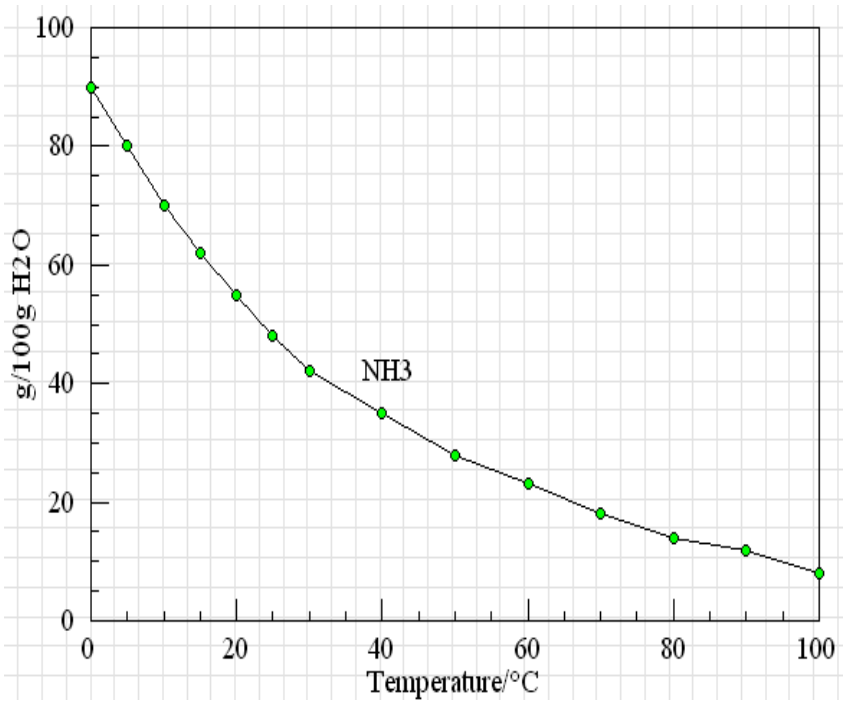

Figure 3.10 NH_3 solubility curve.

We need to keep adding NH_3OH to keep stable pH. Further, increasing temperature promotes reaction (4) which enhanced the hydrolysis of $(NH_2)_2CS$ and the formation of S^{2-}. The increase of S^{2-} will promote the reaction (5) and promote the homogenous mechanism. It is very important to control the temperature to optimize the reaction.

Figure 3.11 shows the dependence of grown CdS film thickness on temperature. As temperature increases, the deposition rate also increases. When the temperature is below 64℃, the hydrolysis of $(NH_2)_2CS$ is very slow which results in the low deposition rate. It is better to control the temperature around 85℃. From Figure 3.11, we can also find that the deposition rate above 80℃ increase almost linear in the first twenty minutes and increase greatly between twenty to thirty minutes and increase slowly between thirty minutes and forty minutes.

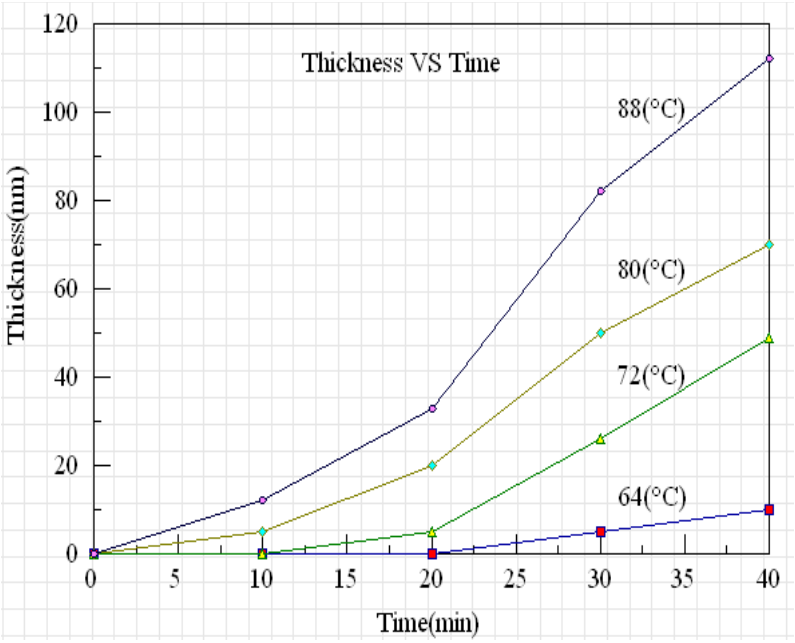

Figure 3.11 Film thickness versus temperature.

In the first twenty minutes, the concentration of $(NH_2)_2CS$ and S^{2-} is very low. The reaction is controlled by heterogeneous mechanism. The result is a good quality transparent, uniform and adherent CdS film. During twenty to thirty minutes, the increase concentration of $(NH2)_2CS$ and S^{2-} promote the reaction (5). The reaction is controlled by both homogenous and heterogeneous mechanisms. In this stage, the CdS colloidal particles precipitated homogeneously from the bulk solution and adsorb randomly on the growing film. During 30 to 40 minutes, the high concentration of $(NH_2)_2CS$ and S^{2-} promote greatly the reaction (5). Besides, the decrease of NH_3 in solution result in the decrease the concentration of $Cd(NH_3)_4^{2+}$, which impede the heterogeneous mechanism. In this stage, the reaction is controlled by the homogenous mechanism. The CdS film is opaque, non-uniform and poorly adherent.

From Figure 3.11, we can also find that the deposition rate below 72℃ is almost linear because the hydrolysis of $(NH_2)_2CS$ is very low and the concentration of S^{2-} is also

very low. This impedes the reaction (5). Therefore, the reaction below 72℃ is controlled by heterogeneous mechanism. However, the good quality CdS deposition rate is too slow.

3.4.5 Effect of $(NH_2)_2CS$ / $CdCl_2$ on the Deposition Rate

The ratio of $(NH_2)_2CS$ and $CdCl_2$ has great influence to the deposition rate. Figure 3.12 shows that the deposition rate decreases with the increase of $(NH_2)_2CS$ / $CdCl_2$, because the increase of $(NH_2)_2CS$ / $CdCl_2$ will increase the hydrolysis of $(NH_2)_2CS$. The higher concentration of S^{2-} will promote the homogenous mechanism and decrease the deposition rate. When the ratio of $(NH_2)_2CS$ and $CdCl_2$ small than 1, in the first 20 minutes, the deposition rate is almost 0, because the concentration of S^{2-} is too low to produce CdS. During the second 20 minutes, the reaction is controlled by heterogeneous mechanism at ratio 1. When the ratio is 2, the first 20 minutes thickness is almost equal to the thickness of the last 20 minutes of ratio 1 since are controlled by heterogeneous mechanism. Further, the thickness at 40 minutes is almost double that at 20 minutes, which means the whole process is controlled by heterogeneous mechanism. When the ratio is 2 to 4, the deposition rate of last 20 minutes is smaller than that of the first 20 minutes, which means the last 20 minutes is affected by the homogenous mechanism. The effect of homogenous mechanism increases with the increasing ratio. When the ratio is bigger than 4, the deposition rate of last 20 minutes is totally controlled by homogenous mechanism. Besides the first 20 minutes is also affected by the homogenous mechanism when the ratio is higher than 4. It explains why the thickness of CdS decreases from ratio 4 to ratio 8. It is better to choose ratio 2 as the deposition condition.

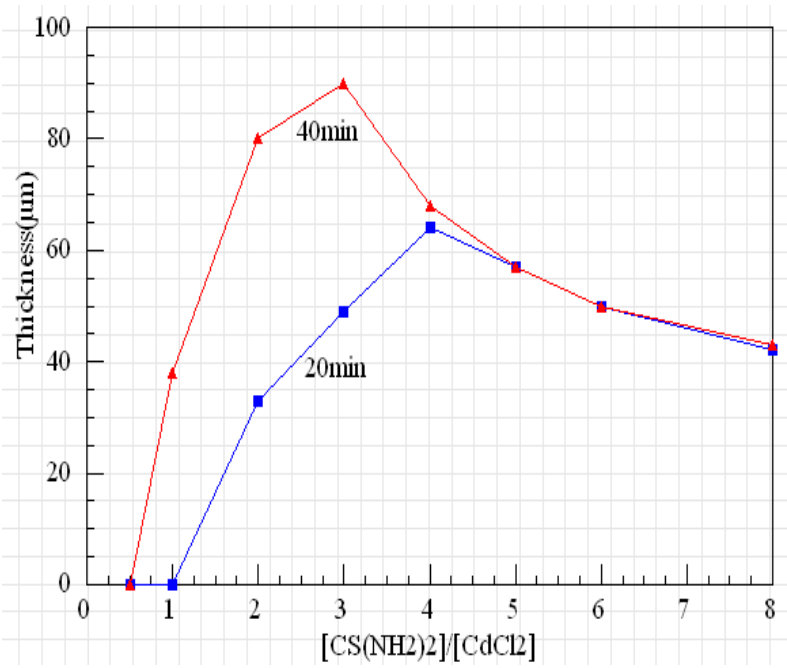

Figure 3.12 Film thickness versus S/Cd.

3.4.6 Effect of NH_4AC on the Deposition Rate

NH_4Ac increases the concentration of NH_4^+ which promotes the reverse reaction (1) and more produced NH_3 will promote the reaction (2). The increasing $Cd(NH_3)_4^{2+}$ and decreasing Cd^{2+} will promote the heterogeneous mechanism and impede the homogenous mechanism. That is why the thickness increases with the increasing of NH_4AC concentration (Figure 3.13). However, an excess of NH_4Ac will decrease the concentration of OH- ions, which will slow the hydrolysis of $(NH_2)_2CS$ and decrease the deposition. That is why the deposition rate decreases when the NH_4AC concentration is above 0.01mol/l.

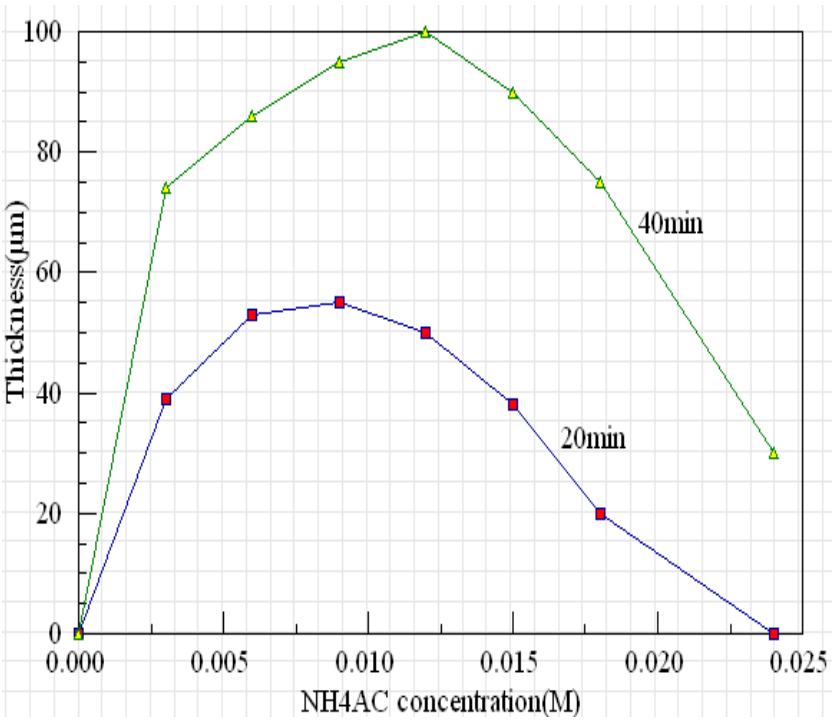

Figure 3.13 Film thickness versus NH_4AC concentration.

3.4.7 Effect of NH_4OH on the Deposition Rate

At low [NH_4OH], Both the concentration of [NH_3] and OH- ions are very low which result in the low concentration of $Cd(NH_3)_4^{2+}A$ and low hydrolysis of $(NH_2)_2CS$. Then the deposition rate is low at the beginning. The deposition rate will increase with the increase of [NH_4OH] (Figure 3.14). However, excess [NH_4OH] will also increase the concentration of OH- ions which promote the homogenous mechanism. That is why the deposition rate decrease when the [NH_4OH] is bigger than 0.4.

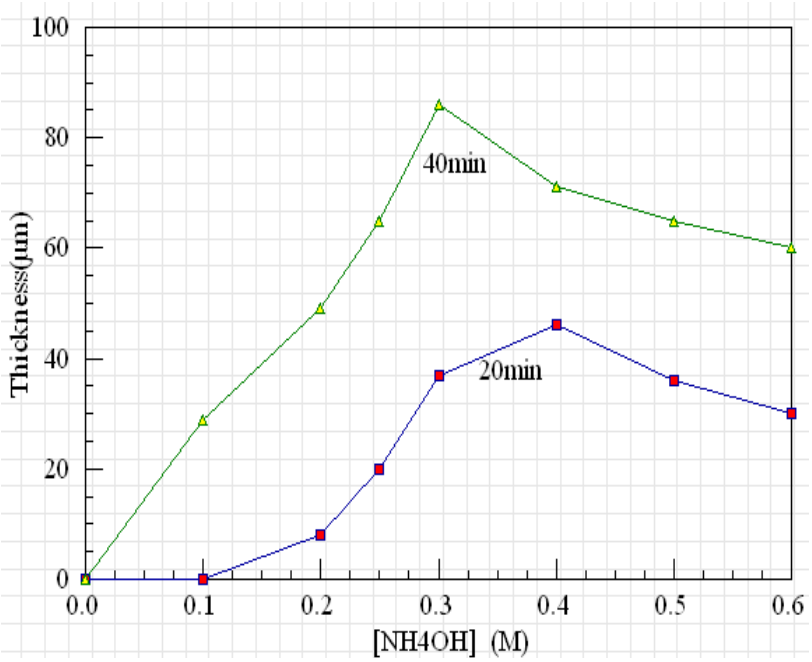

Figure 3.14 Film thickness versus NH_4OH concentration.

3.5. Conclusion

The mechanism of chemical bath deposition and deposition conditions were studied in this paper. We introduced how to promote heterogeneous mechanism and impede the homogenous mechanism by changing the deposition conditions. We also studied different factors of deposition rate which including the temperature and the concentration of Cd^{-} salt, NH_4OH, NH4AC and the ratio of thiourea/Cd-salt. We are currently studying large volume production CdS by CBD.

CHAPTER 4

GROWTH MODEL OF CDTE THIN FILM BY CLOSE SPACED SUBLIMATION

4.1 Introduction

Close spaced sublimation (CSS) has attractive features for high-rate deposition of CdS/CdTe thin film solar modules. CSS has been successfully implemented in commercial production of CdTe solar panels with size of 0.6 m x 1.2 m and 1.2 m x 1.6 m. A CSS growth model is a useful tool to guide the CdTe thin film deposition and the design of CSS. In this paper, a growth model was developed for CdTe deposition including diffusion limited, sublimation limited and reaction limited with the presence of oxygen. The model can explain the effect of source and substrate temperature, ambient gas pressure and the separation between source and substrate on the growth rate of CdTe by CSS. Cadmium telluride (CdTe) thin film photovoltaic has been shown to be the most promising solar cells because of its long term stable performance, easy scale-up for large area production, high absorption coefficient and optimum band gap. Due to the high absorption coefficient and optimum band gap of CdTe, a film thickness of 2 μm should be sufficient to absorb most of the solar spectrum. Compared to several hundred micrometer silicon solar cells, it reduced many materials and save lots of cost. In 2016, a new world record conversion efficiency 22.1% for CdTe solar was announced by First Solar. Besides, a new world record for cadmium-telluride (CdTe) photovoltaic (PV) module conversion efficiency 18.2% was confirmed by the U.S. Department of Energy's National Renewable Energy Laboratory (NREL). CdTe thin films solar cell has been deposited by several techniques. Among the methods, CSS and VTD technique are

expected to have the highest deposition rate and were successfully used in industry. Compare to the successful VTD by First Solar, the CSS by Abound, GE and CTF didn't success as we expected. There are many reasons about the failure of CSS in industry. One of the reasons is because the growth model of CSS is still confused and some mistakes in past many papers. This paper summarized the good points of former other papers and clarify some mistakes.

4.2 Effect Factor of CdTe Growth by CSS

The CdTe growth can be influenced by many factors, such as source and substrate temperature, ambient gas pressure, the separation between source and substrate and the CdTe source materials.

4.2.1 Effect of T_{Sou} and T_{Sub}

Hiroshi Nagayoshi (Hiroshi Nagayoshi, 2004) pointed out that the growth rate increase with the increase of source temperature (Figure 4.1).

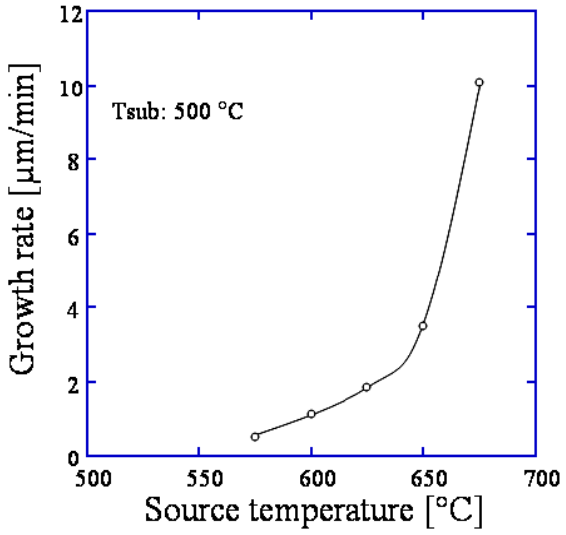

Figure 4.1 Growth rate as a function of source temperature.

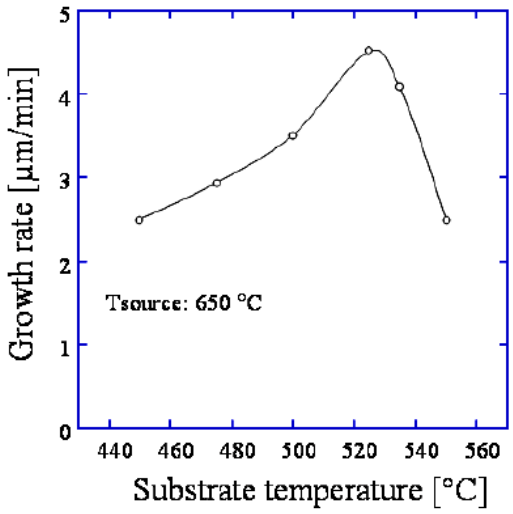

Figure 4.2 Growth rate as a function of substrate temperature.

Source: (Hiroshi Nagayoshi, 2004)

It also increases with the increase of substrate temperature and decrease after the turning point (Figure 4.2).

4.2.2 Effect of $\Delta T=T_{Sou} - T_{Sub}$

The influence of ΔT to the growth rate is very complicated. The growth rate can be increased with the increase of ΔT (Figure 4.1).

Table 4.1 Effect of ΔT on Growth Rate

Deposition time = 60 min		
T_{CdTe} (°C)	T_{glass} (°C)	thickness [µm]
350	250	0
450	350	0.15
500	400	2.25
550	450	18.0

Source: (Stella A., 2007).

It can also be increased with the decreased of ΔT (Figure 4.2) or no change for ΔT (Table 4.1). The influence of ΔT and T_{Sub} is summarized in Figure 4.3(Stella A. 2007).

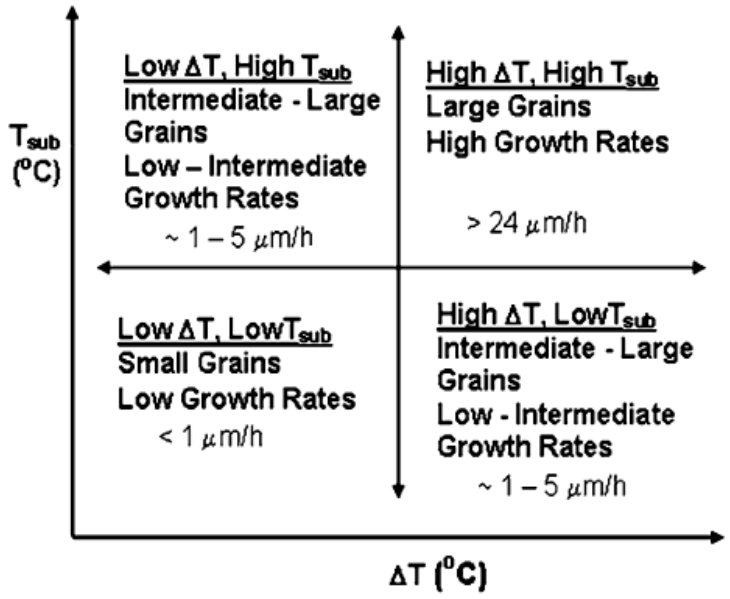

Figure 4.3 Growth rate as a function of ΔT and T_{Sub}.
Source: (Stella A., 2007).

4.2.3 Effect of P_{O_2} and $P_{Inert\ gas}$

The effect of P_{O_2} and $P_{Inert\ gas}$ to the growth rate is very complicated. The growth rate is decreased with the increase of P_{O_2} and $P_{Inert\ gas}$ in the diffusion region. Table 4.2 (Vivienne Denise, et al. 2006) shows the deposition rate increases as pressure decreases down to 1 Torr. This behavior is also predicted by the diffusion limited rate model. Again, the experimental values of the deposition rate were smaller than theoretical values, due the poor adhesion of CdTe film onto the substrate. Further pressure reductions don't affect the rate because at low pressures the rate is limited by free evaporation, a pressure-independent process.

Table 4.2 Effect of P_{Ar} to the Growth Rate

P_{Ar} (Torr)	0.1	1.0	10	20
rate (μm/min)	0.60	0.60	0.20	0.12

Source: (Vivienne Denise, et al., 2006)

Table 4.3 shows that less than 10% oxygen has no bigger difference in the deposition rate. Above 10% oxygen, the deposition rate decreases, the reduction being very steep for those films deposited in presence of pure oxygen. The deposition rate decrease is probably due to the reaction between tellurium and/or cadmium molecules and oxygen molecules, during their transport to the substrate.

Table 4.3 Effect of Oxygen to the Growth Rate

$\%O_2$	0.0	10	20	100
rate (μm/min)	0.20	0.19	0.15	0.08

Source: (Vivienne Denise, et al., 2006)

4.2.4 Effect of Space (h)

The growth rate is decreased with the increase of space d in the diffusion region while the growth rate has no relationship with the space h in the sublimation region. Figure 4.4 (S. N. Alamr, 2003) shows that the growth rate reduces as the separation between the substrate and the baffle (source) increases. Interestingly there is an abrupt change in the slope at a separation of~3 mm, suggesting a change in the deposition mechanism.

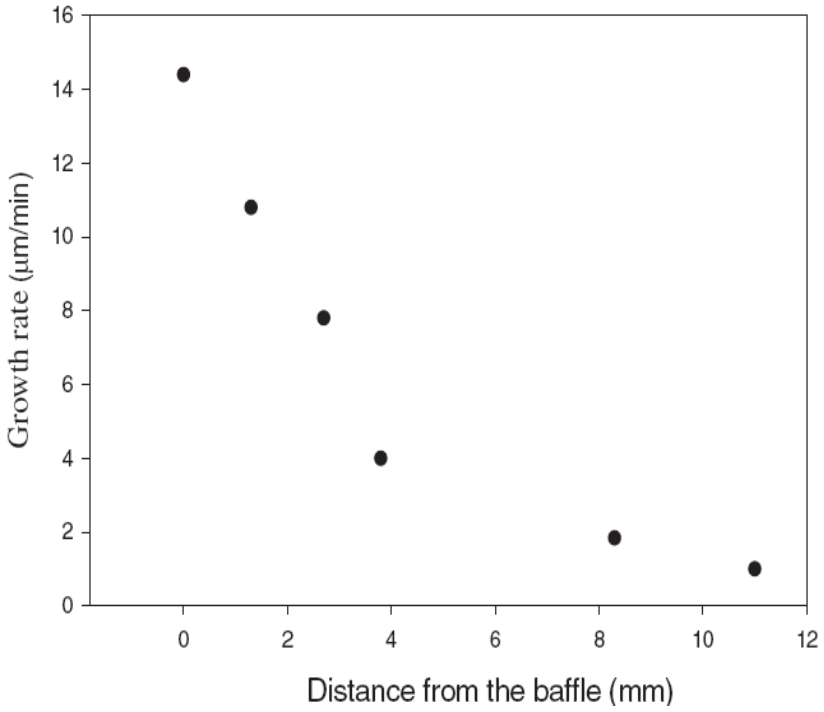

Figure 4.4 Growth rate as a function of space h.

Source: (S. N. Alamr, 2003)

4.2.5 Effect of CdTe Source Materials

The CdTe source materials also have great influence on the growth rate. Figure 4.5 (Wagner Pinheiro, et al, 2006) shows that 1 g powder source gives rise to deposition rates higher than those achieved with the 5 g powder sources, probably due to the temperature gradient along the thickness of the source. Also, comparing the 5 g powder source with the compact powder source (5 g) one observes that the compact powder gives a higher rate, due to better thermal contact among the particles. Both glass and molybdenum substrates gave similar results. The deposition rate is very low, probably due to the introduction of the substrate plate between the material and the graphite block, which reduced the heat transmission to the material.

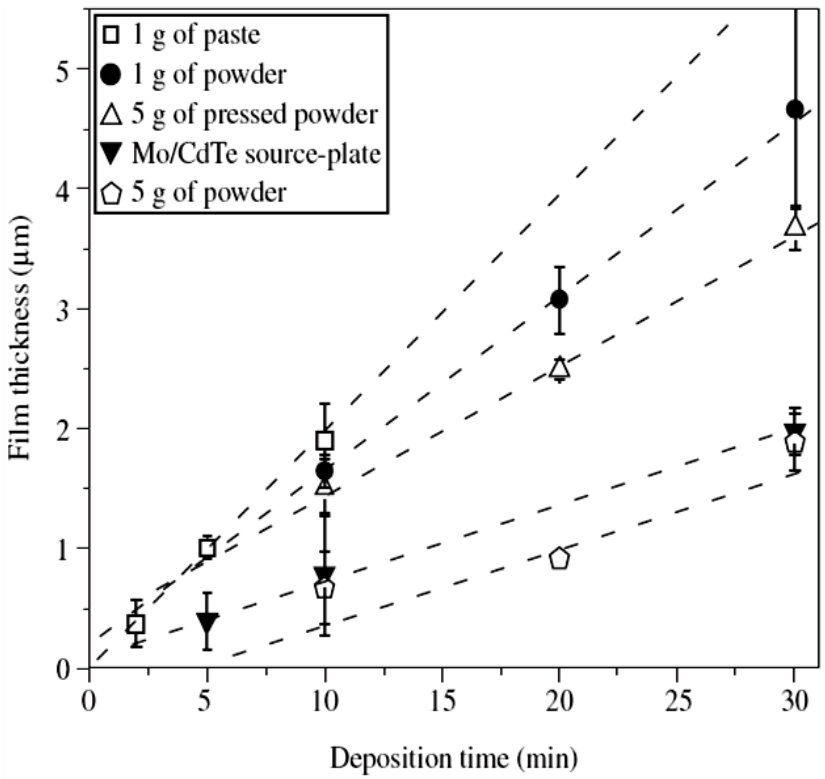

Figure 4.5 Effect of CdTe source on the growth rate.

Source: (Wagner Pinheiro, et al., 2006)

4.3 Different CdTe Growth Model by CSS

4.3.1 Cruz's Model

The CdTe growth process was showed in Figure 4.6. The physical process of the CSS is: First, CdTe source decomposes and sublimates; Second, the diffusion process of Cd and Te_2 from source to substrate; Third, Cd and Te_2 combine into CdTe and CdTe resublimates if T_{sub} is very high.

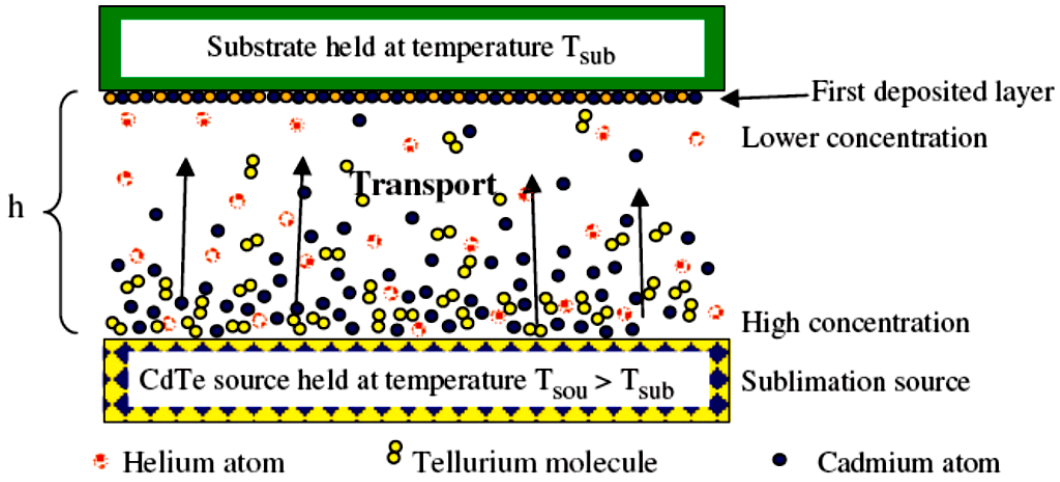

Figure 4.6 Schematic illustrating of CdTe growth by CSS.

Source: (Jose Cruz, 2009)

Jose's diffusion growth model (Jose Cruz, 2009) can be calculated by Fick's Law:

$$F_{Cd} = D_{Cd}^{He} \frac{C_{Sub}^{Cd} - C_{Sou}^{Cd}}{h} \text{ (Fick's law)}$$

$$F_{Cd} = \frac{D_{Cd}^{He}}{kh} \left(\frac{P_{Sou}^{Cd}}{T_{Sou}} - \frac{P_{Sub}^{Cd}}{T_{Sub}} \right) \text{ (idea gas)}$$

$$P_{gas}^{Cd} = 2P_{gas}^{Te_2} \quad \text{(stoichiometry)}$$

$$P_{gas}^{Cd} + P_{gas}^{Te_2} = P_{Solid}^{CdTe}$$

$$P_{gas}^{Cd} = \frac{2}{3} P_{Solid}^{CdTe}$$

$$\mathrm{P}_{solid}^{CdTe} = 101,325 * 10^{6.823 - 10,000 T^{-1}}$$

$$GR_{Diff}(m/s) = \alpha F_{Cd} \frac{m_{CdTe}}{\rho_{CdTe} * NA}$$

Figure 4.7 observed that the growth rate has an exponential dependence on temperature for the three different separation distances. The growth rate will be the same for separation distances between 0 and 5mm as the growth rate is sublimation-limited for this condition and the separation distance has no influence. In contrast, at separation distances greater than 5mm, the growth rate is diffusion-limited.

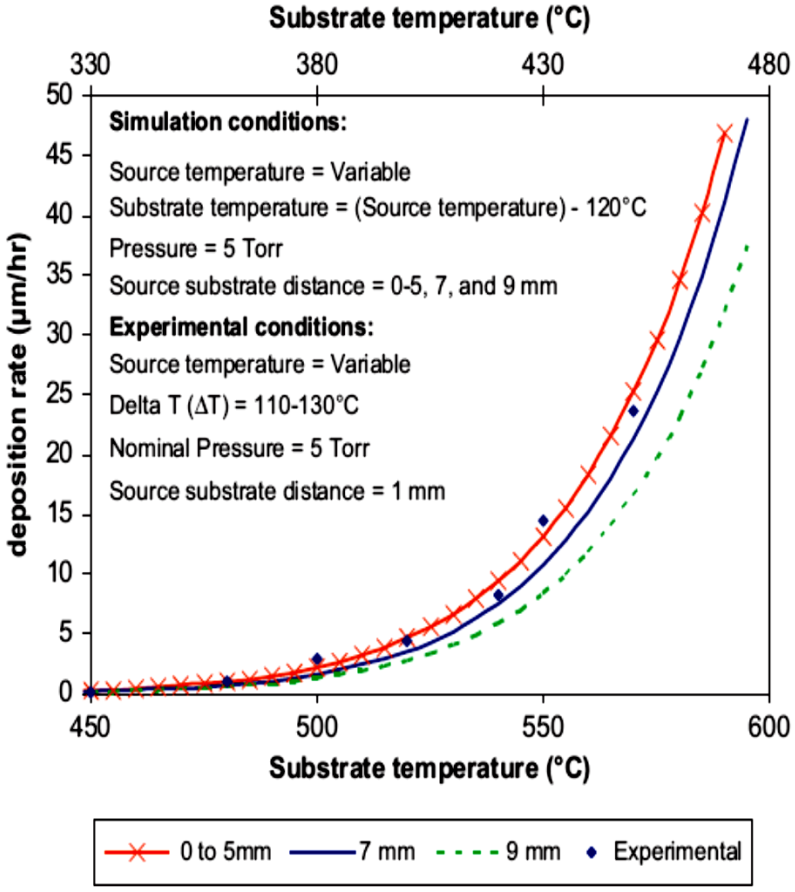

Figure 4.7 Deposition rate vs. T_{Sou} and T_{Sub} .
Source: (Jose Cruz, 2009)

Figure 4.8 observed that the growth rate remains constant at low pressure (T<30Torr), because it is sublimation-limited. The growth rate decrease with the increase of the pressure when the pressure is above 30 Torr, because it is diffusion-limited growth.

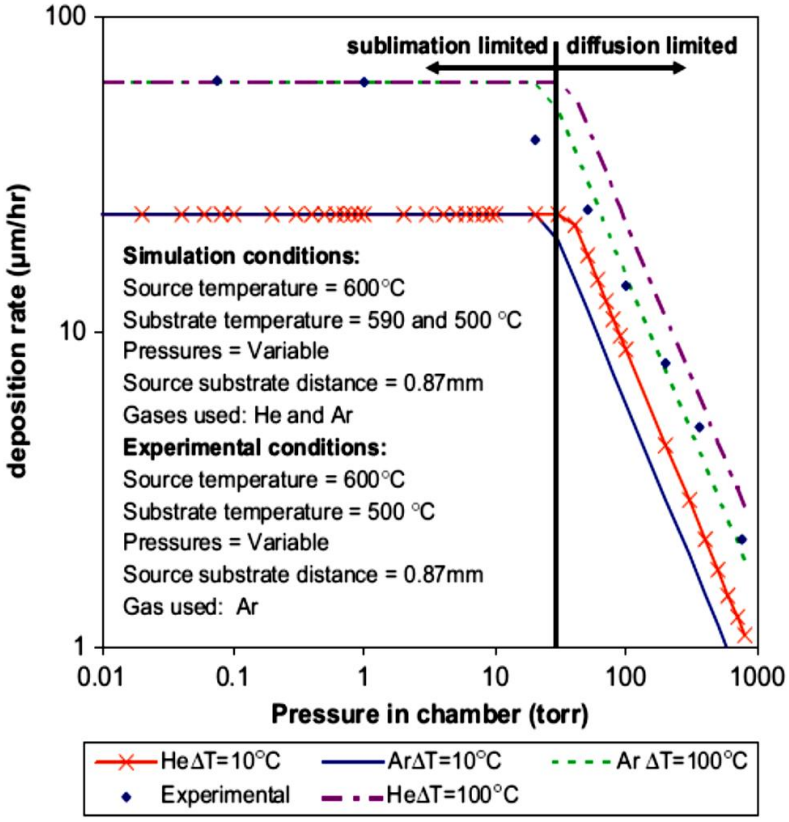

Figure 4.8 Deposition rate vs. $P_{Inert\ gas}$.

Source: (Jose Cruz, 2009)

4.3.2 Bube's Model

Bube's model (T.C. Anthonyi, 1984) is also based on the Fick's law and $J_{cd} = 2 J_{Te_2}$

$$\triangle G_{CdTe(T_{Sub})} = 68.64 - 44.94 \times 10^{-3} \mathrm{T\ kcal/mol}$$

$$\mathrm{K}(0) = P_{Cd}(0) P_{Te_2}(0)^{1/2} = \exp[\frac{-\triangle G_{CdTe(T_{Sou})}}{RT_{Sou}}] \qquad (1)$$

$$\mathrm{K}(h) = P_{Cd}(h) P_{Te_2}(h)^{1/2} = \exp[\frac{-\triangle G_{CdTe(T_{Sub})}}{RT_{Sub}}] \qquad (2)$$

$$J_{cd} = \frac{D_{cd,j}}{khT_{ave}}\left[P_{Cd}(0) - P_{Cd}(\mathrm{h})\right] = J \tag{3}$$

$$J_{Te_2} = \frac{D_{Te_2,j}}{khT_{ave}}\left[P_{Te_2}(0) - P_{Te_2}(h)\right] = \frac{J}{2} \tag{4}$$

It is 4 equations with five unknown. $P_{Cd}(0)$, $P_{Cd}(h)$, $P_{Te_2}(0)$, $P_{Te_2}(h)$, J. Bube assumes that $\Delta T \geq$ **70**℃, $P_{Cd}(0)$ =10* $P_{Cd}(h)$. $P_{Cd}(h)$, $P_{Te_2}(h)$ can be neglected. So it became 3 equations and 3 unknown: $P_{Cd}(0)$, $P_{Te_2}(0)$, J.

$$\mathrm{K}(0) = P_{Cd}(0)P_{Te_2}(0)^{1/2} = \exp[\frac{-\Delta G_{CdTe(T_{Sou})}}{RT_{Sou}}] \tag{1}$$

$$J_{cd} = \frac{D_{cd,j}}{khT_{ave}}\left[P_{Cd}(0) - P_{Cd}(\mathrm{h})\right] = J \tag{2}$$

$$J_{Te_2} = \frac{D_{Te_2,j}}{khT_{ave}}\left[P_{Te_2}(0) - P_{Te_2}(h)\right] = \frac{J}{2} \tag{3}$$

Bube's model is accurate when $\Delta T \geq 70$℃. If $\Delta T \leq 70$℃, then Bube's model is not accurate.

4.3.3 Chin's Model

Chin's Model added two more equations ($P_{Te} = H_0 + aH_1 + a^2H_2$) for both substrate and source. So it is become five equations and five unknown. Chin's model (Ken K. Chin, et al., 2015) based on Henry's law and Greenberg's paper data which is vapor pressure of stoichiometry of CdTe (Figure 4.9).

$$K(0) = P_{Cd}(0)P_{Te_2}(0)^{1/2} = \exp[\frac{-\Delta G_{CdTe(T_{Sou})}}{RT_{Sou}}] \quad (1)$$

$$K(h) = P_{Cd}(h)P_{Te_2}(h)^{1/2} = \exp[\frac{-\Delta G_{CdTe(T_{Sub})}}{RT}] \quad (2)$$

$$J_{cd} = \frac{D_{cd,j}}{khT_{ave}}[P_{Cd}(0) - P_{Cd}(\mathrm{h})] = 2\ J_{Te_2} \quad (3)$$

$$P_{Te}(0) = H_0(0) + a(0)H_1(0) + a(0)^2 H_2(0) \quad (4)$$

$$P_{Te}(h) = H_0(h) + a(h)H_1(h) + a(h)^2 H_2(h) \quad (5)$$

The five unknowns are $P_{Cd}(0)$ $P_{Te_2}(0)$ $P_{Cd}(h)$ $P_{Te_2}(h)$ $a(h)$.

$a(0)$ is known and determined by the CdTe composition and the temperature.

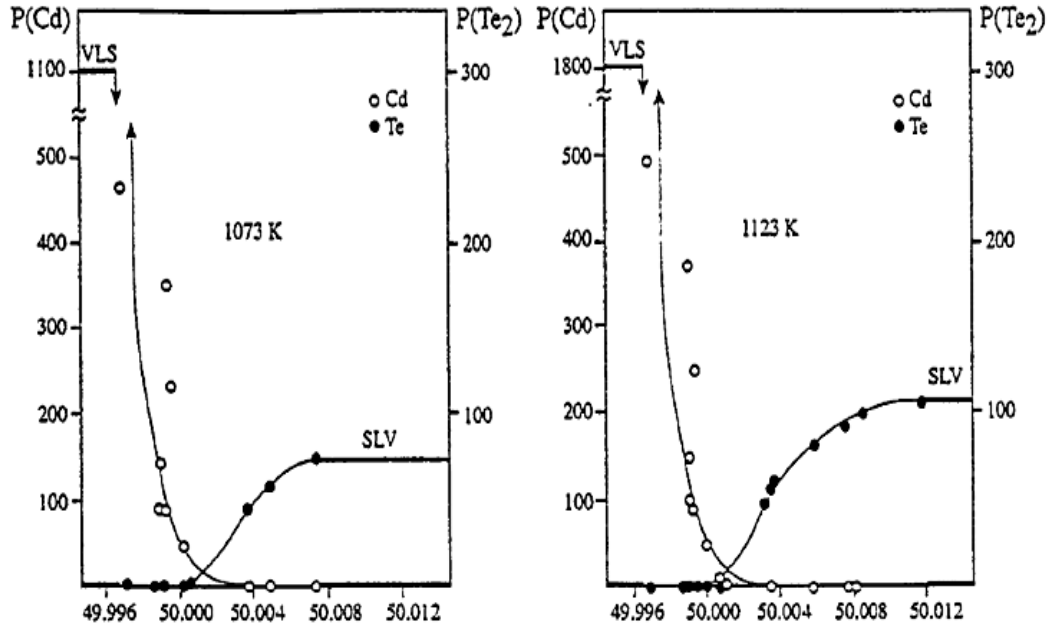

Figure 4.9 Isotherms of partial pressure of P_{Cd} and P_{Te}.

Source:(J. H. Greenberg, 1996)

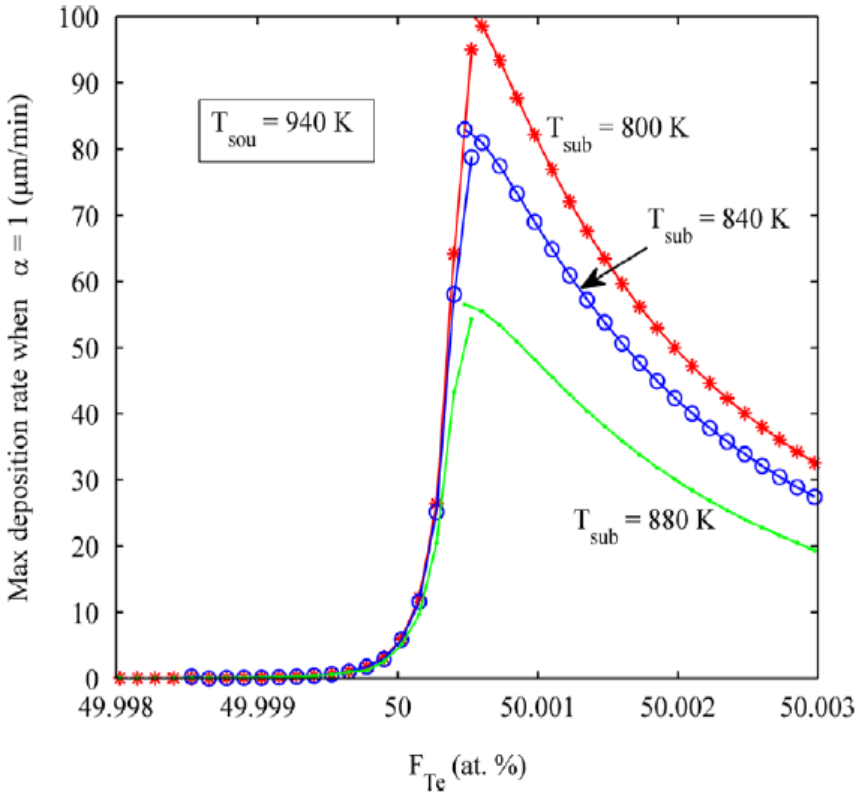

Figure 4.10 Isotherms of partial pressure of P_{Cd} and P_{Te}.

Source: (Ken K.Chin, et al., 2015)

Figure 4.10 show the CdTe growth rate as the function of temperature and the composition of Te. When the CdTe resource is Cd rich, the growth rate is almost 0. When the CdTe resource is Te rich, the growth rate is pretty good. However, if the Te% is above 50.001%, the growth rate is decrease. Therefore, it is important to control the Te between 50% and 50.001%.

4.4 Liu's Model

We cut glass to 4*6 inch. The glass is cleaned by sonication in a 1% solution of liquinox soap in hot DI water. The CdS was deposited on the cleaned substrates by CBD. The CdS substrate is then loaded in the deposition chamber as shown in Figure 4.11.

Figure 4.11 CSS deposition system.

The CdS substrate was annealed at 400 ℃ for 15 min in 30 torr H_2 to reduce oxygen-related defects. After cooling to 200 ℃, the CdTe deposition sequence is initiated. The CdTe deposition by CSS is based on the principle of reversible dissociation of CdTe at high temperatures. Then the elemental gases diffuse to the substrate and the gases recombine on the substrate with lower temperature than the source (Figure 4.12).

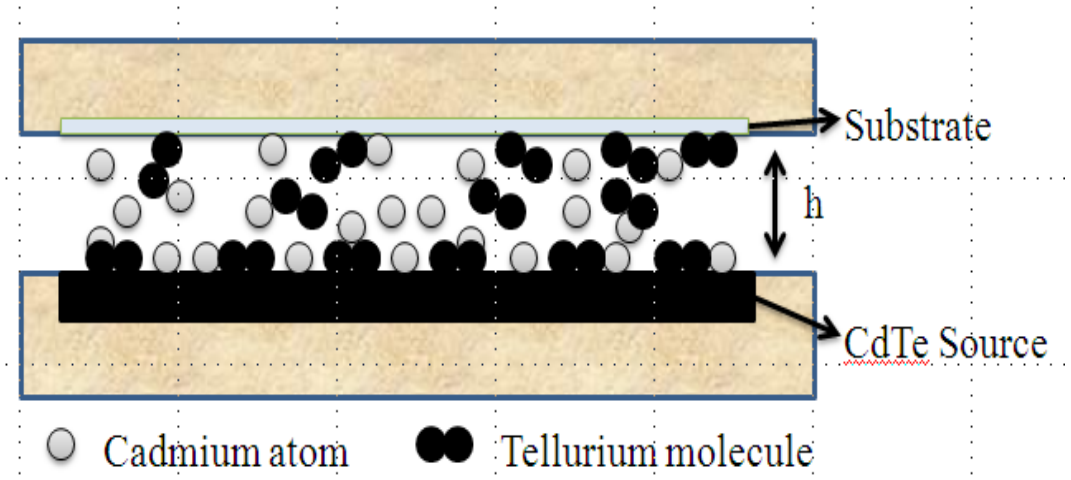

Figure 4.12 Schematic diagram of CSS deposition chamber.

The CdTe deposition chemical process equation by CSS is below:

1. $CdTe(s) \rightarrow Cd(g) + \frac{1}{2} Te_2(g)$

In the source, CdTe decomposes at the source temperature T_{Sou}. The equilibrium constant is: $K_{CdTe}(T_{Sou}) = P_{Cd}(0) P_{Te_2}(0)^{1/2}$ where $P_{Cd}(0)$ and $P_{Te_2}(0)$ are the equilibrium pressure of Cd and Te_2 at the temperature of T_{Sou} .The equilibrium constant can be calculated from the expression given by deLargy et al.

$$K_{CdTe}(T_{Sou}) = P_{Cd}(0) P_{Te_2}(0)^{1/2} = \exp[\frac{-\triangle G_{CdTe(T_{Sou})}}{RT_{Sou}}] \qquad (4.4.1)$$

$$\triangle G_{CdTe(T_{Sub})} = 68.64 - 44.94 \times 10^{-3} T \text{ kcal/mol}$$

2. $Cd(g) + \frac{1}{2} Te_2(g) \rightarrow CdTe(s)$

In the substrate, the Cd and Te_2 combines into CdTe at substrate temperature T_{Sub}. The equilibrium constant is: $K_{CdTe}(T_{Sub}) = P_{Cd}(h) P_{Te_2}(h)^{1/2}$ where $P_{Cd}(h)$ and $P_{Te_2}(h)$ are the equilibrium pressure of Cd and Te_2 at the temperature of T_{Sub} .The equilibrium constant is

$$K_{CdTe}(T_{Sub}) = P_{Cd}(h) P_{Te_2}(h)^{1/2} = \exp[\frac{-\triangle G_{CdTe(T_{Sub})}}{RT_{Sub}}] \qquad (4.4.2)$$

The growth model of CdTe is very complicated. To simplify the growth model, we just consider the situation of steady state, stochiometrical CdTe deposition. The growth rate depends on several interrelated parameters: the space between the source and the substrate, the temperatures of the source T_{sou} and the substrate T_{sub}, and the pressure,

temperature and composition of gases in the deposition chamber. According to different situation, we classify the growth model into two parts:

4.4.1 Sublimation Model

If the mean free path of Cd atoms and Te_2 molecules is longer than the space between the source and substrate (λ >h), then it is sublimation model.

$$\lambda = \frac{KT}{\sqrt{2}\pi d^2 P} \tag{4.4.3}$$

where k is Boltzmann's constant, P is the pressure (Pa), T is the source temperature (K) and d is the molecular diameter of Cd and Te_2.

In the sublimation model, the growth rate is proportional to the equilibrium vapor pressure difference between the source and the substrate.

$$G_{Subi}(m/s) = \frac{\alpha\beta(P^i_{\text{sou}}T_{\text{sou}} - P^i_{\text{sub}}T_{\text{sub}})N_A}{\sqrt{\pi m_i R T_{av}}}\left(\frac{m_i}{\rho_i}\right) \tag{4.4.4}$$

where α and β are coefficients with values between 0and1; P^i_{sou} and P^i_{sub} are the vapor pressure (Pa) of i in the source and substrate; m_i represents the molar mass of the source material(kg/mol); R is the universal gas constant (J/(kg.mol)); T_{sou}, T_{sub}, and T_{av} are the source, substrate, and average temperatures, respectively (K); NA is Avogadro's number; and ρ_i represents the density of the substance evaporated (kg/m^3).

4.4.2 Diffusion Model

If the mean free path of Cd atoms and Te_2 molecules is longer than the space between the source and substrate (λ <h), then it is diffusion model. In the diffusion model, the growth rate can be calculated by Fick's law.

$$J_{cd} = \frac{D_{cd,j}}{khT_{ave}}(P_{Cd}(0) - P_{Cd}(h)) \tag{4.4.5}$$

Where k is Boltzmann's constant(J/K), T_{ave} is the average temperature between source and substrate, $D_{cd,j}$ is the binary coefficient of diffusion of cadmium diffusing into inert gas j (m^2/s); This coefficient will be calculated using the Stefan–Boltzmann model given as

$$D_{Cd,j} = \frac{(NA(KT_{av}/\pi)^3 * (1/m_{Cd} + 1/m_j))^{1/2}}{3(P_{Cd,av} + P_j)\sigma_{Cd,j}^2} \tag{4.4.6}$$

where m_{Cd} and m_j are the molar masses of cadmium and helium (kg/mol), $P_{Cd,av}$ is the vapor pressure (Pa) of Cd evaluated at the average of the substrate and source temperatures T_{av} (K), P_j is the chamber pressure (Pa), NA is Avogadro's number, k is Boltzmann constant, and $\sigma_{Cd,j}$ is the average molecular diameter $\sigma_{Cd,j} = \frac{\sigma_{Cd} + \sigma_j}{2}$.

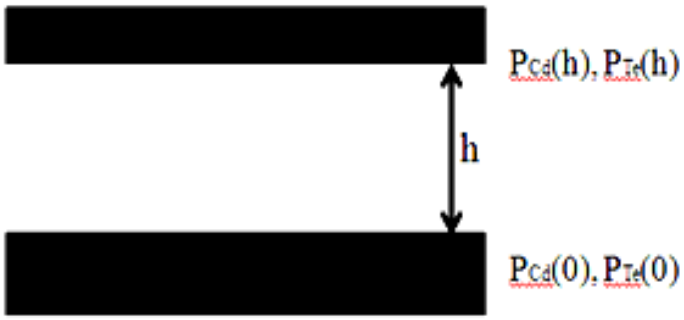

Figure 4.13 Schematic diagram of CSS growth model.

In our model (Figure 4.13), we introduced ∂ as the ratio of pressure of Te and Cd and we assume the ratio in the source and substrate is the same because of the equilibrium and stoichiometry. Then we get 6 equation with 6 unknows: $P_{Cd}(0)$ $P_{Te_2}(0)$ $P_{Cd}(h)$ $P_{Te_2}(h)$ ∂ J

$$\mathrm{K}_{CdTe}(T_{Sou}) = P_{Cd}(0)P_{Te_2}(0)^{1/2} = \exp[\frac{-\triangle G_{CdTe(T_{Sou})}}{RT_{Sou}}] \quad (1)$$

$$\mathrm{K}_{CdTe}(T_{Sub}) = P_{Cd}(h)P_{Te_2}(h)^{1/2} = \exp[\frac{-\triangle G_{CdTe(T_{Sub})}}{RT_{Sub}}] \quad (2)$$

$$J_{cd} = \frac{D_{cd,j}}{khT_{ave}}\left[P_{Cd}(0) - P_{Cd}(\mathrm{h})\right] = J \quad (3)$$

$$J_{Te_2} = \frac{D_{Te_2,j}}{khT_{ave}}\left[P_{Te_2}(0) - P_{Te_2}(h)\right] = \frac{J}{2} \quad (4)$$

$$P_{Cd}(0) = \partial P_{Te_2}(0) \quad (5)$$

$$P_{Cd}(h) = \partial P_{Te_2}(h) \quad (6)$$

$$G(um/\min) = \eta J_{cd}\frac{M_{CdTe}}{\rho_{CdTe}}60*10^6$$

We simplify the equation and can get three equations and 3 unknown:

$P_{Cd}(0)$ $P_{Cd}(h)$ ∂

$$\frac{1}{\partial^{\frac{1}{2}}}P_{Cd}(0)^{\frac{3}{2}} = \exp[\frac{-\triangle G_{CdTe(T_{Sou})}}{RT_{Sou}}] \quad (1)$$

$$\frac{1}{\partial^{\frac{1}{2}}}P_{Cd}(h)^{\frac{3}{2}} = \exp[\frac{-\triangle G_{CdTe(T_{Sub})}}{RT_{Sub}}] \quad (2)$$

$$\partial = 2\frac{D_{Te_2,j}}{D_{cd,j}} \quad (3)$$

After calculation, we get ∂ =1.05 at T_{sub}=600 ℃; T_{sou}=640 ℃;

The growth rate (um/min) can be calculate from the material flux by

$$G(um/\min) = \alpha J_{cd}\frac{M_{CdTe}}{\rho_{CdTe}}60*10^6$$

Where the coefficient α is sticking coefficient. The fitting parameter value α=0.36, M_{CdTe} is molar mass in Kg/mol and ρ_{CdTe} is the density in Kg/m^3.

At the T_{sub}=600 ℃; T_{sou}=640 ℃; h=2 mm, we calculate the deposition rate is 4.02 um/min. It is very close to the experiment data of 4.33um/min. Table 4.4 shows the deposition rate for different substrate temperature at T_{sou}=640 ℃. Table 4.5 shows the deposition rate and the ratio ∂ for different source temperature at T_{sub}=400 ℃.

Figure 4.14 shows that the growth rate almost kept the same with the increase of T_{sub} when the T_{sub} is below to 550 ℃. The growth rate decrease greatly with the increase of T_{sub} when the T_{sub} is above to 550 ℃. It is because of the re-sublimation of CdTe on the substrate.

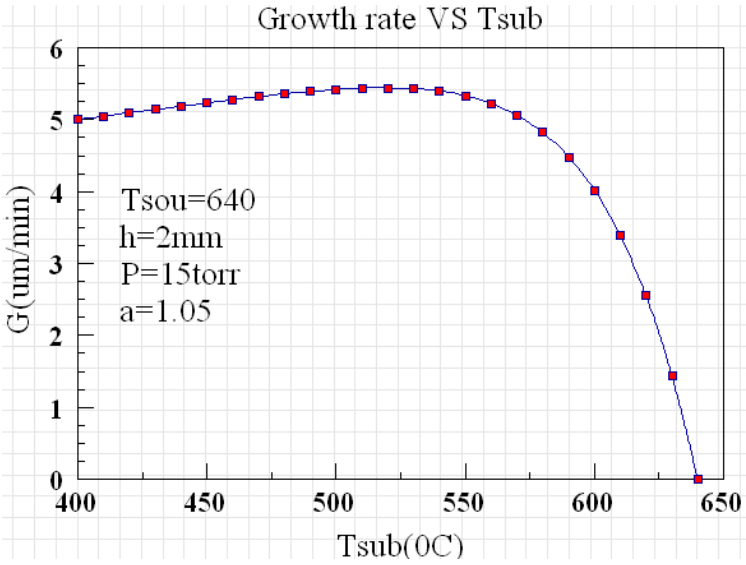

Figure 4.14 Growth rate at different substrate temperature.

Figure 4.15 compare the diffusion model with the former model (Guogen Liu, 2015) and the experimental data. The diffusion model is very accurate.

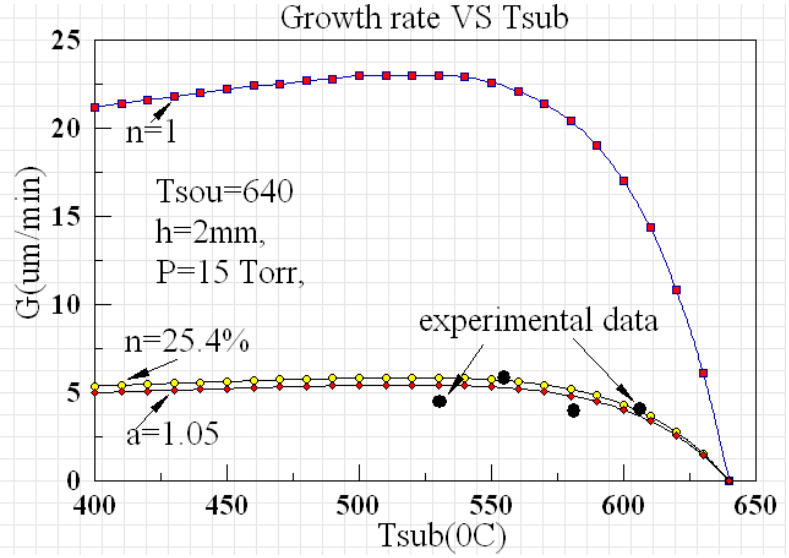

Figure 4.15 Growth rate compare with experimental data.

Table 4.4 Deposition Rate at Different Substrate Temperature (T_{sou}=640 ℃)

T_{sub} (℃)	400	410	420	430	440	450	460	470	480	490
G (um/min)	5	5.05	5.10	5.14	5.19	5.23	5.28	5.32	5.36	5.39

T_{sub} (℃)	500	510	520	530	540	550	560
G (um/min)	5.42	5.44	5.44	5.43	5.40	5.33	5.22

T_{sub} (℃)	570	580	590	600	610	620	630	640
G (um/min)	5.06	4.82	4.48	4.02	3.39	2.55	1.44	0

Table 4.5 Deposition Rate and ∂ at Different Source Temperature (Tsub=400 ℃)

T_{sou} (℃)	400	410	420	430	440	450	460	470
∂	2	1.071	1.07	1.069	1.068	1.067	1.065	1.064
G(um/min)	0	0.0003	0.0009	0.0018	0.0033	0.0055	0.0089	0.0139

T_{sub} (℃)	480	490	500	510	520	530	540	550
∂	1.063	1.062	1.061	1.06	1.059	1.058	1.057	1.056
G(um/min)	0.0215	0.0325	0.0486	0.072	0.104	0.151	0.216	0.306

T_{sub} (℃)	560	570	580	590	600	610	620	630	640
∂	1.055	1.054	1.053	1.052	1.051	1.05	1.049	1.048	1.047
G(um/min)	0.43	0.6	0.83	1.138	1.551	2.1	2.82	3.768	5

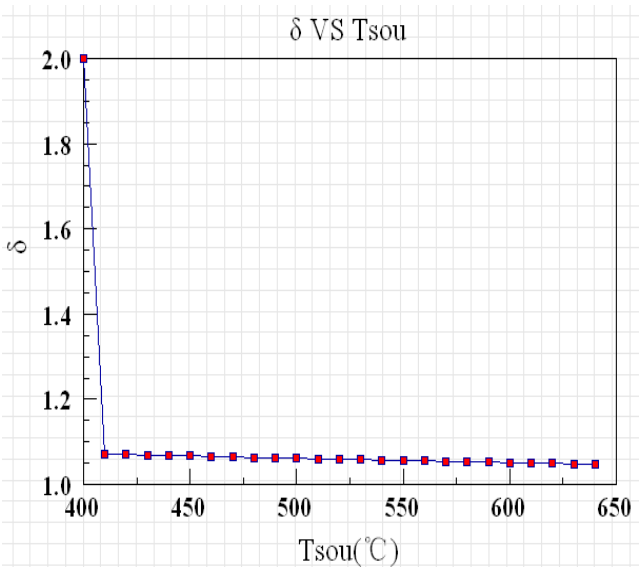

Figure 4.16 ∂ for different source temperature at T_{sub}=400 ℃.

Figure 4.16 shows that the ratio ∂ decreases with the increase of the T_{sou}. When the T_{sou}=400 ℃, ∂ =2, because it is congruent sublimation. With the increase of source temperature, the sublimation rate is increase but the ∂ decrease. It may because of the increase of Te sublimation because the Te melting points is higher than Cd. The higher T_{sou}; the more Te sublimation.

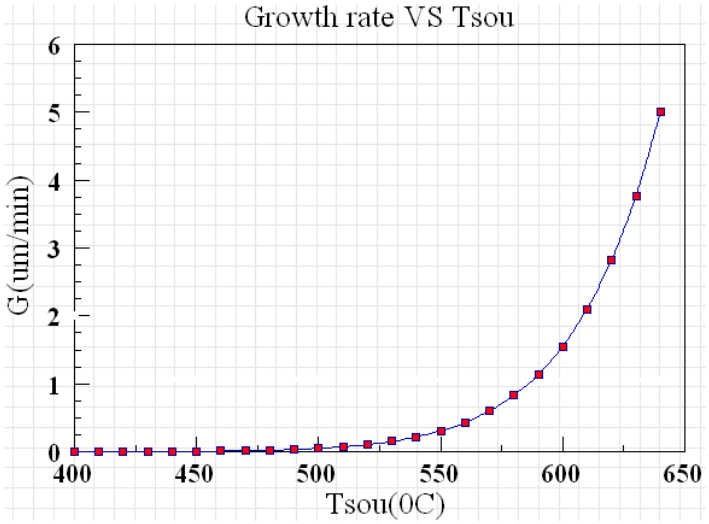

Figure 4.17 Growth rate vs T_{sou} at T_{sub}=400 ℃.

Figure 4.17 shows that the growth rate increases with the increase of T_{sou}. When T_{sou} is between 400 ℃-500 ℃, the growth rate is almost zero, because CdTe evaporate very slowly. Above 500 ℃, CdTe evaporate faster and the growth rate increase fast.

4.5 Results

4.5. 1 Microscope

We use the microscope to exam the process of the CdTe deposition. From Figure 4.18, we can see the CdTe thin film is deposited by an island mechanism, because the bonds between atoms within the film are stronger than the film-substrate bonds.

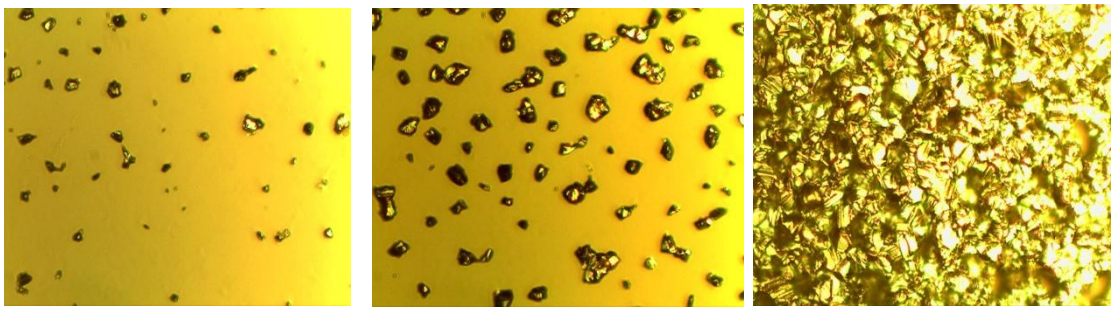

Figure 4.18 The CdTe deposition process.

4.5.2 XRD

The XRD spectra of CdTe are shown in Figure 4.19. From the XRD, we can see the CdTe are highly oriented along the (111) direction.

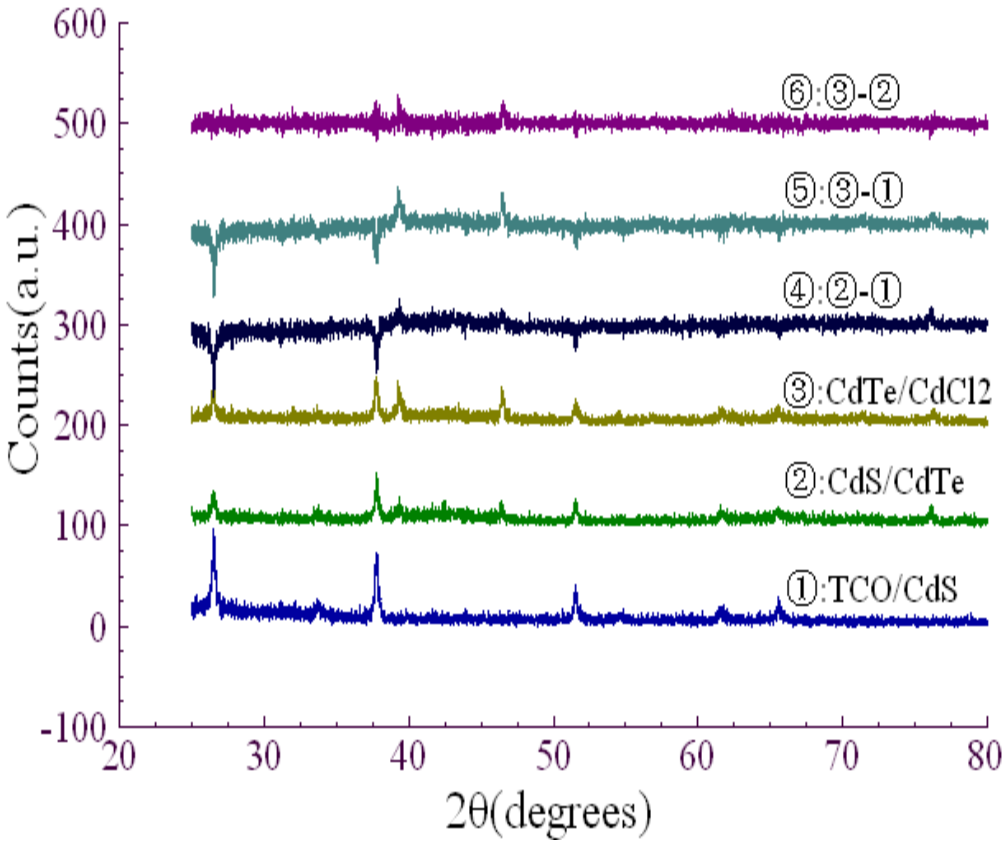

Figure 4.19 XRD of CdTe film.

4.6 Conclusion

In this paper, we present three different growth models in CdTe deposition by CSS. We present mean free path to decide the sublimation and diffusion model. If the mean free path of Cd atoms and Te_2 molecules is shorter than the space between the source and substrate (λ < h), it is sublimation model. If λ > h, it is diffusion model. If the inert gas has oxygen input, then we need to consider the reaction model. The growth models are affected by several important parameters: spacing, ambient gas, ambient gas pressure, substrate temperature and source temperature. They all have independent control over the growth rate.

REFERENCES

Alamr, S. N., "The growth of CdTe thin film by close space sublimation system," phys. stat. sol. (a) 200, No. 2, 352–360 (2003).

Anthony, T. C., Fahrenbruch, A. L., Bube, R. H., "Growth of cadmium telluride films by close-spaced vapor transport". J. Vac. Sci. Technol., A: Vac., Surf., Films (1984).

Arango, S., et al., "Coating and Surface Treatments on Orthodontic Metallic Materials," Coatings 2013, 3(1), 1-15 (2012).

Chin, K. K., Cheng, Z. M., Delahoy, A. E., "Nonstoichiometric composition shift in Physical Vapor Deposition of CdTe thin films," Journal of Crystal Growth,(2015).

Cruz-Campa, J. L., "CdTe thin film growth model under CSS conditions," Solar Energy Materials & Solar Cells 93 15– 18 (2009).

Cunningham, R., "Cadmium telluride PV module manufacturing at BP Solar," Prog. Photovolt., 10, 159–168 (2002).

Dahmani, B. et al., "Material for use in the manufacturing of luminous display devices," WO2004023436 A2 (2003).

Delahoy, A. E., Guo, S. Y., "Handbook of photovoltaic science and engineering," Second edition, Edited by Luque, A., Hegedus, S., John Wiley & Sons, Ltd. (2011).

Dharmadasa, I. M., "New ways of developing glass/conducting glass/CdS/CdTe/metal thin-film solar cells based on a new model," Semicond. Sci. Technol. 17, 1238–1248 (2002).

Falc ão, V. D., Pinheiro, W. A., "Influence of Deposition Parameters on the Properties of CdTe Films Deposited by Close Spaced Sublimation," Materials Research, Vol. 9, No. 1, 29-32 (2006).

Gonz ález, J., et al., "PV solar market in the global energy industry," http://whitewallenergy.com/blog/PV-solar-market-in-global-energy-industry/ (2015).

Green, M. A., et al., "Solar cell efficiency tables," Prog. Photovolt. Res. Appl. 21, 827–837 (2013).

Singh, G., "Exploit nature-renewable energy technologies," Aditya Books Pvt. Ltd. (2013).

Liu, G. G., et al., "The Growth Model of CdTe Thin Film by Close Spaced Sublimation," at 42th IEEE PVSC (2015).

Nagayoshi, H., et al., "Growth of thick CdTe films by close-space sublimation technique," IEEE. Volume:7 (2004).

Sculati-Meillaud, F., "Thin Film Silicon Solar Cells on Glass,"

http://pvlab.epfl.ch/thin_film_on_glass (2016)

Mathias, "NREL sets new world record with two-junction solar cell," http://energyinformative.org/nrel-efficiency-record-two-junction-solar-cell (2013).

"How does solar water heating work?"http://info.cat.org.uk/questions/solar-water-heating/how-does-solar-water-heating-work.

Crossley, Reed, "The sun to rule them all? solar energy's potential,"

http://learn.revolvesolar.com/the-sun-to-rule-them-all-solar-energys-potential (2016)

Grana, Paul. "Five Solar Debates: the Efficiency Race," http://thegreenstalk.com/2010/08/.(2010).

"Available Technologies," http://www.aessolar.co.uk/.

"CTF Solar," http://www.ctf-solar.com/.

Cook, Charlie, "The Growth of Solar Power,"

https://charlieonenergy.wordpress.com/2015/12/07/solar-and-moores-law/ (2015)

Kranz, L., et al., "Doping of polycrystalline CdTe for high-efficiency solar cells on flexible metal foil," Nature Communications (2013).

Martinez, M. A., et al., "Cadmium sulphide growth investigations on different SnO2 substrates," Appl. Surf. Sci. 140-182 (1999).

Matin, M. A., et al., "Ultra thin high efficiency CdS/CdTe thin film solar cells," proceedings of the 8th WSEAS int. conf. on non-linear analysis, non-linear systems and chaos ISSN: 1790-2769 (2009).

Occupy theory, "Advantages and disadvantages of renewable energy," http://occupytheory.org/advantages-and-disadvantages-of-renewableenergy/(2014).

Pinheiro, W. A., et al., "Comparative study of CdTe sources used for deposition of CdTe thin films by close spaced sublimation technique," Materials Research, Vol. 9, No. 1, 47-49 (2006).

Powalla, M., et al., "Thin-film solar cells based on the polycrystalline compound semiconductors CdS and CdTe," Advances in OptoElectronics, Volume 2007, Article ID 97545, 6 pages (2007).

Powell, R. C., et al., "Technology support for initiation of high-throughput processing of thin-film CdTe PV modules," Phase 3 final technical report (1998).

Quinones, S. A., "SEM characterization of CdTe growth on CdTe(111) by close-spaced sublimation," J Mater Sci: Mater Electron. 18:1085–1091 (2007).

Rinkesh, "Fossil Fuel," http://www.conserve-energy future.com/ (2013).

Kuhaimi, S. A., "Influence of preparation technique on the structural, optical and electrical properties of polycrystalline CdS films," Vaccum 51 349 (1998).

Seitz, et al., “Ökoeffizienz analyse von photovoltaik module,” Bifa Umweltinstitut, 62. ISSN 0944-5935 (2013).

Solar irradiance, https://en.wikipedia.org/wiki/Solar_irradiance#cite_note-1 (2015).

Scholten, M. D., and Schottler, M., “Solar as an environmental product: thin-film modules – production processes and their environmental assessment,” Presented at Thin Film Industry Forum. ECN (2009).

Woodford, C., “Renewableenergy,” http://www.explainthatstuff.com/renewable energy.html (2015).

Zweibel, K. J., Mason, V. F., “A solar grand plan,” Scientific American. (2008).